474-00049
Effective Date: May 8, 2014
Revision B

GSFC JPSS CMO
August 18, 2014
Released

Joint Polar Satellite System (JPSS) Ground Project
Code 474
474-00049

Joint Polar Satellite System (JPSS) VIIRS Aerosol Optical Thickness (AOT) and Particle Size Parameter Algorithm Theoretical Basis Document (ATBD)

For Public Release

The information provided herein does not contain technical data as defined in the International Traffic in Arms Regulations (ITAR) 22 CFC 120.10.
This document has been approved For Public Release.

National Aeronautics and Space Administration

Goddard Space Flight Center
Greenbelt, Maryland

Joint Polar Satellite System (JPSS) VIIRS Aerosol Optical Thickness (AOT) and Particle Size Parameter Algorithm Theoretical Basis Document (ATBD)

JPSS Electronic Signature Page

Prepared By:

Ray Godin
JPSS Data Products and Algorithms, EDR Lead
(Electronic Approvals available online at https://jpssmis.gsfc.nasa.gov/mainmenu_dsp.cfm)

Approved By:

Eric Gottshall
DPA Manager
(Electronic Approvals available online at https://jpssmis.gsfc.nasa.gov/mainmenu_dsp.cfm)

Preface

This document is under JPSS Ground AERB configuration control. Once this document is approved, JPSS approved changes are handled in accordance with Class I and Class II change control requirements as described in the JPSS Configuration Management Procedures, and changes to this document shall be made by complete revision.

Any questions should be addressed to:

JPSS Ground Project Configuration Management Office
NASA/GSFC
Code 474
Greenbelt, MD 20771

Change History Log

Revision	Effective Date	Description of Changes (Reference the CCR & CCB/ERB Approve Date)
Original (Rev -)	04/22/2011	**474-CCR-11-0064**: This version baselines D43313, VIIRS Aerosol Optical Thickness (AOT) and Particle Size Parameter Algorithm Theoretical Basis Document (ATBD), Rev F dated 02/16/2010 as a JPSS document, version Rev –. This is the version that was approved for NPP launch. Per NPOESS CDFCB - External, Volume V – Metadata, doc number D34862-05, this has been approved for Public Release into CLASS. This CCR was approved by the JPSS Ground Algorithm ERB on April 22, 2011.
A	06/26/2013	**474-CCR-11-1053:** This is the first post-launch update by the JPSS cal/val team that includes accurate description of current algorithm, description of post-launch changes to algorithm and PCT, preliminary validation and future plans. This CCR was approved by the JPSS Ground Algorithm ERB on June 26, 2013.
B	05/08/2014	**474-CCR-14-1687:** This CCR was approved by the JPSS Ground Algorithm ERB on May 8, 2014. Affects Table C.1 and C.3.

SUOMI- NATIONAL POLAR-ORBITING PARTNERSHIP (NPP)

VIIRS AEROSOL OPTICAL THICKNESS (AOT) AND PARTICLE SIZE PARAMETER (APSP) ALGORITHM THEORETICAL BASIS DOCUMENT (ATBD) (D43313 Rev F)

ELECTRONIC APPROVAL SIGNATURES:

The following individuals are recognized for their contributions to the current or previous versions of this document.

Istvan Laszlo Shobha Kondragunta Sid Jackson Lorraine A. Remer Hongqing Liu Jingfeng Huang	Ho-Chun Huang Hai Zhang Min Oo Andrew Sayer Edward Hyer Heather Cronk	Doug Hoyt Heather Kilcoyne Richard Slonaker Scott Vibert Eric Vermote Xuepeng (Tom) Zhao

Revision/ Change Record		Document Number D43313	
Revision	Document Date	Revision/Change Description	Pages Affected
----	1/18/2007	Initial PCIM Release to bring document into Matrix Accountability. Reference original document number: Y2388 delivered in 2006	All
A	8/14/2007	Updated for changes to the science code baseline implemented by SPCR ALG00001205	All
B	9/17/2007	Updated for changes to the science code baseline implemented by SPCR ALG00001222	55-58
C	3/11/2008	Updated for changes to the science code baseline implemented by SPCR ALG00001279	21-22
D	11/18/2008	Updated for changes to the science code baseline implemented by i-iii, x, 1, 3, SPCR ALG00001358	6, 9, 11, 1317, 27, 29, 31-35, 40, 42, 47, 58, 59
E	12/10/2008	Updated for changes to the science code baseline implemented by SPCR ALG00001387	71-74
F	2/16/2010	In preparation for Public Release of this ATBD, the following administrative changes were made: all ITAR markings were removed, and Distribution Statement F added. ECR A-184A. Approved for Public Release per Contracts Letter 100610-02	All

TABLE OF CONTENTS

LIST OF FIGURES

LIST OF TABLES

GLOSSARY OF ACRONYMS

6S	Second Simulation of the Satellite Signal in the Solar Spectrum
AERONET	Aerosol Robotic Network
AE	Ångström exponent
AMI	Aerosol Model Information
AOT	Aerosol Optical Thickness
APSP	Aerosol Particle Size Parameter
ATBD	Algorithm Theoretical Basis Document
ATMS	Advanced Technology Microwave Sounder
AVHRR	Advanced Very High Resolution Radiometer
BRDF	Bidirectional Reflectance Distribution Function
CALIOP	Cloud-Aerosol Lidar with Orthogonal Polarization
CALIPSO	Cloud-Aerosol Lidar and Infrared Pathfinder Satellite Observations
CERES	Clouds and Earth's Radiant Energy System
CrIS	Cross-track Infrared Sounder
EDR	Environmental Data Record
EOS	Earth Orbiting System
FNMOC	Fleet Numerical Meteorology and Oceanography Center
IP	Intermediate Product
IR	InfraRed
LUT	Look-up Table
MAN	Maritime Aerosol Network
MIRA	Middle Infrared Anomaly
MISR	Multi-angle Imaging SpectroRadiometer
MODIS	Moderate Resolution Imaging Spectroradiometer
MSS	Multispectral Sensor
NAAPS	Navy Aerosol Analysis and Prediction System
NASA	National Aeronautics and Space Administration
NCEP	National Center for Environmental Prediction
NDVI	Normalized Difference Vegetation Index

NIR	Near InfraRed
NOAA	National Oceanic and Atmospheric Administration
NOGAPS	Navy Operational Global Atmospheric Prediction System
NPOESS	National Polar-orbiting Operational Environmental Satellite System
NPP	National Polar-orbiting Partnership
OMPS	Ozone Mapping Profiling Suite
PCT	Processing Coefficient Table
POES	Polar Orbiting Environmental Satellites
POLDER	POLarization and Directionality of the Earth's Reflectances
RDR	Raw Data Record
RGB	Red Green Blue
S-NPP	Suomi-National Polar-orbiting Partnership
SDR	Sensor Data Record
SM	Suspended Matter
SWIR	Short Wave InfraRed
TM	Thematic Mapper
TOA	Top of the Atmosphere
VCM	VIIRS Cloud Mask
VIIRS	Visible Infrared Imaging Radiometer Suite
VRA	Visible Reflectance Anomaly

ABSTRACT

This document describes the operational retrieval algorithm of the Visible Infrared Imager Radiometer Suite (VIIRS) aerosol optical thickness, particle size parameter and suspended matter products. The aerosol optical thickness product consists of the vertically-integrated column total extinction for a range of wavelengths from 0.4 to 2.25 μm. The particle size parameter product consists of the Ångström Exponent computed from the optical thicknesses at two separate wavelengths. Retrieval of these products is performed globally in daylight except over bright surfaces and under cloudy conditions. The aerosol optical thickness is calculated over both land and ocean using look-up tables (LUT) of pre-computed values for several atmospheric parameters in order to simplify the radiative transfer calculations. The aerosol LUTs are computed for multiple aerosol types, optical thickness values, and sun-sensor viewing geometries. The LUT accounts for multiple scattering in the atmosphere by molecules and aerosol particles. Because the reflective properties of ocean and land are very different, separate retrieval approaches are used over the land and the ocean. Over the ocean, the surface BRDF is computed based on wind speed and the BRDF-atmosphere coupling is included in the radiative transfer calculations. Over the land, a dark pixel approach is used, and the retrieval is based on matching surface reflectance ratios to expected values. The aerosol retrieval over land uses a Lambertian surface reflectance assumption in the inversion. The aerosol particle size parameter is the Ångström Exponent computed from the aerosol optical thickness values at two different wavelengths. The suspended matter product is a classification of the aerosol type into categories consisting of volcanic ash, dust, smoke, sea salt, not determined and none, and is a by-product of the retrievals over land and ocean, or is input from the VIIRS Cloud Mask. The aerosol algorithm is applied to every VIIRS pixel at moderate resolution to form an Intermediate Product at nominal 0.75 km (nadir) resolution. Then an aggregation algorithm is applied that makes use of the associated quality flags to create a nominal 6 km Environmental Data Record product. Suspended matter is not aggregated and is made available at moderate resolution.

VIIRS aerosol products have been compared with a total of 10 months (2 May to 14 Oct 2012 and 28 Nov 2012 through March 2013) of MODIS, AERONET and CALIOP products to evaluate and perform a preliminary validation. These results show the ocean AOT in very close agreement with both MODIS and AERONET, and the ocean Ångström Exponent agreeing better with AERONET than does MODIS. VIIRS AOT over land correlates with MODIS and AERONET AOT, but was initially biased high. Changes to the expected values of the spectral surface reflectance ratios used in the over-land aerosol retrieval, implemented 22 Jan. 2013, eliminated much of the global bias in AOT over land. Further plans for change should reduce much of the scatter that still exists between VIIRS and validation data sets in AOT over land. VIIRS Ångström Exponent over land and suspended matter products over land and ocean are not yet showing skill against validation data sets. Plans are being executed to address some of these issues.

1.0 INTRODUCTION

We live in a time of increasing awareness of the environmental challenges facing our present and future, and this awareness is coupled with an increasing commitment to provide the tools necessary to provide the information to understand and meet those challenges. One important environmental challenge is to understand the role of atmospheric aerosols in climate processes and in the degradation of air quality. These small suspended liquid and solid particles in our atmosphere such as mineral dust, smoke, volcanic ash, particulate pollution, sea salt and biogenic compounds play an active role in the Earth's energy balance, hydrological cycle and atmospheric chemistry. At the same time these particles cause ill health effects when breathed into the lungs, and degrade visibility, which can interfere with military operations and civilian flight safety. Because these particles and their precursors are emitted into the atmosphere from a variety of sources, undergo chemical transformation as they are transported globally and are removed from the atmosphere by various processes on the order of one or two weeks, their compositions and distributions are characterized by a high level of temporal and spatial variability. A global view of the aerosol system can be best achieved by space-based observations that complement ground-based and airborne observations, which provide a more detailed characterization of the particles but with significantly poorer temporal and/or spatial sampling.

The Visible Infrared Imager Radiometer Suite (VIIRS) launched aboard the Suomi National Polar orbiting Partnership (NPP) satellite in October 2011 is continuing in a tradition of providing a key set of aerosol products based on daily observations from space. These products are designed to match the precedent established by NASA's Earth Observing System (EOS) MODerate resolution Imaging Spectroradiometer (MODIS) that has produced near-real time aerosol data products for over a dozen years. The climate, air quality, research, applied, private, governmental and military communities have all embraced the MODIS aerosol product and have come to rely on it for their research, forecasts, communication and policy decisions. The VIIRS aerosol products to be described here are designed to provide the same level of quality aerosol information in a timely manner that will continue to satisfy the needs of these many communities.

1.1 Purpose of document

This Algorithm Theoretical Basis Document (ATBD) describes the algorithms used to retrieve the Suomi-NPP VIIRS aerosol products that include Aerosol Optical Thickness (AOT) and Aerosol Particle Size Parameter (APSP) and Suspended Matter (SM) Environmental Data Records (EDRs). Also described in this ATBD are the Aerosol Optical Thickness (AOT) and Aerosol Model Information (AMI) Intermediate Products (IP). The EDRs are being archived and released to the public. The IP products may be released at a future time. These products are summarized in Table 1.1 and described in Section 1.2. Specifically, this document identifies the sources of input data, both VIIRS and non-VIIRS, required for retrievals; provides the physical theory and

mathematical background underlying the use of this information in the retrievals; includes implementation details; and describes assumptions and limitations of the proposed approach.

This ATBD is the first post-launch formal description of the VIIRS aerosol algorithms, and it includes some preliminary comparison of the on-orbit product with heritage products from other sensors, and some preliminary validation against ground-truth data from the Aerosol Robotics Network (AERONET) and the Marine Aerosol Network (MAN). This ATBD supersedes the earlier version (D43313 Rev F; Baker et al., 2011) written before launch. Significant revisions to the algorithms took place between the previous ATBD and the at-launch aerosol algorithms described here. Those earlier documents should now be considered obsolete.

1.2 VIIRS aerosol products

The VIIRS aerosol products are summarized in Table 1.1. Aerosol optical thickness is sometimes referred to as the aerosol optical depth. It is the integrated aerosol extinction coefficient over a vertical column of unit cross section through the atmosphere, defined by,

$$AOT_\lambda = \int_{z=0}^{z=TOA} \sigma_{ex_\lambda} \, dz \tag{1.1}$$

where *TOA* is the top of the atmosphere, σ_{ex}, the extinction coefficient in units of inverse length, is the fractional depletion of radiance per unit path length. The extinction coefficient and thus the AOT are functions of wavelength, λ. AOT is the degree to which aerosols prevent the transmission of light by absorption and/or scattering of light, and is related to the transmission (T_λ) by aerosols by,

$$T_\lambda = \exp\left(-\frac{AOT_\lambda}{\cos\theta_0}\right) \tag{1.2}$$

where θ_o is the solar zenith angle and AOT_λ is defined for the vertical column and not the slant path towards the direction of the sun. It is an extensive variable like length or mass, so that when air masses of $AOT = x$ and $AOT = y$ are mixed, the resulting air mass has $AOT = x+y$. Thus, AOT is used as a measure of the aerosol loading, the amount of aerosol in the air mass.

The VIIRS APSP currently in production and described in this ATBD is the Ångström Exponent (AE). This parameter expresses the spectral dependence of the AOT and is defined as,

$$AOT_\lambda = AOT_{\lambda_0}\left(\frac{\lambda}{\lambda_0}\right)^{-AE} \tag{1.3}$$

where λ_o represents any reference wavelength. Equation (1.3) assumes that the spectral dependence of the AOT in log-log space is linear so that a single exponent can represent the spectral dependence across all wavelengths. This means that given the AOT at any wavelength and the AE, then the AOT at any other wavelength is known. Conversely, given the AOT at any two wavelengths, the AE can be derived, as well. Equation (1.3) is a reasonable approximation, although many aerosol types result in curvature of the AOT-wavelength relationship on a log-log plot that introduces complexities and contradict the inherent assumption (Eck et al., 1999; O'Neill et al. 2001). These complexities will not be addressed in the current APSP algorithm, nor further described in this document. Through Mie theory (Mie, 1908) we know that the spectral dependence of AOT is a function of particle size. Therefore, AE is a qualitative measure of particle size with larger AE corresponding to smaller particles, and vice-versa. This is how AE fills the VIIRS criteria for APSP. The AE is an intensive or intrinsic property, like temperature, so that when air masses of $AE=x$ and $AE=y$ are mixed, the resulting air mass will not be characterized by the sum of the individual AEs. Thus, AE represents particle properties, namely size, and not aerosol loading.

The third VIIRS aerosol product is Suspended Matter (SM). This product is a simple classification of the aerosol type. The aerosol retrieval is categorized into dust, smoke, sea salt, volcanic ash, unknown and none. The classification is based primarily on the derived AOT and fine mode weight over ocean and AOT and land aerosol model over land.

Table 1.1 Summary of aerosol products

Parameter name	Units	Horizontal cell size	Comments
Aerosol Optical Thickness (AOT)	dimensionless	6 km (nadir) EDR 0.75 km (nadir) IP	Retrieved globally during daylight except over cloudy areas and bright surfaces. Reported at 11 wavelengths 0.412 to 2.25 μm
Aerosol Particle Size Parameter	Ångström Exponent (dimensionless) Goal: Effective radius (μm)	6 km (nadir) EDR 0.75 km (nadir) IP	Retrieved globally during daylight except over cloudy areas and bright surfaces.
Aerosol Suspended Matter	Aerosol type Dimensionless with an exception being smoke for which concentrations in	0.75 km (nadir) EDR	Reports on aerosol type for moderate to heavy aerosol loading, for AOT > specified threshold.

	μg/m^3 are also reported.		

1.3 Scope

This document covers the algorithm theoretical basis for the retrieval of the products listed in Table 1.1 of VIIRS on Suomi-NPP, and provides preliminary comparison to heritage products and ground-truth. This document is not a User's Guide. It does not give details on how to acquire data, read data files or interpret Quality Flags in the data. The VIIRS Aerosol Product User's Guide (http://www.star.nesdis.noaa.gov/jpss/ATBD.php#S126472) does provide that level of detail. In this document, Section 1.0 describes the purpose and scope of this document. Section 2.0 is an overview of the aerosol retrievals. The theoretical description and implementation of the algorithm are described in Section 3.0. A preliminary validation is summarized in Section 4.0. Future updates are discussed in Section 5.0. References for citations in the text are listed in Section 6.0, followed by Appendices.

2.0 EXPERIMENT OVERVIEW

2.1 Suomi-NPP and VIIRS mission

The Suomi-NPP mission is a joint endeavor between NOAA and NASA to understand, monitor and predict the parameters affecting long-term climate change and short-term weather conditions. Suomi-NPP carries five instruments: the Advanced Technology Microwave Sounder (ATMS) for temperature and moisture profiles, the Cross-track Infrared Sounder (CrIS) for monitoring meteorological variables of the atmosphere, the Ozone Mapping and Profiler Suite (OMPS) for measuring ozone from space, the Clouds and Earth's Radiant Energy System (CERES) for monitoring Earth's radiation budget and the Visible Infrared Imaging Radiometer Suite (VIIRS) to measure land, oceanic and atmospheric parameters including aerosols. The spacecraft is in a polar orbit at an altitude of 824 km with an ascending equator crossing time of 1:30 pm Local Time. In this way the orbit is similar to NASA's A-Train satellite orbits. However, because Suomi-NPP's orbit is at a higher altitude than the A-Train satellites (705 km), flight track coincidences occur every two or three days for about 3 hours, if the requirement is for overlap of the two satellites to occur within 5 minutes of each other.

The VIIRS sensor is a 22-band cross-track scanning radiometer that measures reflected and emitted radiation from the Earth-atmosphere system in narrow discrete bands, similar to the MODIS instrument. Wavelengths span the range from 0.412 to 12.01 μm. VIIRS has a wider swath width than MODIS (3000 km vs. 2330 km), which allows VIIRS to fully sample the Earth every day, not every two days. Furthermore VIIRS's on-board data retention algorithms eliminate redundant views of the same Earth scenes, which mitigates the "bow tie" effect at swath edges that characterized MODIS imagery. Furthermore, the pixel aggregation and better geometric strategy reduces the spreading of the pixel sizes towards the swath edge. While a MODIS pixel spreads to

4x its resolution at nadir, the VIIRS spread is roughly 2x nadir. VIIRS produces some bands at 0.371 x 0.387 km nadir resolution and others at 0.742 x 0.776 km nadir resolution. Like MODIS, VIIRS views each scene at only one angle per day, and does not measure polarization. These radiances are processed into a variety of products that include information on wildfires, vegetation dynamics, ocean productivity, sea surface temperature, clouds and aerosols.

2.1.1 VIIRS data levels

The VIIRS sensor produces four levels of data. The raw measurements of reflected and thermal radiance are presented as dimensionless "counts" and stored in Raw Data Records (RDRs). The RDRs are processed with calibration and geo-location information, and are presented with engineering units of radiance and quality flags as Sensor Data Records (SDRs). SDRs are used to derive geophysical parameters such as cloud identification and aerosol optical thickness. The geophysical parameter processing occurs in steps. The first step results in an Intermediate Product (IP). The primary use of an IP is by one or more other algorithms within the VIIRS processing environment. Thus, the VIIRS cloud mask (VCM) is an IP used by the aerosol algorithm and many other algorithms to identify the location of the clouds. There is an aerosol IP that is used by other subsequent processing. Some IPs are discarded after use, some are archived and some will be made available to the public. The second step in the geophysical parameter processing is the creation of Environmental Data Records (EDRs). EDRs are created from SDRs, IPs and ancillary data, and are expected to reach different stages of validation in which the uncertainty of the retrieved products are well-characterized.

2.2 VIIRS band characteristics

The narrow band measurements of the VIIRS sensor in the 0.412 to 2.25 μm range are used to derive the aerosol parameters. Other bands are used to create the VIIRS Cloud Mask (VCM), which the aerosol algorithms use as input and in internal tests to characterize surface conditions. The visible and near infrared channels used to derive optical thickness are all within window regions and their bandwidths are narrow. As a result, the contamination of gas (such as O_2, O_3, H_2O) absorption is minimized. Table 2.1 summarizes the VIIRS Moderate Resolution Bands. The "M-bands" denote moderate spatial resolution of 0.742 x 0.776 km at nadir (1.60 x 1.58 km at edge of scan), and the I-bands denote higher resolution (0.371 x 0.387 km at nadir and 0.80 x 0.789 km at edge of scan) imagery bands. The Day-Night Band (DNB) has a broad bandwidth and is used for imagery at night (0.742 x 0.742 km across the entire swath). The aerosol algorithms use the following bands: M1, M2, M3, M5, M6, M7, M8, M10 and M11 to derive aerosol, and M4, M9, M12, M15 and M16 as part of internal screening tests.

Table 2.1 VIIRS band characteristics

Band name	Wavelength (μm)	Bandwidth (μm)	Nadir horizontal	End of scan horizontal	Use in aerosol algorithm

			resolution (km) Downtrack x crosstrack	resolution (km) Downtrack x crosstrack	
M1	0.412	0.020	0.742 x 0.776	1.60 x 1.58	Inversion over land
M2	0.444	0.014	0.742 x 0.776	1.60 x 1.58	Inversion over land
M3	0.486	0.019	0.742 x 0.776	1.60 x 1.58	Inversion over land; internal tests land and ocean
M4	0.551	0.021	0.742 x 0.776	1.60 x 1.58	Internal tests ocean
I1	0.638	0.082	0.371 x 0.387	0.80 x 0.789	
M5	0.672	0.020	0.742 x 0.776	1.60 x 1.58	Inversion over land and ocean; internal tests land
M6	0.745	0.015	0.742 x 0.776	1.60 x 1.58	Inversion over ocean
I2	0.862	0.039	0.371 x 0.387	0.80 x 0.789	
M7	0.862	0.039	0.742 x 0.776	1.60 x 1.58	Inversion over ocean; internal tests land
DNB	0.7	0.4	0.742 x 0.742	0.742 x 0.742	
M8	1.238	0.027	0.742 x 0.776	1.60 x 1.58	Inversion over ocean; internal tests land and ocean
M9	1.375	0.015	0.742 x 0.776	1.60 x 1.58	Internal tests land
I3	1.61	0.06	0.371 x 0.387	0.80 x 0.789	
M10	1.600	0.059	0.742 x 0.776	1.60 x 1.58	Inversion over ocean; internal tests land and ocean
M11	2.257	0.047	0.742 x 0.776	1.60 x 1.58	Inversion over land and ocean;

					internal tests land and ocean
I4	3.743	0.387	0.371 x 0.387	0.80 x 0.789	
M12	3.697	0.191	0.742 x 0.776	1.60 x 1.58	Internal tests land
M13	4.067	0.163	0.742 x 0.776	1.60 x 1.58	
M14	8.578	0.323	0.742 x 0.776	1.60 x 1.58	
M15	10.729	0.989	0.742 x 0.776	1.60 x 1.58	Internal tests land and ocean
I5	11.501	1.880	0.371 x 0.387	0.80 x 0.789	
M16	11.845	0.864	0.742 x 0.776	1.60 x 1.58	Internal tests land and ocean

2.3 Aerosol retrieval strategies

There has been a progression of retrieving aerosol optical thickness and other aerosol products from reflected solar radiance in the visible and near-IR bands, measured by satellite, beginning in the 1970s. Retrievals were made initially with the Multispectral Sensor (MSS) and Thematic Mapper (TM) on board the Landsat series of satellites (Griggs, 1975; Fraser, 1976; Mekler et al., 1977), then from the Advanced Very High Resolution Radiometer (AVHRR) on board NOAA's Polar Orbiting Environmental Satellites (POES) (Rao et al., 1989; Stowe et al.,1990, 1997, Higurashi and Nakajima, 1999; Geogdzhayev, and Mishchenko et al.,1999) and most recently using the Earth Observing System (EOS) era satellite sensors. The EOS-era satellite sensors in this category include the MODerate resolution Imaging Spectroradiometer (MODIS) (Remer et al., 2005; Levy et al. 2007), the Multi-angle Imaging SpectroRadiometer (MISR) (Diner et al., 1998; Kahn et al., 2010) and the POLarization and Directionality of the Earth's Reflectances (POLDER) (Tanré et al., 2011). Of these three sensors, MODIS with its broad spectral range, single angle look at each target and lack of polarization measurements is the closest in design to VIIRS. The aerosol retrieval algorithms of these heritage sensors match satellite-measured radiances to pre-computed values in Look-Up Tables. The aerosol retrieval algorithms were originally applied only over ocean and then over dark land targets to minimize uncertainties introduced from separating the atmospheric component from the land surface component in the measured reflectance received at satellite. Multiple wavelengths were used together to extend to over brighter land surfaces and to extract information on particle size as well as the AOT for aerosol loading. When multiple angles and/or polarization capabilities were added to the sensor design (MISR and POLDER), more information on particle properties became possible.

MODIS is also a cross-track scanning radiometer with a similar wide spectral range and narrow bandwidths as VIIRS. The MODIS aerosol product is produced over both ocean and land, with the

ocean products including both spectral AOT and several aerosol particle size parameters (APSP) including two Ångström exponents at different parts of the spectrum to identify curvature on the AOT-wavelength log-log plot (Section 1.2). Over land, the publicly available MODIS aerosol product includes only AOT. There are other MODIS aerosol algorithms that do not produce a public aerosol product, but instead produce an intermediate product that is used in the atmospheric correction to obtain surface reflectance values over land and over ocean. The surface products are publicly available, even though the aerosol information used to obtain those products are not. MODIS aerosol and surface products have a 13-year post-launch history. They have well-characterized uncertainties and are widely used throughout the community. Because of the similarities between the sensors and MODIS's long history in the aerosol community, the VIIRS aerosol algorithms are based on the MODIS heritage.

An approach similar to MODIS, but with a higher spatial resolution product, is applied to VIIRS. Reflected spectral solar reflectances measured by a satellite sensor in well-selected multiple channels of visible and near-IR are used to derive the aerosol optical thickness and size parameter simultaneously over land and ocean. The core of the approach is to use Look-Up Tables (LUTs), which are pre-computed for multiple values of the AOT and multiple aerosol models by using sophisticated radiation transfer models (such as Second Simulation of the Satellite Signal in the Solar Spectrum [Vermote et al., 1997a; Kotchenova et al., 2006]). The measured spectral reflectances in several channels are compared with the reflectances computed using the values of atmospheric parameters stored in the LUTs and surface parameters computed within the AOT code to identify the best solution for both AOT and the set of intrinsic aerosol optical properties called the *aerosol model*.

2.3.1 Aerosol optical thickness retrievals over water

The relatively homogeneous surface of the ocean enables the direct application of the LUT approach to find the aerosol optical thickness and size distribution. The observed reflectances at the top of the atmosphere (TOA) are inverted using the LUTs and the surface Bidirectional Reflectance Distribution Function (BRDF) computed as a function of wind speed and wind direction to find a preliminary value of optical thickness for each candidate aerosol model. Ancillary information on the total column water vapor and ozone are input and used to correct for species absorption in the inversion. The solution exhibiting minimum residual is the best fit to the observations, and its corresponding AOT is the retrieved value. The aerosol models (sets of intrinsic aerosol properties) used over ocean are dynamic. There are separate models for an aerosol fine mode, approximately submicron-sized particles, and an aerosol coarse model, approximately supermicron-sized particles. A single fine mode and a single coarse mode may be combined with any relative weight between them to form the dynamic aerosol model. This method is based on MODIS heritage and is a direct adaptation of the algorithm developed by Tanré et al. (1999). Details are described in Section 3.3.

2.3.2 Aerosol optical thickness retrievals over land

Over land retrievals are more challenging due to brighter and more variable surface conditions (i.e., noisier inversion conditions). The algorithm constrains the surface conditions for aerosol retrieval by assuming spectral relationships between specific VIIRS channels. The spectral relationships in the form of simple ratios are applied globally to all dark surfaces, for all seasons, and the surface is currently assumed to be Lambertian. Future versions of the retrieval may introduce a non-Lambertian surface to the retrieval. The aerosol models over land are limited to a set of five static models, determined from spectral radiance measurements. The VIIRS aerosol land algorithm is based on the MODIS atmospheric correction heritage (Vermote et al., 1997b; Vermote et al., 2002; Kotchenova et al. 2006), which deviates from the algorithm producing publicly available AOT over land. Surface reflectance, aerosol optical thickness, and aerosol model are solved simultaneously based on the expected spectral albedo ratios of vegetated surfaces derived from atmospheric correction using AERONET data and a limited set of 5 static aerosol models. A priori assumptions of spectral albedo ratio and limitations in model freedom are necessary given the number of free parameters and inherently noisier retrieval. Details are described in Section 3.4.

2.3.3 Aerosol Size Parameter Retrievals

The aerosol models producing the least residual when compared with VIIRS-measured spectral radiances define the spectral dependence of the AOT. There is information about particle size in the AOT spectral dependence and the Ångström Exponent can be calculated from the optical thicknesses in two channels (Eq. (1.3)). The band pairs used for the Ångström Exponent retrieval are M2 (445 nm) and M5 (672 nm) over land, and M7 (865 nm) and M10 (1610 nm) over ocean. Other size parameters can be determined from this retrieved spectral dependence. Particle effective radius is one such parameter, but it is not derived or reported at this time.

2.3.4 Suspended Matter retrievals

The suspended matter product is a simple classification of the aerosol into particle type: volcanic ash, dust, smoke, sea salt, undetermined and none. The procedure uses the results of the retrievals to separate between these aerosol types. Over land, the retrieval returns the aerosol model that best fits the spectral radiances. When this retrieved model is dust, the suspended matter product identifies dust. When it is smoke, suspended matter is smoke. If none of these, then the return is undetermined. Over ocean the dust category is determined for retrievals with small fine mode fraction and relatively high AOT. Small fine mode fraction and a more moderate AOT will return sea salt. The smoke category represents both smoke and pollution, basically particles emitted as a result of combustion processes. The smoke category is determined for high fine mode fraction. The undetermined category, over ocean, is for any aerosol with at least moderate loading, but with ambiguous fine mode fraction. The volcanic ash category is identified by the VIIRS cloud mask, an input to the aerosol algorithm. The aerosol algorithm simply repackages the information and outputs it as part of the aerosol algorithm.

3.0 ALGORITHM DESCRIPTION

The aerosol algorithm uses data from VIIRS and from outside sources. The Read Input Module reads in the ancillary data that have been pre-processed by the Gridding module and readies the data for use by the aerosol module. The input data not directly used by the module for the aerosol optical thickness, size parameter or suspended matter calculation are used for pixel selection. Section 3.1 describes the inputs to the aerosol algorithm.

Over both ocean and land, the top-of-atmosphere radiance received by the satellite is a combination of contributions from two sources: the atmospheric path radiance and the contribution from the surface (including coupling between the surface and atmosphere). The algorithms to derive aerosol information from VIIRS measurements require modeling the radiation received by the satellite from these two sources as a function of the aerosol contribution. Common to both ocean and land is the need to account for contributions and modifications of the radiance in its path from sun-to-surface-to-satellite, caused by non-aerosol constituents of the atmosphere. These non-aerosol components of the model include absorbing gases and molecular (Rayleigh) scattering. The details of the algorithm's handling of gaseous absorption and molecular scattering are described in Section 3.2.

Aerosol retrievals are made only in non-cloudy daytime conditions over dark surfaces. Snow/ice, water with suspended sediments and strong sunglint are considered to be bright surfaces, along with surfaces of bare soil, rock or senescent vegetation. The VIIRS Cloud Mask IP provides information on cloud cover, land/water, snow/ice, fire and sunglint in each pixel. The aerosol algorithm uses the cloud confidence, cloud shadow, fire, snow/ice, land/water flag, adjacent pixel cloud confidence and cirrus detected bits from the VIIRS Cloud Mask. The land/water flag is used to determine which optical thickness retrieval method to employ since land and oceans each have different methods of retrieval. The other cloud mask information is used in conjunction with procedures internal to the aerosol algorithm to avoid clouds, strong sunglint, snow/ice and fire etc. The VIIRS Cloud Mask IP is produced by a standard VIIRS algorithm with its own ATBD and User's Manual, and the reader is directed to those documents for further information on that product. Any pixel that is identified with these bright conditions or with clouds is not used in the aerosol retrieval, and is flagged as "not produced". Pixel selection for retrieval and the masking of inappropriate situations is a fundamental part of any aerosol retrieval. Here the masking is tailored specifically for either ocean or land procedures, and will be described in Sections 3.3.1 and 3.4.1, respectively.

For the aerosol products "cloudy" has been defined as any cloud cover within a pixel. The definition of "daytime" has been established to be solar zenith angles less than 65^{o}. "Extended daytime" (solar zenith angles between 65^{o} and 80^{o}) pixels are processed identical to "daytime" but are flagged to indicate their illumination state and suspect quality. "Twilight" (solar zenith angles between 80^{o} and 85^{o}) pixels are either assigned values from the Navy Aerosol Analysis and Prediction System (NAAPS) model or climatology, or use interpolation from surrounding pixels. Night pixels are filled with data either from climatology or from NAAPS, and flagged as high quality, even if no actual retrieval is performed.

Over the ocean, the surface is relatively homogeneous and the surface reflectance is relatively constant. A lookup table accounting for multiple scattering in the atmosphere by molecules and aerosol particles is used along with the known reflectance of the ocean surface to calculate the aerosol optical depth. The water-leaving radiance is dependent upon the chlorophyll content, or ocean color, and the turbidity. Because the water leaving radiance is small in the red, near infrared (NIR) and shortwave infrared (SWIR) channels are used in the ocean inversion and constant value of chlorophyll can be used without much error contribution. This is not true for turbid water; therefore, no retrieval is performed over water with significant turbidity. In rough seas, sea foam and whitecaps can reflect additional sunlight; therefore, the whitecap coverage is calculated as a function of wind speed. Sunglint is an additional contributor to the TOA radiance and is calculated using the Cox and Munk (1954) model. In areas of significant sunglint, the optical thickness is not calculated since the sunglint depends on wind speed and direction, which are not precisely known. The aerosol retrieval over ocean is described in detail in Section 3.3.

Over the land, the surface albedo varies with wavelength and surface type. Areas of dark, dense vegetation have a low reflectance in the red and blue bands. Aerosols will make these regions appear brighter because they scatter the light as it travels back to the sensor from the surface. In the SWIR, the wavelength of the radiation is too long to be affected by this scattering by most particle types, and thus, provides a more accurate representation of the surface. Previous work by Kaufman et al. (1997) for MODIS has established a relationship between the surface reflectances in the SWIR, specifically the MODIS 2.13 μm band, and in the red and blue bands. This statistical relationship is used to constrain surface reflectance in the visible range using the measured reflectance in the SWIR. VIIRS builds on this empirical work to assume ratios between surface reflectance of several different wavelengths. A process of elimination finds regions dark enough for these relationships to hold. A pixel must meet a series of criteria in order to be considered dark, thus preventing bright pixel (e.g., snow and sand) selection. The aerosol retrieval over land is described in Section 3.4.

Figure 3.1 is a flowchart schematic of the logic that governs the overall processing, pixel by pixel, and how each pixel is checked for specific conditions and how quality flags are set.

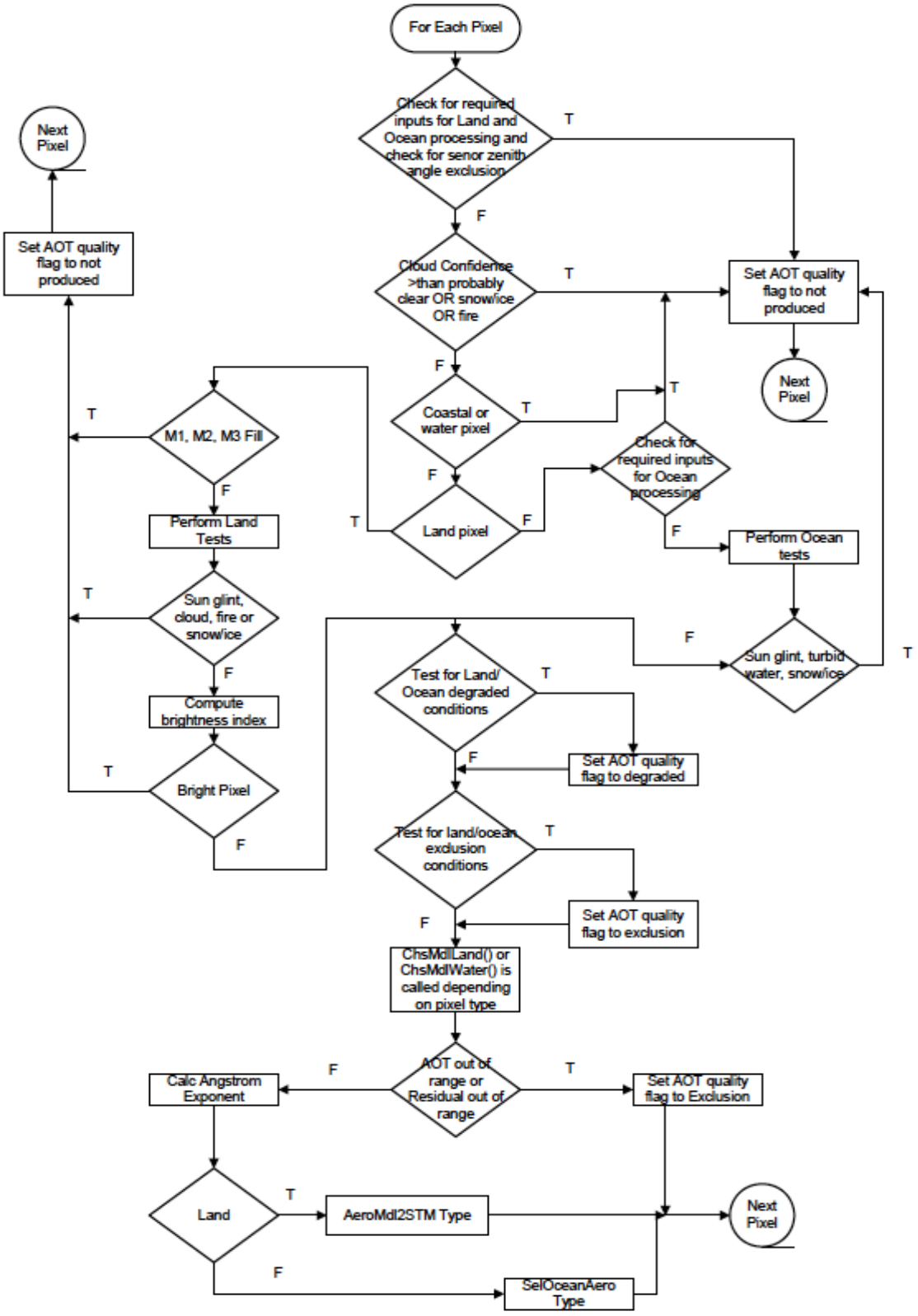

Figure 3.1 Flowchart describing overall logic of retrieval algorithm and how quality flags are set at each decision point.

The aerosol atmospheric LUT contains pre-computed values of the atmospheric components of top-of-atmosphere (TOA) reflectance vs. AOT and aerosol model spanning the envelope of viewing and illumination geometries. The algorithm simply brackets the observed TOA reflectance with the TOA reflectance calculated from the viewing geometry interpolated LUT parameters (i.e., searches for the closest values, both larger and smaller than observed, within the LUT) and interpolates on the corresponding AOT values. AOT retrievals are performed for each aerosol model (i.e., 5 for land and 20 for ocean). The optimal model is the one for which the residual is minimized. The residual is defined as the sum of the squares of the differences between observed and calculated reflectances for all VIIRS bands used in the model determination. Over-Land and Over-Ocean processing differs with respect to the aerosol models used and the surface reflectance calculation. For ocean processing there is a separate aerosol sun glint LUT, which is used to compute the effect of the ocean BRDF on light scattered by the atmosphere. As noted previously, the direct sun glint contribution is computed analytically.

3.1 Algorithm Input

The algorithm requires VIIRS Sensor Data Records (SDRs) for bands M1, M2, M3, M5, M6, M7, M8, M10 and M11 that contain VIIRS-measured calibrated and geo-located reflectances. These reflectances are used directly to retrieve the aerosol information and also for pixel selection. Additional data used by the algorithm for pixel selection comes from other VIIRS products, most commonly the VIIRS Cloud Mask IP, but also from additional VIIRS SDRs not used directly for aerosol retrieval (M4, M9, M12, M15, and M16). Because the reflectance measured at satellite is affected by atmospheric constituents other than aerosols, the effects of these other constituents: absorbing and scattering gases, must be calculated and included in the inversion. To calculate the transmission of the absorbing gases (water vapor, ozone and other gases) and the reflectance of molecular (Rayleigh) scattering, ancillary information on total column concentrations of the gaseous absorbers, and elevation and surface pressure for the molecular scattering is required. Ancillary information is also needed to choose between the land or ocean algorithm, and to avoid clouds, sunglint, snow/ice, turbid water and bright land surfaces. Some of the ancillary information comes from outside sources, most often from the National Center for Environmental Prediction (NCEP) model. If NCEP model data is not available, back-up options include the Fleet Numerical Modeling Ocean Center (FNMOC) Navy Operational Global Atmospheric Prediction System (NOGAPS) model data or climatology.

Table 3.1 summarizes the VIIRS-derived data sets ingested by the VIIRS aerosol algorithms and used to derive the aerosol products. Just because an ancillary data set is used in a masking procedure within the algorithm, it does not mean that the masking is solely dependent on that ancillary data set. There are several internal procedures that rely on the basic set of VIIRS calibrated radiances to mask clouds, sunglint, snow, etc. without ancillary data. These procedures are described in Sections 3.3.1 and 3.4.1 where the retrievals over ocean and land are described.

A “SDR” denotes a “Sensor Data Record”, which is a VIIRS observation at satellite-level after calibration is applied and the observation is geo-located. An SDR carries with it information on

latitude, location, elevation and the solar-satellite geometry of each pixel, in addition to the reflectance. An "IP" denotes an "Intermediate Product". This is a basic pixel level retrieval. The aerosol IP product will be both archived and publicly released. See Section 2.1.1 for further clarification. "NCEP" is the National Center for Environmental Prediction. NAAPS is the Navy Aerosol Analysis and Prediction System. The use of the NAAPS model data as a gap filler in the aerosol product is explained in Section 3.7.1.

Table 3.1 Algorithm inputs

Input Data	Source of Data	Use in aerosol algorithm
Calibrated reflectances	VIIRS calibrated TOA reflectance SDR for bands M1,M2, M3, M5, M6, M7, M8, M10 and M11	• Matching LUT values for aerosol retrieval. • Some bands are also used in masking and pixel selection.
	VIIRS calibrated TOA reflectance SDR for bands M4 and M9	Internal tests, masking and pixel selection (turbid/shallow water, cirrus cloud)
Solar, zenith and azimuth angles	Included in the VIIRS calibrated TOA reflectance SDR as part of the geolocation	Indexing the LUT for matching the VIIRS values for aerosol retrieval.
Sensor geometry	Included in the VIIRS calibrated TOA reflectance SDR as part of the geolocation	Indexing the LUT for matching the VIIRS values for aerosol retrieval.
Ozone concentration (atm-cm)	Pre-processed to VIIRS 0.75 km resolution, originates from NCEP (50 km spatial resolution)	Gaseous transmission for ozone
Total precipitable water (cm)	Pre-processed to VIIRS 0.75 km resolution, originates from NCEP (50 km spatial resolution)	Gaseous transmission for water vapor
Surface pressure (hPa)	Pre-processed to VIIRS 0.75 km resolution, originates from NCEP (50 km spatial resolution)	• Molecular reflectance • Gaseous transmission for other gases than ozone and water vapor
750 m digital elevation (m)	Included in the VIIRS calibrated TOA reflectance SDR as part of the geolocation	Molecular reflectance
Land/Water Information	VIIRS Cloud Mask IP	Directs algorithm to either land or ocean procedure
Cloud Information	• VIIRS Cloud Mask IP	Cloud identification and

	• VIIRS calibrated TOA reflectance SDR for band M9	avoidance
Heavy aerosol flag	• VIIRS Cloud Mask IP	Identifies situation identified as cloud by the VCM but is likely retrievable as aerosol
Sunglint Information	VIIRS Cloud Mask IP	Sunglint avoidance over ocean
Wind speed (m/s)	Pre-processed to VIIRS 0.75 km resolution, originates from NCEP (50 km spatial resolution)	• Sunglint avoidance over ocean and land • Sea foam model for water leaving radiance
Wind direction (degrees from North)	Pre-processed to VIIRS 0.75 km resolution, originates from NCEP (50 km spatial resolution)	Sunglint avoidance over ocean
Fire information	VIIRS Cloud Mask IP	• Sunglint avoidance over land • Fire avoidance over land
Snow/Ice Information	VIIRS Cloud Mask IP	Snow/ice avoidance over ocean and land
2 m Surface air temperature (^{o}K)	NCEP	• Snow/ice avoidance • Sunglint avoidance over land
Calibrated brightness temperatures	VIIRS calibrated brightness temperature (SDR for band M12, M15 and M16)	• Snow/ice avoidance • Sunglint avoidance over land
Volcanic ash information	VIIRS Cloud Mask IP	Suspended matter product
AOT gap filler data	NAAPS	Provides AOT values for all pixels not retrieved by the aerosol algorithm. Aerosol IP only.

3.2 Calculation of gaseous absorption and molecular reflectance

In the core of the inversion, over both ocean and land, the reflectance at the top of the atmosphere is modeled as a function of reflectance from the surface, molecules and aerosols that has been attenuated by absorption from gases. The retrieval inverts this model to arrive at the aerosol component of the top of atmosphere reflectance. The procedure requires that all other constituents in the model, specifically the gaseous transmission and the molecular (Rayleigh) reflectance, be well-defined, with only the aerosol component acting as a free variable. Here we define the parameters that are required by the governing equations for both the ocean and land retrieval, Eqs. (3.12) and (3.23), respectively. Parameters required specifically for ocean are described in Section 3.3, and for land in Section 3.4.

3.2.1 Calculation of gaseous absorption

The VIIRS bands were designed to avoid most of the gaseous absorption in the atmosphere. Figure 3.2 shows the bandwidths of both the moderate resolution, "M-bands" and imagery resolution, "I-bands", above the atmospheric transmission function for a Mid-Latitude Summer atmosphere. Significant absorption bands of various absorbing gases are noted in the figure. Clearly the VIIRS reflectances will be minimally affected by absorption, except for M9, which is used for cloud identification, not the aerosol retrieval directly. We note the placement of band M11 at 2.25 μm, rather than where MODIS' comparable band is located (2.13 μm), avoids much of the necessary water vapor correction required by MODIS. However, ozone absorption in the Chappius bands will affect reflectance in the visible region, and water vapor and other gases will also have a small effect on the retrieval.

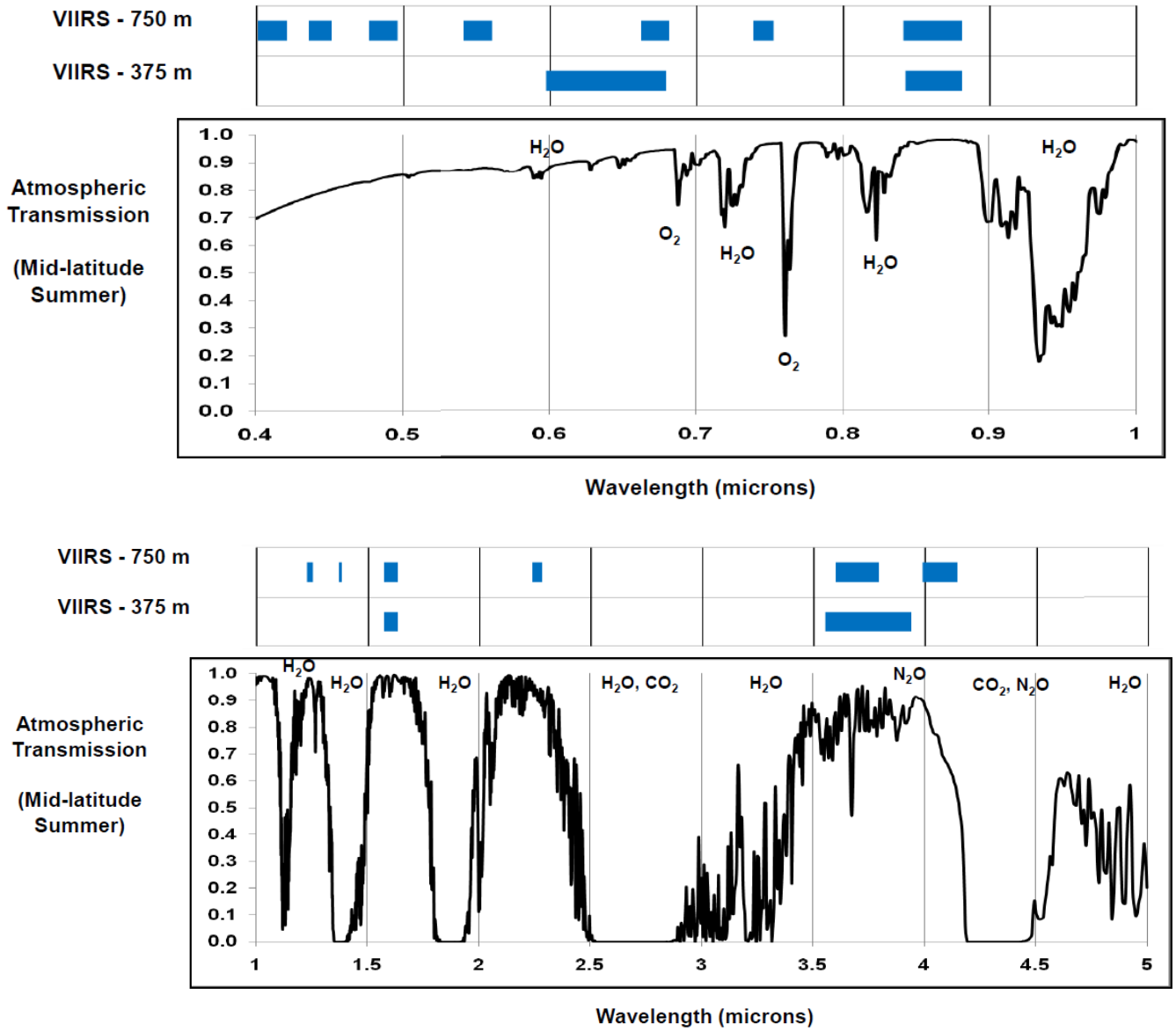

Figure 3.2 VIIRS spectral coverage (from Guenther et al., Performance Continuity of the A-Train MODIS Observations: Welcome to the NPP VIIRS, poster presentation available at http://www.star.nesdis.noaa.gov/jpss/documents/meetings/2011/AMS_Seattle_2011/Poster/A-TRAIN%20%20Perf%20Cont%20%20MODIS%20Observa%20-%20Guenther%20-%20WPNB.pdf

For each type of gaseous absorption: ozone, water vapor and constant gas species, the transmission function is given as an empirical fitting based on running a radiative transfer code forward for a wide variety of geometrical situations between the sun and satellite sensor, and a wide variety of absorber amounts. Then fitting the resulting transmissions as an empirical relationship based on the air mass, M, (defined in Eq. (3.2) below) and the absorber amount. The 6S radiative transfer code was used for these calculations. The calculation was done for 10 of the

11 VIIRS solar reflectance bands, with the central wavelengths of each band given in APPENDIX A. The bandwidths for each band were calculated from pre-launch test measurements of the relative spectral response.

3.2.1.1 Ozone transmission (Tg_{O3}^{λ})

The total column amount of ozone is required by the aerosol algorithm in order to calculate the ozone transmission functions. Ozone column concentrations vary slowly both in time and space around the globe, but concentrations do vary. Because of this, calculations of global daily ozone concentrations are obtained from NCEP Global Forecast System (GFS) model system, which is provided at a spatial resolution of half a degree. This is much larger than the input reflectance resolution of 0.742 x 0.259 km or of the VIIRS EDR product spatial resolution of approximately 6 km at nadir. However, ozone varies more slowly over distance than does aerosol, making this spatial resolution discrepancy unimportant. The NCEP ozone product is a 3-hr output from the Global Forecast System. The ozone field from forecast output is interpolated to VIIRS observation time. If the NCEP product is unavailable, the Fleet Numerical Modeling Ocean Center (FNMOC) Navy Operational Global Atmospheric Prediction System (NOGAPS) model data (http://www.usno.navy.mil/FNMOC/fnmoc) can be used as a substitute. An accuracy of 0.015 atm-cm will provide adequate ozone input for the correction.

Once the total column ozone concentration, (U_{03}), is obtained in units of atm-cm, the transmission function (Tg_{03}) for each band (λ) is calculated from,

$$T_{gO3}^{\lambda}(M, U_{O3}) = \exp\left(-M\, a_{O3}^{\lambda} U_{O3}\right) \tag{3.1}$$

where M is the air mass defined as

$$M = \frac{1}{\cos\theta_0} + \frac{1}{\cos\theta_S} \tag{3.2}$$

θ_o is the solar zenith angle and θ_s is the sensor zenith angle. The constants a_{03} are the absorption coefficients, and are functions of wavelength band, given by Kneizys et al., (1980). APPENDIX A lists the coefficients for Eq. (3.1) for each of the 11 wavelengths used.

3.2.1.2 Water vapor transmission (Tg_{H2O}^{λ})

Even though the VIIRS bands were chosen in spectral window regions to avoid most of the water vapor in the atmosphere, a residual correction is necessary. In contrast to column ozone concentrations, total column water vapor concentrations, called total precipitable water vapor, vary rapidly both in time and space. Thus, ancillary data giving water vapor concentrations is required. NCEP model data provides the primary source for this parameter. Once the total column

water vapor concentration in units of g/cm^2 = cm (U_{H2O}), is obtained, the transmission function (Tg_{H2O}) for each band (λ) is calculated from,

$$T_{gH2O}^{\lambda}(M,U_{H2O}) = \exp\left[\begin{array}{r} M\, a_{H2O}^{\lambda} U_{H2O} + b_{H2O}^{\lambda} \ln(MU_{H2O}) \\ + c_{H2O}^{\lambda}\, MU_{H2O} \ln(MU_{H2O}) \end{array}\right] \quad (3.3)$$

where M is the air mass defined in Eq. (3.2). The constants, a_{H2O}, b_{H2O} and c_{H2O} are functions of wavelength, and are given in APPENDIX A.

3.2.1.3 Transmission of other gases (Tg_{OG}^{λ})

The other absorbing gases in the atmosphere included in the aerosol retrieval are carbon dioxide (CO_2), oxygen (O_2), carbon monoxide (CO), oxides of nitrogen (NOx) and methane (CH_4). These are well-mixed in the atmosphere and do not vary temporally or spatially. Computing their transmission function does not require ancillary data sets that explicitly provide their concentrations. Instead their transmission functions are linked to the amount of atmosphere traversed by the incoming and outgoing light, which is quantified by the air mass, M, and scaled atmospheric pressure, P. The transmission of other gases (Tg_{OG}) is given by,

$$T_{g_{OG}}^{\lambda}(M,P) = \exp\left[\begin{array}{r} M\left(a_0^{\lambda} P + a_1^{\lambda} \ln(P)\right) + \ln(M)\left(b_0^{\lambda} P + b_1^{\lambda} \ln(P)\right) \\ + M \ln(M)\left(c_0^{\lambda} P + c_1^{\lambda} \ln(P)\right) \end{array}\right] \quad (3.4)$$

a_0, a_1, b_0, b_1, c_0 *and* c_1 are constants for each wavelength band and are given in APPENDIX A. M is the air mass defined by Eq. (3.2). Note $P = P_{sfc}/P_0$ where P_0 = 1013 mb, and P_{sfc} is the surface pressure obtained from NCEP. P = 1 is standard pressure where all of the *ln(P)* terms are zero. So, Eq. (3.4) can be approximated as,

$$T_{g_{OG}}^{\lambda}(M,P) = \exp\left[M\, a_0^{\lambda} P + b_0^{\lambda}\, P \ln(M) + c_0^{\lambda}\, PM \ln(M)\right] \quad (3.5)$$

3.2.2 Molecular (Rayleigh) reflectance and transmission

The molecular reflectance and transmission are functions of the amount of molecules traversed by the incoming and outgoing light, which is dependent on the sun-satellite geometry (θ_o, θ_s, ϕ) and the atmospheric pressure of the surface target (P). In the VIIRS aerosol algorithm, the molecular reflectance at standard pressure, $\rho_R^{\lambda}(\theta_o, \theta_s, \phi, P_o)$ is calculated based on the simplification of Vermote and Tanré (1992), and depends on a pre-computed molecular (Rayleigh) optical thickness τ_R^{λ}, calculated for a standard atmospheric pressure (P_o). The pre-computed τ_R^{λ} are given in APPENDIX A and their calculation is described in the 6S manual under the subroutine,

ODRAYL and references therein. The adjustment for actual pressure, *P*, to obtain the molecular reflectance for the actual pressure, $\rho_R^\lambda(\theta_o, \theta_s, \phi, P)$, is done by adjusting the molecular optical thickness,

$$\tau_R^\lambda(P) = P\,\tau_R^\lambda \tag{3.6}$$

where *P* is the normalized surface pressure, P_{sfc}/P_0. Note the wavelength dependence of the molecular reflectance and molecular optical thickness. Molecular scattering has a strong spectral signature, which requires accurate spectral registration of the VIIRS bands to maintain a high accuracy in the aerosol retrieval.

The molecular (Rayleigh) transmission at standard pressure based on the two-stream approximation is,

$$T_R^\lambda(\theta, P_0) = \frac{\left[\frac{2}{3} + \cos\theta\right] + \left[\frac{2}{3} - \cos\theta\right] e^{-\tau_R^\lambda/\cos\theta}}{\frac{4}{3} + \tau_R^\lambda} \tag{3.7}$$

where θ denotes the solar zenith angle (θ_o), the sensor zenith angle (θ_s) or both, depending on the path traversed. The molecular transmission at actual pressure, $T_R^\lambda(\theta, P)$, is calculated from Eq. (3.7) using the pressure-adjusted molecular optical thickness (Eq. (3.6)).

Because the molecular reflectance and transmission depend on surface atmospheric pressure, which can vary over small spatial scales in a complex terrain, the 50 km NCEP surface pressure is pre-processed to VIIRS resolution outside of the aerosol algorithm and input at nominally 0.75 km resolution as one of the algorithm's inputs. The pre-processed surface correction is performed as,

$$P_{pixel} = P_{model}\,\frac{e^{-H_{digital}/8.24}}{e^{-H_{model}/8.24}} \tag{3.8}$$

where P_{pixel} and P_{model} are actual pixel-level and model surface pressures; $H_{digital}$ and H_{model} are high-resolution digital and low-resolution model surface elevations, respectively. A constant scale height of 8.24 km is assumed in this pressure correction.

3.3 Theoretical Description of Aerosol Retrievals over Ocean

The retrieval of the aerosol properties over ocean is a direct adaptation of the algorithm developed by Tanré et al. (1999). The algorithm uses VIIRS-measured radiances in 6 bands, (M5, M6, M7, M8, M10 and M11), in the wavelength range 0.672 to 2.25 μm. The strategy is to retrieve aerosol optical thickness and an aerosol model consisting of one fine mode and one coarse mode.

The retrieval is sensitive to two pieces of information: namely the aerosol loading in one wavelength and the relative contribution of each mode to the total AOT. When one mode clearly dominates the signal, then the effective radius of that dominant mode can sometimes be retrieved. There are 4 possible small-mode models, 5 possible large-mode models and 101 different fractional amounts of each pair are possible. The procedure (1) selects the appropriate pixels for retrieval, (2) uses pre-calculated parameters for gaseous transmission and molecular scattering (Section 3.2), (3) matches the spectral top-of-atmosphere spectral radiances measured by VIIRS with the pre-calculated values in a Look-Up Table (LUT) for each combination of possible fine mode and coarse mode, and for each possible fraction of each of the 20 pairs of modes. There are 2020 possibilities in all. In the following subsections the pixel selection process, the possible aerosol mode models, surface models and inversion procedure are described in detail.

3.3.1 Selection Process for Appropriate Pixels for Aerosol Retrieval Over Ocean

The ocean algorithm is designed to retrieve aerosol properties over a well-characterized ocean surface. Any obstruction to that surface, such as a cloud, or any ocean condition that is difficult to characterize such as strong sun glint or suspended sediments in the water, are avoided by the algorithm. Pixels that are identified as having adverse conditions for aerosol retrieval are not processed and flagged as such. The algorithm bases its decision on whether or not to process the pixel by using information supplied from the VIIRS cloud mask, one of the algorithm's inputs, in conjunction with internal tests within the ocean procedure of the aerosol algorithm. Some of these internal procedures, such as the sun glint calculation, require ancillary data.

3.3.1.1 Cloud avoidance

The aerosol algorithms are designed to work only in cloud-free conditions; thus, cloudy pixels must be identified so that the algorithm avoids making a retrieval in unacceptable conditions. The problem is that often the cloudiness condition of a pixel is ambiguous, especially when clouds cover only a portion of the pixel. The VIIRS cloud mask (VCM) is an independent VIIRS IP product that has been designed, implemented and tested to identify clouds for a variety of purposes employed by other VIIRS algorithms within the processing environment (VCM ATBD, released 2013). The cloud mask is based on a cascade of threshold, spectral and spatial variability tests covering the wide spectrum of the VIIRS radiances from the visible to the thermal infrared.

When some algorithms, such as aerosol, need partially-cloudy pixels marked as "cloudy", and other algorithms, such as cloud retrieval algorithms, need partially-cloudy pixels marked as "clear", a binary "yes/no" cloud mask is impossible. For this reason, the VIIRS cloud mask returns an array of flags, each indicating a different level of confidence in the cloudiness of a specific pixel and also offering a variety of other important information about that pixel. There are four levels of confidence: Confidently Cloudy, Probably Cloudy, Probably Clear and Confidently Clear. The aerosol algorithm ingests these data, uses them to decide whether or not to retrieve, and then if retrieving uses them again to assess the quality of the aerosol retrieval and probability of cloud contamination in the retrieval.

Heavy aerosol flag from VCM

In addition to the four level designation of confidence in the cloudiness of each pixel, the VCM offers a list of other information about that pixel in the form of binary flags. An important VCM flag for the aerosol algorithm is the "heavy aerosol flag" (VCM ATBD released 2013). This flag uses spectral information in the form of ratios of measured reflectance and spatial variability to call back pixels already designated as Confidently Cloudy and mark them as appropriate for an aerosol retrieval. Such is the case for heavy aerosols that sufficiently brighten the background to trigger visible cloud tests. The logic used by the heavy aerosol test in the VCM is as follows.

For day time, confidently cloudy pixels that are not snow or ice, over land all liquid phase clouds are marked as possible candidates for heavy aerosol. Over ocean a spectral test applied to liquid phase clouds identifies candidates for heavy aerosol. If M1/M5<2.0 and M1<0.3, the pixel is identified as candidate for dust. If M11/M1< a specified threshold, which varies with scan angle, the pixel is identified as candidate for smoke.

The next step tests the spatial variability of the candidate pixels using the standard deviation of reflectance of the 0.65 μm I-band in a 1.5 x 1.5 km^2 area. Because these are I-band pixels there are 16 pixels in this area. If there is only one candidate pixel in the area, that pixel is assumed to be a cloud edge and no heavy aerosol flag is set.

If there are at least two pixels identified as candidates in that area, over ocean, those candidate pixels are set as heavy aerosol if the standard deviation is less than 0.01. If the standard deviation exceeds 0.01, those pixels are set as liquid clouds. Over land, if NDVI > 0.3 and the standard deviation is less than or equal to 0.02, the pixels are heavy aerosol; otherwise, they are liquid phase cloud.

Volcanic ash logic for ocean and land are then performed. The pixel is set to heavy aerosol if the volcanic ash is detected.

The aerosol algorithm will attempt a retrieval on all Confidently Clear and Probably Clear pixels, or on any pixel with a positive heavy aerosol flag, regardless of the cloudiness of the pixel. Thus the 'heavy aerosol flag' over rides all other cloud masking criteria. Currently the heavy aerosol flag test is applied only to Confidently Cloudy pixels. That is set to change in summer 2013, where it will be applied to both Confidently Cloudy and Probably Cloudy pixels. The change will allow more retrievals of dust plumes in the Atlantic, but introduce noise in cloud fields and partly cloudy conditions. The changes will be under tight scrutiny after implementation and may require tuning or change.

Based on the information in the VIIRS cloud mask and other indicators within the aerosol algorithm itself, quality flags are set within the aerosol algorithm and output with the other aerosol products to specify areas where clouds may contaminate the retrieval. These flags will affect the aggregation procedure in which the aerosol IP product at ~0.75 km at nadir is used to create the aggregated EDR product at ~6 km at nadir. See Section 3.7.2.

Some pixels will be classified as "probably clear" which indicate that there is a possibility of contamination by small clouds. The aerosol algorithm retrieves on these probably clear pixels, producing an IP product, without degradation in any of the IP quality flags. See Appendix C1. The presence of clouds in adjacent pixels will cause a quality flag to be set. The presence of nearby clouds can generate several artifacts in the retrieval of aerosol: (a) mixed pixels probably exist at the border of the cloud and are not detected, (b) shadows may contaminate the pixel and not be properly flagged (c) cloud could generate scattering either by the atmospheric scattering (molecular) or by the instrument. Retrievals flagged as adjacent to clouds should also be used with caution.

An additional thin cirrus check is applied over land using band M9 is performed internally. This allows a more conservative test to be applied for screening thin cirrus than is appropriate for the VIIRS cloud mask.

The description of the cloud avoidance in the processing applies to the over land procedure, as well as the over ocean.

3.3.1.2 Sun glint calculation and avoidance

The aerosol algorithm for over ocean retrieval is not designed to work for pixels in strong sun glint. Therefore sun glint information is needed in order to avoid those pixels affected by glint. There are two sources for this information. Sun glint information is available from the ingested VIIRS Cloud Mask that calculates the glint based on geometry, flagging all pixels within 36^{o} of specular reflection as sun glint. However, the primary source of sun glint information is calculated dynamically inside the aerosol retrieval code using the approach described in 6S (Vermote et al., 1997). This approach accounts for variable wind speed and wind direction, which can affect the spread and intensity of the sun glint pattern, and is not included in the sun glint flag provided by the VIIRS Cloud Mask. The wind speed is used to calculate the Fresnel reflection on the sea surface using the Cox and Munk (1954) rough ocean model. The surface wind speed and direction are ingested as ancillary data obtained from NCEP. The threshold for the sun glint mask is 3% of the value of the reflectance corrected for gaseous absorption and molecular scattering observed at 1.24 μm. Calculated values of sun glint below 3% of the corrected observed 1.24 μm reflectance value will be used in the aerosol retrieval. Values above that value will not be used. In the case where the VIIRS Cloud Mask identifies a broader sun glint exclusion region than the internal test, this broader exclusion region shall supersede the narrower internal calculation. Thus, 36^{o} from specular reflection constitutes the minimum possible extent of the sunglint mask.

3.3.1.3 Sea ice avoidance

The primary method for the over ocean procedure to identify sea ice pixels is through the information provided in the VIIRS cloud mask (VCM ATBD released 2013). Additionally the split window surface temperature is used to identify scenes that are likely to be ice. The surface

temperature is calculated using the same formula applied over land and given by Eq. (3.19) in Section 3.4.1.3. If sea surface temperature is < 275°K, no retrieval is made.

3.3.1.4 Turbid and shallow water

The MODIS heritage turbid/shallow water test described in Li et. al. (2003) is used to identify turbid water containing suspended sediments and also shallow water, in which reflection from the sea bottom is visible. Neither of these conditions is sufficiently well-characterized to be used in the aerosol retrieval and must be avoided. The sediment masking algorithm follows: the observed reflectances at 0.488, 1.24, 1.61, and 2.25 μm are used to derive the power law fit using least squares minimization. Expected reflectances at 0.555 μm based on the power law fit are computed. Since a Rayleigh plus aerosol scattering atmosphere is expected to have a path reflectance which is a power law in wavelength, the differences between the observed reflectances and the calculated reflectances in these bands approximately correspond to the water leaving reflectance introduced by sediments. For clear water, the differences are close to zero; while for turbid water the differences are all greater than 0.01. The specific criteria to trigger that the pixel is affected by turbid water are:

$$\begin{aligned} &\rho_{0.555}^{ob} - \rho_{0.555}^{ex} > 0.015 \\ &\rho_{0.488} < 0.25 \\ &\rho_{2.25} < 0.10 \end{aligned} \qquad (3.9)$$

The thresholds on the 0.488 μm and 2.25 μm channels call back pixels that are most likely heavy dust or smoke, and not sediments. Significant bottom reflection will also cause a deviation from the expected power law fit, and can be identified and avoided using the same procedure. The test must be performed for a retrieval to take place. If one of the channels is bad and the test is not performed, the quality flag will be designated as "excluded" and it is as if the retrieval is not produced.

3.3.2 Aerosol models for over ocean retrieval

Table 3.2 describes the four fine mode models and five coarse mode models used in the VIIRS aerosol retrieval over ocean. All 9 aerosol models are assumed to be spherical particles and each can be used in a Mie calculation to produce a unique set of optical properties. The optical properties include absorption and scattering coefficients and phase function, which form the basis to derive spectral extinction, single scattering albedo, asymmetry factor, and Ångström exponent. Table 3.3 gives some of the calculated optical properties of these models.

Table 3.2 The 4 fine mode and 5 coarse mode models used in the VIIRS aerosol retrieval over ocean.

	λ=0.47 to 0.86 μm	1.24 μm	1.65μm	2.25 μm	r_v (μm)	σ_v (μm)	comments
1	1.45-0.0035i	1.45-0.0035i	1.43-0.0035i	1.40-0.001i	0.1	0.40	Wet water soluble type
2	1.45-0.0035i	1.45-0.0035i	1.43-0.0035i	1.40-0.001i	0.15	0.60	Wet water soluble type
3	1.40-0.0020i	1.40-0.0020i	1.39-0.0005i	1.36-0.0003i	0.2	0.60	Water soluble with humidity
4	1.40-0.0020i	1.40-0.0020i	1.39-0.0005i	1.36-0.0003i	0.25	0.60	Water soluble with humidity
5	1.45-0.0035i	1.45-0.0035i	1.43-0.0035i	1.43-0.0035i	0.98	0.60	Wet sea salt type
6	1.45-0.0035i	1.45-0.0035i	1.43-0.0035i	1.43-0.0035i	1.48	0.60	Wet sea salt type
7	1.45-0.0035i	1.45-0.0035i	1.43-0.0035i	1.43-0.0035i	1.98	0.60	Wet sea salt type
8	1.53-0.003i (0.47) 1.53-0.001i (0.55) 1.53-0.000i (0.66) 1.53-0.000i (0.86)	1.46-0.000i	1.46-0.001i	1.46-0.000i	1.48	0.60	Dust like type
9	1.53-0.003i (0.47) 1.53-0.001i (0.55) 1.53-0.000i (0.66) 1.53-0.000i (0.86)	1.46-0.000i	1.46-0.001i	1.46-0.000i	2.5	0.80	Dust like type

Shown are complex refractive index as a function of wavelength, modal radius (r_g), width of the mode (s), mode effective radius (R_{eff}) and a generic description of the aerosol type represented by the mode. Models 1-4 are fine mode. Models 5-9 are coarse mode.

Table 3.3 Normalized extinction coefficients as a function of wavelength (in μm), single scattering albedo (ω_0) and asymmetry parameter (g) at 550 nm and Ångström Exponent (AE) for the 0.47-0.86 μm wavelength pair, for each of the models defined in Table 3.2.

	0.47	0.67	0.86	1.24	1.65	2.25	ω_0	g	AE
1	1.5066	0.5731	0.2677	0.0815	0.0303	0.0075	0.9651	0.4772	2.8596
2	1.3117	0.6814	0.3930	0.1557	0.0642	0.0201	0.9758	0.6372	1.9948
3	1.2600	0.7165	0.4401	0.1903	0.0838	0.0287	0.9857	0.6991	1.7409
4	1.2053	0.7564	0.4961	0.2345	0.1108	0.0405	0.9863	0.7256	1.4692
5	0.9697	1.0320	1.0389	0.9454	0.7583	0.5444	0.9468	0.7339	-0.1141
6	0.9721	1.0442	1.1002	1.1344	1.0619	0.8972	0.9199	0.7506	-0.2049
7	0.9795	1.0348	1.0911	1.1696	1.1858	1.1094	0.8963	0.7733	-0.1786
8	0.9721	1.0379	1.0993	1.1558	1.1081	0.9577	0.9727	0.7058	-0.2035
9	0.9780	1.0259	1.0632	1.0890	1.0682	0.9934	0.9638	0.7240	-0.1382

The results of the Mie calculation are used as input into the radiative transfer calculation that calculates the apparent reflectance at the top of the atmosphere. The components required to make that radiative transfer calculation that are dependent on the optical properties of each aerosol model shown in Table 3.2 include the (a) atmospheric intrinsic reflectance sometimes called the path radiance, the (b) total (direct and diffuse) downward and upward atmospheric transmission, (c) the diffuse downward and upward atmospheric transmission, and (d) the atmospheric spherical albedo.

These optical properties are obtained from forward calculations of the radiative transfer code, 6S (Vermote et al., 1997; Kotchenova et al., 2006), for each of the 6 wavelength bands and each of the 9 models for a range of geometries and optical thicknesses. The step in solar zenith angle is 4 degrees from 0 to 80 degrees The sensor zenith angle is computed at the first 20 of 24 Gauss quadrature angles (with the nadir added) spanning 0 to 70 degrees. The step is kept constant in scattering angle (4°), Θ, defined as,

$$\cos\Theta = -\cos\theta_0 \cos\theta_S - \sin\theta_0 \sin\theta_S \cos\phi \qquad (3.10)$$

This results in a variable number of steps for each θ_o, θ_s configuration. Though more expensive and more complicated to interpolate, this structure achieves a higher precision with a reduced size LUT.

The step in AOT is variable to provide more information for the interpolation at the lower end. The AOT values used are as follows: 0.01, 0.05, 0.10, 0.2, 0.3, 0.4, 0.6, 0.8, 1.0, 1.2, 1.4, 1.6, 1.8 and 2.0.

3.3.3 Ocean surface reflectance

There are three components that affect the ocean surface reflectance: the water leaving reflectance, white caps (sea foam), and the sun glint. While the strong sun glint is identified and avoided by the algorithm (Section 3.3.1.2), the weaker glint continues to affect the retrieval and must be characterized.

The water leaving reflectance depends on chlorophyll content (ocean color) and turbidity caused by suspended sediments. Water with suspended sediments tends to be localized, concentrating at river outflows. The VIIRS aerosol algorithm identifies these situations using a procedure described in Section 3.3.1.4 and avoids making a retrieval using pixels affected by turbid water. Chlorophyll content varies across the ocean both in time and space, which could create difficulty in characterizing the ocean surface reflectance for aerosol retrieval. However, ocean color is strongly spectrally dependent, making nearly no contribution to the water leaving reflectance at longer wavelengths. The VIIRS aerosol algorithm avoids much of the problem by using only bands with wavelengths equal to or longer than 0.672 μm (M5 to M11, except M9) in the retrieval. The chlorophyll concentration is assumed to be a constant value of 0.4 mg m^{-3} across all the oceans. This results in a water leaving reflectance of 0.001 in M5 and zero for the other five bands used.

Whitecap reflectance is spectrally independent and a product of its effective reflectance (0.22) and coverage. This, in turn, is dependent upon wind speed. Following Koepke et al., (1984), the white cap coverage is modeled as:

$$\text{Whitecap Coverage} = 2.95\text{E-}06\ [\text{Wind Speed (m s}^{-1})]^{3.52}. \qquad (3.11)$$

The individual wavelength water leaving reflectance and whitecap reflectance are simply summed to yield a single term, ρ_{w+wc}.

The sun glint directional reflectance, ρ_G, is computed from the following inputs: wind speed (ms^{-1}), seawater index of refraction (n_d), seawater extinction coefficient (n_d), relative wind azimuth (solar azimuth – wind azimuth adjusted to be within the range 0^o-360^o), solar zenith angle, sensor zenith angle, and relative satellite azimuth angle. The index of refraction and extinction coefficients are both band-specific constants set according to Table 3.4.

Table 3.4 Seawater index of refraction and extinction coefficient values for VIIRS bands.

VIIRS band	Index of refraction	Extinction coefficient
M5	1.33700	0.0
M6	1.33600	0.0
M7	1.33432	0.0
M8	1.32936	0.00004
M10	1.32270	0.00009
M11	1.29793	0.00045

The procedure for calculating ρ_G makes use of the Cox and Munk (1954) model for wave slope distribution and Fresnel's reflection coefficients as described in Born and Wolf (1975). A full description is given in the 6S manual in subroutines OCEABRDF and SUNGLINT.

3.3.4 Core ocean aerosol retrieval

The core VIIRS aerosol inversion over ocean is shown schematically as a flow chart in Figure 3.3. It attempts to minimize the difference between the observed spectral reflectance in the six VIIRS bands and the reflectance pre-computed in two look-up tables (LUTs). The atmospheric LUT contains the path reflectance from the atmosphere only. Computed for each wavelength, each of the 9 models, a range of aerosol optical thicknesses and a range of solar zenith, sensor zenith and relative azimuth angles. The sun glint LUT contains $\overline{\rho}_G$ which is the integral of the downwelling skyshine reflected from the ocean BRDF into the sensor line of site. The value of $\overline{\rho_G^*}$, the integral of multiple scattering of direct sun glint from the ocean BRDF away from the sensor line of sight back into the sensor line of sight, is obtained from the same LUT by using the solar zenith angle instead of the sensor zenith angle.

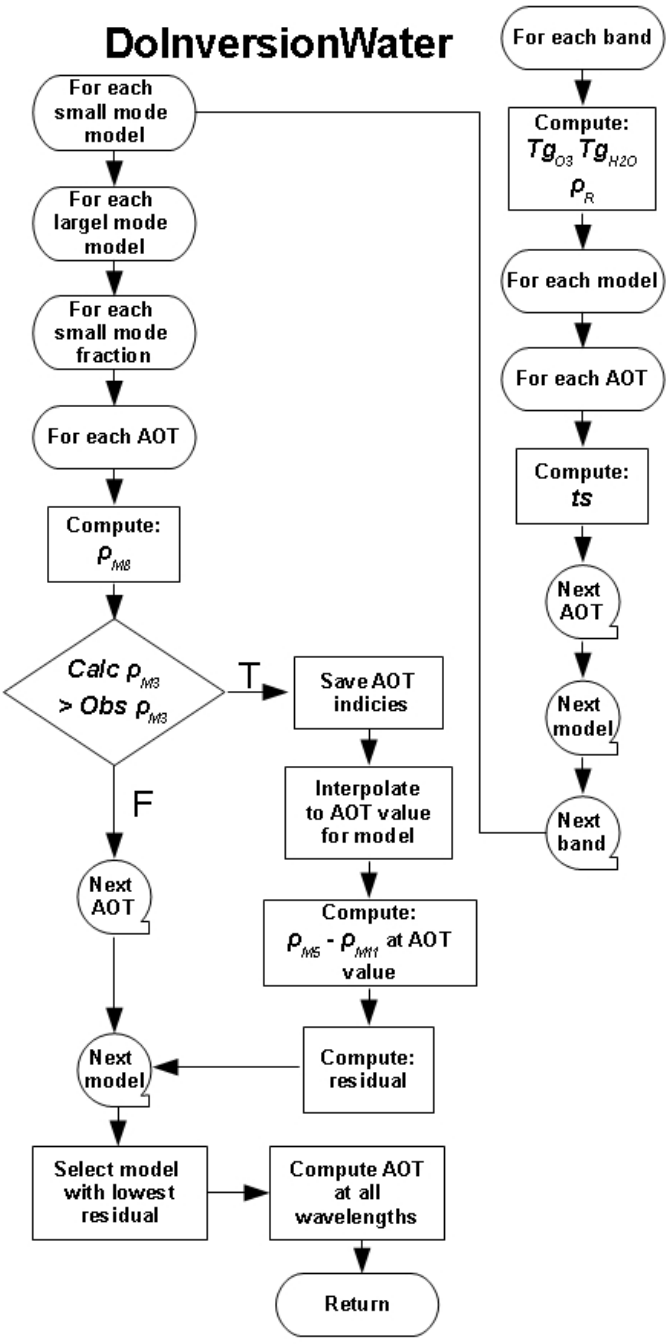

Figure 3.3 Flow chart for core ocean inversion algorithm.

The top of atmosphere reflectance is obtained from the following equation:

$$\rho^{LUT} = T_g^{OG} T_g^{O3} \left\{ \begin{array}{l} \left(\rho_{R+A} - \rho_{R+A}(P_0)\right) T_g^{H2O}\left(\frac{U_{H2O}}{2}\right) + \rho_R(P) \\ + T_g^{H2O}(U_{H2O}) \left[\begin{array}{l} \frac{T_{R+A}(\theta_0) T_{R+A}(\theta_S) \rho_{w+wc}}{1 - S_{R+A}\rho_{w+wc}} + e^{-M\tau_{R+A}} \rho_G \\ + t^d_{R+A}(\theta_0) e^{\frac{\tau_{R+A}}{\cos\theta_S}} \overline{\rho_G} + t^d_{R+A}(\theta_S) e^{-\frac{\tau_{R+A}}{\cos\theta_0}} \overline{\rho^*_G} \\ + t^d_{R+A}(\theta_0) t^d_{R+A}(\theta_S) \overline{\overline{\rho_G}} \\ + \frac{T_{R+A}(\theta_0) T_{R+A}(\theta_S) S_{R+A} \overline{\overline{\rho_G}}^2}{1 - S_{R+A}\overline{\overline{\rho_G}}} \end{array} \right] \end{array} \right\} \quad (3.12)$$

where the explicit notation indicating wavelength and model dependence have been dropped. The subscript "*R*" denotes "Rayleigh" and refers to molecular scattering alone. The subscript "*R+A*" denotes "Rayleigh + Aerosol" and refers to the total atmospheric contribution that includes aerosol. Parameters involving the total atmosphere (*R+A*) are dependent on aerosol model, as are those terms involving the coupling between atmosphere and surface reflectance, $\overline{\rho_G}$ and $\overline{\overline{\rho_G}}$. θ_o and θ_s are the solar and sensor zenith angles, respectively. The definitions and locations in this document where the parameters in Eq. (3.12) are described are given below:

ρ^{LUT}, the reflectance at top-of-atmosphere for a specific set of conditions in the LUT,

T_g^{OG}, the gaseous transmission of the other gases (Section 3.2.1.3 and Eq. (3.5)),

T_g^{O3}, the gaseous transmission of ozone (Section 3.2.1.1 and Eq. (3.1)),

$T_g^{H2O}(U_{H2O})$ and $T_g^{H2O}(U_{H2O}/2)$, the gaseous transmission of water vapor (Section 3.2.1.2 and Eq. (3.3)) for the total column precipitable water vapor (U_{H2O}) and the half column of water vapor ($U_{H2O}/2$), accounting for the assumption that aerosol and water vapor are probably well mixed,

$\rho_R(P)$ and $\rho_R(P_o)$, the molecular (Rayleigh) intrinsic reflectance at actual pressure (P) and reference pressure (P_o) (Section 3.2.2),

ρ_{R+A}, the atmospheric intrinsic reflectance (molecules and aerosols) (Sections 3.2.2),

M the air mass (Section 3.2.1.1 and Eq. (3.2)),

ρ_{w+wc}, the combined water leaving and whitecap reflectance (Section 3.3.4),

ρ_G, the sun glint directional reflectance (Section 3.3.4),

$T_{R+A}(\theta_0)$ and $T_{R+A}(\theta_s)$ the total (direct and diffuse) downward and upward transmission, respectively ,

$t^d_{R+A}(\theta_0)$, the diffuse downward transmission, $=T_{R+A}(\theta_0) - \exp[-(\tau_R + \tau_A)/\cos\theta_o]$,

$t^d_{R+A}(\theta_s)$, the diffuse upward transmission, $=T_{R+A}(\theta_s) - \exp[-(\tau_R + \tau_A)/\cos\theta_s]$,

S_{R+A}, the atmospheric spherical albedo adjusted for actual surface pressure (APPENDIX B),

$\overline{\rho_G}$ is the pre-computed normalized integrated downward irradiance by sunglint directional

reflectance, and $\overline{\rho_G^*}$ is the reciprocal of $\overline{\rho_G}$ found by swapping solar zenith and sensor zenith angles. Each is dependent on aerosol model, AOT and geometry, including relative azimuth of sun and sensor views. (APPENDIX B).

$\overline{\overline{\rho_G}}$ is the sunglint spherical albedo, dependent only on wavelength (APPENDIX B).

τ_{R+A}, the total optical thickness of both gases and aerosol.

Thus, ρ^{LUT} is available for each of the 9 aerosol models at each wavelength for the specific viewing geometry and for a variety of AOT values. The inversion mixes two aerosol modes, one fine and one coarse, using the equation in Tanré et al. (1998) based on the Wang and Gordon (1994), which approximates the top of the atmosphere reflectance for the combination of the fine and coarse mode as a linear combination of the reflectance of the fine mode, $\rho^{f,LUT}$ and the coarse mode $\rho^{c,LUT}$:

$$\rho^{LUT}(\tau_A) = \eta\,\rho^{f,LUT}(\tau_A) + (1-\eta)\,\rho^{c,LUT}(\tau_A) \qquad (3.13)$$

For each value of τ_A in the LUT for the given viewing geometry the algorithm uses Equations (3.12) and (3.13) to compute 4 (fine mode) x 5 (coarse mode) x 101 (number of η in 1% increments) possible combinations for each of the 6 spectral bands and thus 2020 values of $\rho_{TOA}(\tau_{R+A})$ for each spectral band.

For each possible combination, the optical thickness (τ^{inv}_{R+A}) is inverted for the M7 (0.865 μm) reference band such that

$$\rho^{LUT}(\tau^{inv}_{R+A})^k = \rho^k_{obs} \qquad (3.14)$$

where ρ^k_{obs} is the reflectance observed in the reference band, k = 0.865 μm. In other words, $\tau^{inv}{}_{R+A}$ is the optical thickness that allows the calculated reflectance to match the observed reflectance. Equation (3.10) is computed for the values of τ_A in the LUT to find the two τ_{R+A} values that bracket ρ^k_{obs} (e.g. $\tau^{LUT1}{}_{R+A}$ and $\tau^{LUT2}{}_{R+A}$) so that

$$\rho^{LUT}(\tau^{LUT1}_{R+A})^k \le \rho^k_{obs} < \rho^{LUT}(\tau^{LUT2}_{R+A})^k \qquad (3.15)$$

A simple linear interpolation is used to find $\tau^{inv}{}_{R+A}$ from between the two nodes in the LUT,

$$\tau^{inv}_{R+A} = \tau^{LUT1}_{R+A} + \frac{\tau^{LUT2}_{R+A} - \tau^{LUT1}_{R+A}}{\rho^{LUT}(\tau^{LUT2}_{R+A}) - \rho^{LUT}(\tau^{LUT1}_{R+A})}\left(\rho_{obs} - \rho^{LUT}(\tau^{LUT1}_{R+A})\right) \qquad (3.16)$$

all at the reference wavelength, *k*.

Once the AOT has been retrieved at the reference wavelength, it is used in Equation (3.12) to compute the reflectances at the other 5 wavelengths. These computed reflectances are differenced with the actual observations to produce a residual as follows:

$$\text{Residual} = \frac{1}{N}\sum_{i=1}^{N}\left(\rho^{LUT}(\tau_{R+A}^{inv})^{i} - \rho_{obs}^{i}\right)^{2} \quad (3.17)$$

where N=5, the number of bands used in the residual calculation, and $\rho_{obs}{}^{i}$ is the observed reflectance in band i. The smallest residual from the 2020 possibilities is the retrieved model along with its corresponding AOT at each wavelength. The results of the retrieval are values of AOT that is $\tau^{inv}{}_{R+A}$, at the six wavelength bands, identification of the two modes giving the minimum residual and the η parameter that identifies the weighting of these two modes resulting in the minimum residual. The combination of the two modes and their weighting parameter provides an aerosol model with a unique spectral dependence that is assumed linear in log-log space. This is used to extrapolate the AOT from the six retrieved wavelengths to a total of 11 wavelengths corresponding to M1, M2, M3, M4, M5, M6, M7, M8, M10 and M11, plus a value at 0.55 μm, an important wavelength in a multitude of applications, but not one of the VIIRS channels. Note that the shortest wavelength used in the retrieval is M5, 0.67 μm and that all reported AOT values at shorter wavelengths are extrapolated from longer wavelengths.

After the inversion is performed for each pixel, and the lowest residual is determined, the lowest residual is compared to a predefined threshold (implemented as a configurable parameter). If the lowest residual exceeds the predefined threshold, the quality of that retrieval is downgraded to "excluded". This residual threshold test excludes retrievals with a variety of contamination conditions missed by the pre-inversion data screening including, sub-pixel clouds, cloud shadows and turbid water.

3.4 Theoretical Description of Aerosol Retrievals Over Land

The difference between retrieving aerosol characteristics over land from doing the same over ocean is that the land surface reflectance is more heterogeneous than the ocean, less easily modeled and often times much brighter. The ocean surface can be bright in sun glint, but such situations are much more easily predicted and avoided than bright surfaces over land. Because the land surface reflectance is challenging to predict and model and because aerosol interactions make a smaller proportional contribution to total at-sensor radiance, it is more difficult to separate the atmospheric from the surface signal in the observations received by the satellite. A different type of retrieval is necessary.

There are three major assumptions in the VIIRS aerosol optical thickness retrievals over land. First, the retrieval limits the aerosol optical properties to 5 bimodal models, all assuming spherical particles. The over land algorithm has no flexibility in mixing models, unlike the over ocean algorithm which can retrieve arbitrary mixtures of fine and coarse modes. The assumed aerosol models are described in Section 3.4.2. Second, the VIIRS over land algorithm requires the land surface spectral reflectance to conform to a predetermined spectral signature that is applied uniformly and globally across all pixels deemed appropriate for inversion. Lastly, the land surface

is assumed to be Lambertian. The theoretical and empirical basis of the land surface reflectance assumptions is described in Section 3.4.3.

The VIIRS over land algorithm follows from a heritage algorithm used to produce the MODIS atmospherically corrected surface reflectance (Vermote and Kotchenova, 2008). The algorithm makes use of VIIRS reflectances in the following bands: M1 (0.412 μm), M2 (0.445 μm), M3 (0.488 μm), M5 (0.672 μm) and M11 (2.25 μm). It retrieves surface reflectance across the visible spectrum for a predetermined set of optical depths at 550 nm and a predetermined set of aerosol models. For each aerosol model, the optical depth is selected at which the assumed spectral relationship between the red (M5) and blue (M3) bands is approximately satisfied. This optical depth value is obtained by linear interpolation in surface reflectance residual between the two bounding optical depth bins. Then, for each model, an expected surface reflectance residual is calculated using the other three bands (M1, M2 and M11). The model with the lowest residual is selected and the optical depth value for that model becomes the retrieved value of optical depth at 550nm for that pixel.. The fitting procedure is described in Section 3.4.4. Similar to the ocean algorithm the land algorithm relies on pre-calculated values of the radiative transfer parameters, stored in a Look-Up Table (LUT). However, before the inversion procedure begins, a pixel must be selected for retrieval.

3.4.1 Selection Process for Appropriate Pixels for Aerosol Retrieval Over Land

A pixel entering the aerosol algorithm arrives with associated VIIRS SDRs, VIIRS M-Band Geolocation and an associated set of flags provided by the VIIRS cloud mask. These include indicators of cloud, snow/ice, fire, the angles of the observation (solar zenith, sensor zenith, relative azimuth) and also whether the pixel is land, ocean or coast. If the associated flags indicate extreme solar zenith angle, a high probability of cloud, sunglint, snow/ice or fire, the aerosol algorithm does not produce a retrieval for that pixel and moves on to the next. The aerosol quality flag is set to 'not produced' for that pixel.

After that initial selection process, a pixel identified as 'land' undergoes another series of tests internal to the aerosol algorithm. These are applied to further eliminate cloud, sun glint, fire, ephemeral water and snow/ice surfaces that the VIIRS cloud mask might miss.

3.4.1.1 Cloud avoidance

There is no difference between using the VIIRS cloud mask, combined with a M9 band test for thin cirrus in the land procedure than what was described for the ocean procedure in Section 3.3.1.1. The reader is referred to that section for a description.

3.4.1.2 Sun glint avoidance

Sunglint is also detected over land. This is important because land-based water bodies such as rivers, lakes, ponds and irrigated farmland may not be tagged as water in the land/water mask. In the specular reflection direction these inland water pixels, even puddles, can be misinterpreted to be fires, clouds or clear land pixels. The algorithm calculates sunglint reflectance dynamically (Section 3.3.1.2) over all surfaces (land and ocean). The sunglint pixel is set if visible reflectance anomaly (VRA) is greater than 0.02, middle infrared anomaly (MIRA) is greater than 0.1 and the pixel is free from cloud and fire. The VRA is defined as VRA=M3-0.5*M5.

The middle infrared anomaly (MIRA) is calculated as follows:

$$\text{MIRA} = \rho_{3.7} - (0.87 * \text{M11} - 0.32 * \text{M10}) \qquad (3.18)$$

where $\rho_{3.7}$ is the estimated reflectance at 3.7 μm. This is not the M12 value of radiance because the observed M12 radiance includes both emissive and reflective components, and the emissive part must be subtracted from the total value. M11 and M10 are the observed TOA reflectances in bands M11 and M10, respectively. When the VRA value is greater than 0.02 and the MIRA value exceeds 0.1 in a pixel, but the pixel is not cold enough to be cloud, nor hot enough to be fire, the pixel is flagged as sunglint and the retrieval is not performed. Otherwise, the retrieval is performed. Figure 3.4 illustrates the effect of sunglint in the middle infrared RGB composite and the masking of the sunglint according to the criteria described above.

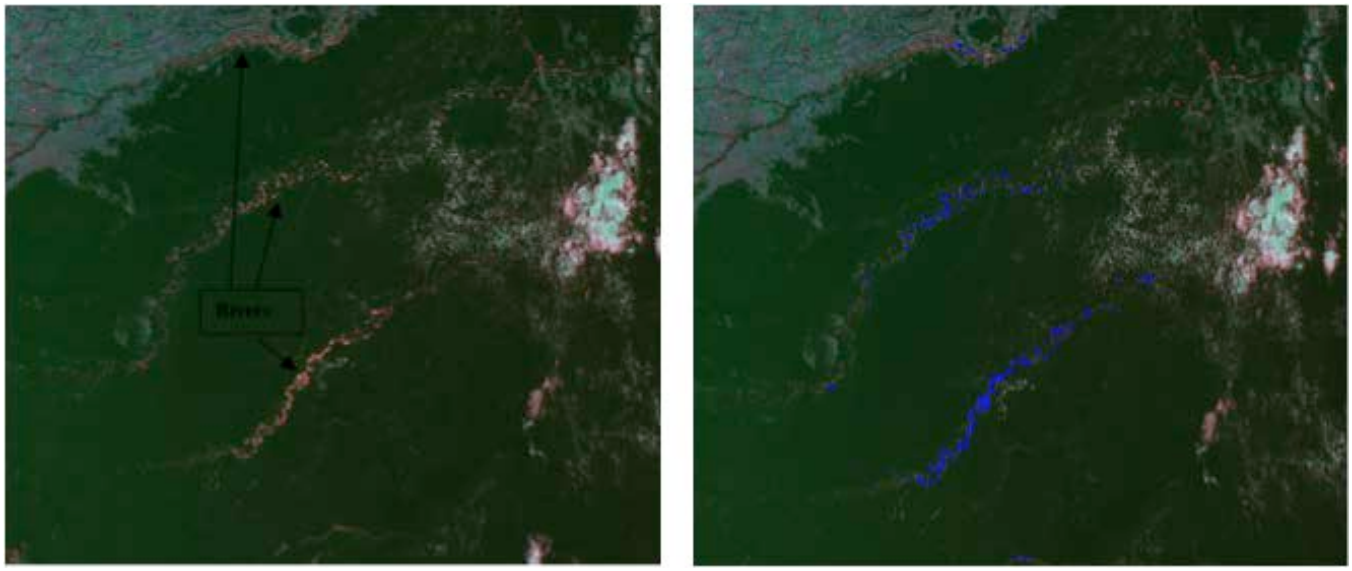

Figure 3.4 MODIS scene from the Amazon in rgb true color (left). The rivers appear reddish because they are in sunglint. The same scene in rgb true color appears on the right, but with the sunglint mask applied, in blue.

3.4.1.3 Snow/ice avoidance over land

The aerosol algorithm is not designed to retrieve over snow or ice. A very minimal amount of snow can introduce substantial error in the retrieval; therefore, a very conservative method has been developed to assure that no snow or mixed pixels are used by the algorithm. Information on snow/ice is passed to the aerosol algorithm via the VIIRS cloud mask, but the primary means for identifying snow is an internal procedure. A specific algorithm based on the MODIS data has been designed to detect snow-contaminated pixels over land. When snow is detected, the aerosol algorithm performs an aggressive filtering of the optical thickness values (based on spectral dependence) around the snow covered area to eliminate contamination by sub-pixel snow as much as possible it is therefore important to limit that process as much as possible to optimize processing time and reduce "false" rejection. The internal mask described previously should not misclassify snow as cloud because it uses quantities that are not sensitive to snow (MIRA and VIIRS band M9) in most conditions. For pixels which have not been classified as cloud, fire or sunglint but still have a high visible reflectance anomaly (blue-red/2), the test using the ratio between band M8 (1.24m) and M7 (0.87m) is used to classify the pixels as snow or not (.M8/.M7 < 0.9). In addition, a condition on the surface temperature (should be <278K) is also required. Surface temperature is given by,

$$T_{surface} = A + B\left(T_{15} - T_{coeff}\right) + C\left(T_{15} - T_{coeff}\right)\left(T_{15} - T_{16}\right) + D\left(T_{15} - T_{16}\right)\left(\frac{1}{\cos\theta_S} - 1\right) + T_{coeff} \quad (3.19)$$

where $T_{coeff} = 273.15°K$, θ_S is the sensor zenith angle, A, B, C, D are coefficients as follows: if $T_{15} - T_{16} \le 0.7$, A=1.110, B=0.9586, C=0.1741, D=1.876; otherwise, A=1.196, B=0.9888, C=0.1300, D=1.627.

3.4.1.4 Fire avoidance

Fire is detected if MIRA is greater than 0.1 and the difference between surface temperature and NCEP model surface air temperature is greater than 5 degrees. This internal test is in addition to fire information passed to the aerosol algorithm from the VCM.

3.4.1.5 Bright pixel avoidance

Pixels that pass all the tests and appear appropriate for aerosol retrieval over land are then subjected to one last test that eliminates bright pixels. Bright pixels are eliminated for two reasons. First, the brighter the surface reflectance, the greater the absolute error in reflectance introduced from small relative deviations from assumed values. Retrieved AOT errors are proportional to absolute error in surface reflectance assumptions. Second, bright pixels indicate a non-vegetative surface that is less likely to conform to the assumed spectral signature used as the inversion fitting metric. This metric is based primarily on empirical evidence from vegetated dark pixel targets. The retrieval places greater confidence on vegetated-dominated pixels.

The bright pixel index is given by

$$\text{Bright\_Index} = \frac{\rho_{1.24} - \rho_{2.25}}{\rho_{1.24} + \rho_{2.25}} \tag{3.20}$$

where $\rho_{1.24}$ and $\rho_{2.25}$ are the top-of-atmosphere M8 and M11 reflectances, respectively. Bright_Index is sometimes referred to as $NDVI_{SWIR}$ (Levy et al., 2007). It provides a measure of how vegetated the pixel is or its greenness. By basing the index on shortwave infrared channels (SWIR), the index is less affected by aerosol than less atmospherically resistant indices based on shorter wavelengths. The VIIRS algorithm identifies a bright pixel when

$$\text{Bright\_Index} < 0.05 \quad \text{AND} \quad \rho_{2.25} > 0.3 \tag{3.21}$$

The algorithm also makes a distinction between vegetated-dominated pixels and those that are less vegetated and assigns quality flags differently for each category. A vegetated-dominated pixel requires

$$\text{Bright\_Index} > 0.2 \tag{3.22}$$

which will be necessary to obtain a quality flag of 'high' quality.

3.4.2 Over-land Aerosol Models

The assumed optical properties (aerosol models) used by the VIIRS aerosol retrieval over land are taken from Dubovik et al., (2002). The models are based on inversions of sky radiance measurements taken by AERONET stations worldwide (Holben et al., 1998; Holben et al. 2001; Dubovik and King 2000). Data from twelve stations are used in the Dubovik et al., (2002) study, each with 300 to 2400 inversions. The models include size distributions and optical properties of the aerosols, and they are dynamic, with some of the parameters varying with magnitude of the AOT (Remer and Kaufman, 1998). Table 3.5 gives the model properties. Five models from this work are used in the VIIRS over-land aerosol retrieval: Dust, Smoke-high absorption, Smoke-low absorption, Urban-clean and Urban-polluted. The Oceanic model is not included due to exclusion of coastal pixels in the land retrieval and the infrequency of oceanic aerosols inland. Subsequent studies to Dubovik et al., (2002) also identify five or six aerosol models, roughly paralleling these five, but with differences, that represent all aerosol types across the AERONET inversion data base (Omar et al., 2009; Levy et al., 2007).

Dust corresponds to desert dust. It is dominated by its coarse mode and absorbs more strongly towards shorter wavelengths. Biomass burning produces smoke with low absorption (high single scattering albedo) when there is a high fraction of woody materials burnt and a strong contribution from the smoldering phase of the fires. Smoke in South America tends to be low

absorption. In southern Africa, fires tend to be primarily savanna fires, with less woody material burnt and a larger contribution from the flaming phase of the fire. This produces a high absorption (relatively low single scattering albedo). Urban-low absorption aerosol is typical of a relatively clean urban-industrial aerosol (e.g. the U.S. and western Europe) that produces sulfate aerosol and organics, but with a minimum amount of black carbon. This type of aerosol easily swells with increasing humidity and is the most dynamic of the models, growing quickly in size and decreasing in the real part of the refractive index as AOT increases. Urban-high absorption aerosol corresponds to a more polluted urban environment, typical of the mega-cities of emerging economies (e.g. Mexico City, Sao Paulo, Indian and Chinese cities). Smoke and urban absorption in the visible is caused by black carbon, which follows a λ^{-1} spectral dependence. This spectral dependence coupled with typical small particle sizes causes the single scattering albedo to decrease with increasing wavelength. Each model has its own size distribution, all are bimodal, all but dust are dominated by the small mode, all allow for some systematic variation with aerosol loading. Figure 3.5 shows the size distributions of all five models. Figure 3.6 shows some of the optical properties of the five models and Figure 3.7 shows the Ångström Exponent of the five models as a function of AOT.

Table 3.5 Land aerosol model parameters.

	dust	**Smoke-low absorption**	**Smoke-high absorption**	**Urban-clean absorption**	**Urban-polluted absorption**
Refractive indices					
Real part	1.48	1.47	1.51	1.41-0.03τ	1.47
Imaginary part	**	0.0093	0.021	0.003	0.014
Size parameter fine mode					
Volume mean radius (μm)	0.12	0.13+0.04τ	0.12+0.025τ	0.12+0.11τ	0.12+0.04τ
Standard deviation	0.49+0.10$\tau_{1.02}$	0.40	0.40	0.38	0.43
Volume concentration ($\mu m^3/\mu m^2$)	0.02+0.02$\tau_{1.02}$	0.12τ	0.12τ	0.15τ	0.12τ
Size parameter coarse mode					
Volume mean radius (μm)	1.90	3.27+0.58τ	3.22+0.71τ	3.03+0.49τ	2.72+0.60τ
Standard deviation	0.63-0.10$\tau_{1.02}$	0.79	0.73	0.75	0.63
Volume concentration ($\mu m^3/\mu m^2$)	0.9$\tau_{1.02}$	0.05τ	0.09τ	0.01+0.04τ	0.11τ

τ refers to AOT at 0.44 μm
$\tau_{1.02}$ refers to AOT at 1.02 μm

** The imaginary part of the index of refraction for dust is defined for the following (wavelength, index of refraction) pairs: (0.350 µm, 0.0025), (0.400 µm, 0.0025), (0.412 µm, 0.0025), (0.443 µm, 0.0025), (0.470 µm, 0.0023), (0.488 µm, 0.0021), (0.515 µm, 0.0019), (0.550 µm, 0.0016), (0.590 µm, 0.0013), (0.633 µm, 0.0010), (0.670 µm, 0.0007), (0.694 µm, 0.0007), (0.760 µm, 0.0007), (0.860 µm, 0.0006), (1.240 µm, 0.0006), (1.536 µm, 0.0006), (1.650 µm, 0.0006), (1.950 µm, 0.0006), (2.250 µm, 0.0006) and (3.750 µm, 0.0006).

These models are used in the 6SV radiative transfer model to produce forward calculations of top of atmosphere reflectance for each wavelength for a variety of geometries and AOTs. Note that the LUT values are indexed by AOT at 0.55 µm, no matter the wavelength of the reflectance being calculated. Because each of the models locks into a specific spectral dependence, knowing the AOT at 0.55 µm and the model, implies that AOT at each wavelength is also known. The results of these calculations are stored in a LUT and used in the core inversion described in Section 3.4.4.

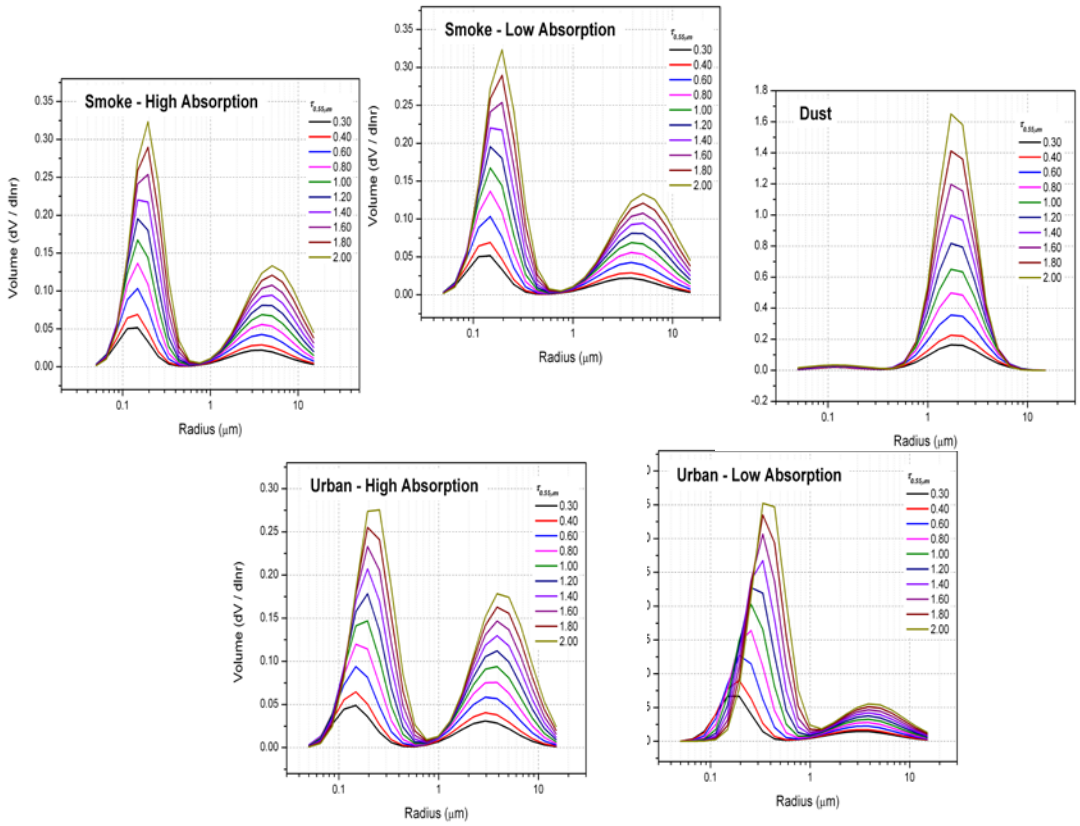

Figure 3.5 Volume size distributions of the five aerosol models used in the land retrieval. Note that size systematically varies as a function of AOT.

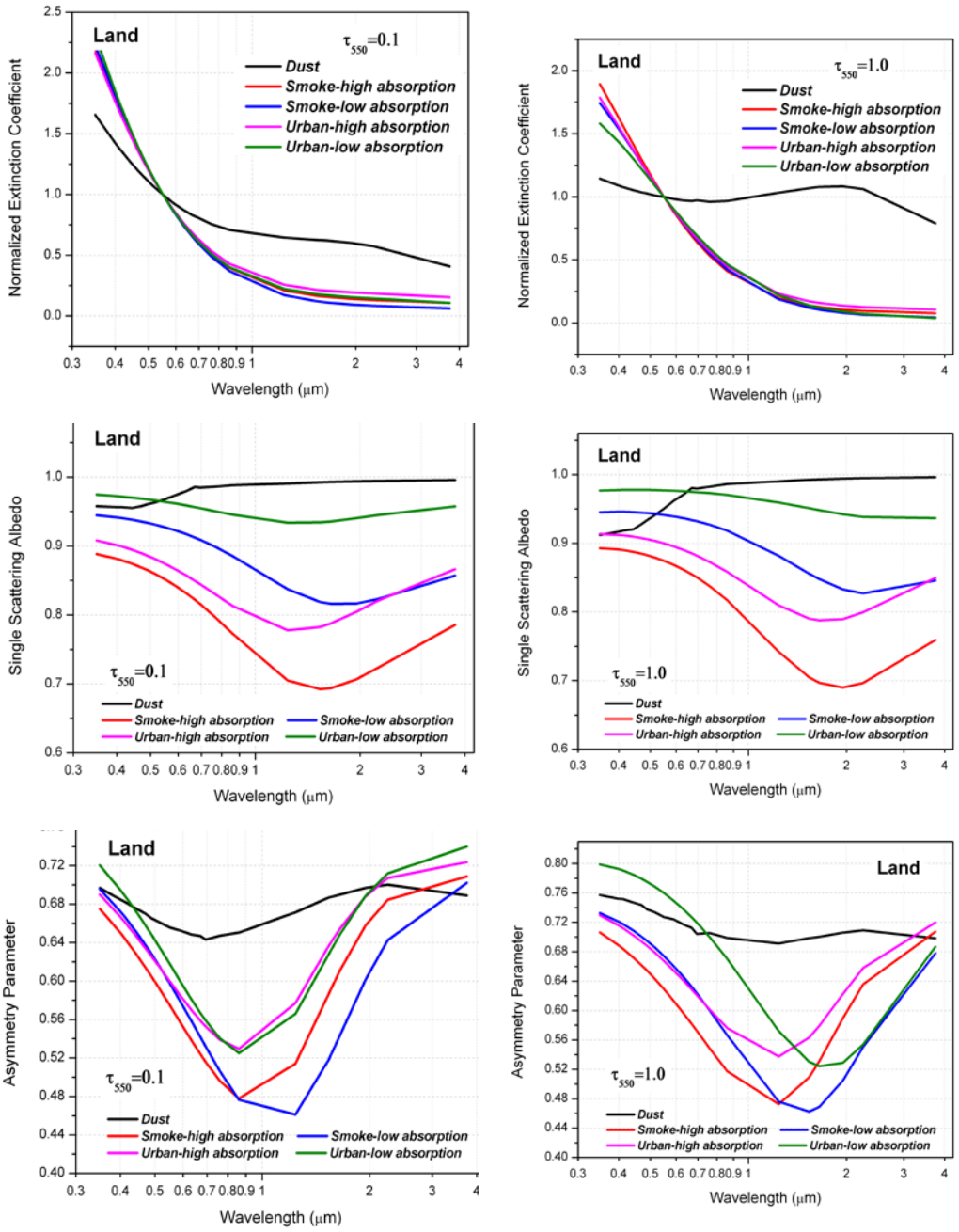

Figure 3.6 Normalized spectral extinction coefficient (top), single scattering albedo (center) and asymmetry parameter (bottom) for AOT = 0.1 (left) and AOT = 1.0 (right) for the five land aerosol models.

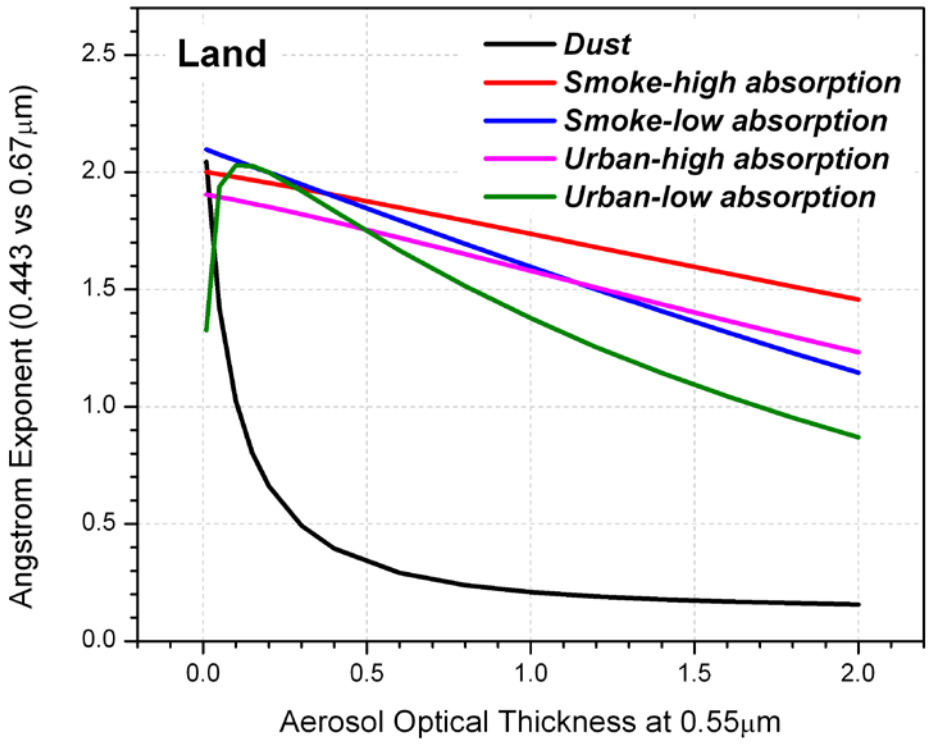

Figure 3.7 Ångström Exponent defined with wavelengths 0.443 μm and 0.67 μm as a function of AOT for the five aerosol models used in the over land retrieval.

Because the model size distributions vary with AOT, the Ångström Exponent of each model will also vary with AOT. For example, dust size distribution in Figure 3.5 at low AOT shows two aerosol modes, each with very low amplitude. As AOT increases, the coarse mode increases, but the fine mode does not. This shifts the Ångström Exponent from high values to low values as the aerosol loading increases from AOT <0.05 to AOT > 0.50.

3.4.3 Spectral surface reflectance in the over land retrieval

The second major assumption in the VIIRS over land retrieval is that surface reflectance conforms to a set of expected spectral ratios that can be applied to all pixels identified as appropriate by the selection criteria of Section 3.4.1. This means that while the appropriate land reflectance itself varies widely from relatively bright sparsely vegetated dry landscapes to dark densely vegetated forests, we expect the variation of specific wavelengths to correlate. As vegetation becomes denser and darker, the reflectances in the blues, red and mid-infrared (λ > 2.0 μm) wavelengths will decrease. Note that not all parts of the spectrum are expected to correlate in this fashion. For example, green, 0.87 μm and 1.6 μm will become brighter, not darker as vegetation becomes

denser. This assumption of universal ratios of specific surface reflectances is based on the following physics. Shadows, vegetation and soil wetness all tend to reduce reflectivity in the mid-infrared and the visible simultaneously. Note that chlorophyll in plant leaves absorbs radiation in the blue and red parts of the spectrum, but chlorophyll exists in solution in those leaves. So, where chlorophyll exists to absorb light in the blue and red, liquid water exists to absorb radiation in the mid-infrared wavelengths. Wet soil is darker in the visible because the water fills in the spaces between soil grains, which effectively changes the net refractive index of the soil to increase forward scattering and darken the soil. Meanwhile the wetness directly absorbs light in the mid-infrared, causing again the correlation between these two parts of the spectrum of surface reflectivity (Kaufman et al., 1997). Robust surface reflectance ratios have been determined from satellite analysis (Kaufman and Remer, 1994; Kaufman et al., 1997), from surface and aircraft measurements (Kaufman et al., 1997; Remer et al., 2001; Karnieli et al., 2001) and from simulations (Kaufman et al., 2002).

The VIIRS algorithm requires ratios between four channels and 0.672 μm. Specifically these are: 0.412 μm, 0.444 μm, 0.486 μm and 2.257 μm. At launch and current values of these ratios, including the trivial value of $\rho_{0.675}/\rho_{0.65}$ is given in Table 3.6.

Table 3.6 Surface reflectance ratios used by the VIIRS algorithm.

wavelength	at-launch ratio $\rho_\lambda / \rho_{0.675}$	current ratio $\rho_\lambda / \rho_{0.675}$
0.412 μm	0.3905	0.513
0.444 μm	0.475	0.531
0.486 μm	0.578	0.645
0.672μm	1.0	1.0
2.257 μm	2.0	1.788

These represent the expected spectral dependence of the surface reflectivity.

There is an important point to note about the current values of the ratios. The values are derived at an AERONET stations, and these locations may not represent truly global surface reflectivity characteristics. The actual surface spectral reflectance may vary under different conditions, so that any set of mean values applied globally may introduce a significant amount of scatter in the aerosol retrieval. Parameterizing these different conditions and applying a modified set of reflectance ratios that adjust to changing situations may reduce some of the scatter. This issue has been explored, and proposed updates that parameterize the surface reflectance ratios in terms of $NDVI_{SWIR}$ (Eq. (3.20)) are presented in Section 5.1.

3.4.4 Core inversion for the over land retrieval

The core inversion is based on performing atmospheric correction on the VIIRS-observed reflectance in several channels in the visible and then matching the retrieved spectral surface reflectance with the spectral signature expected from the empirical study of Section 3.4.3.

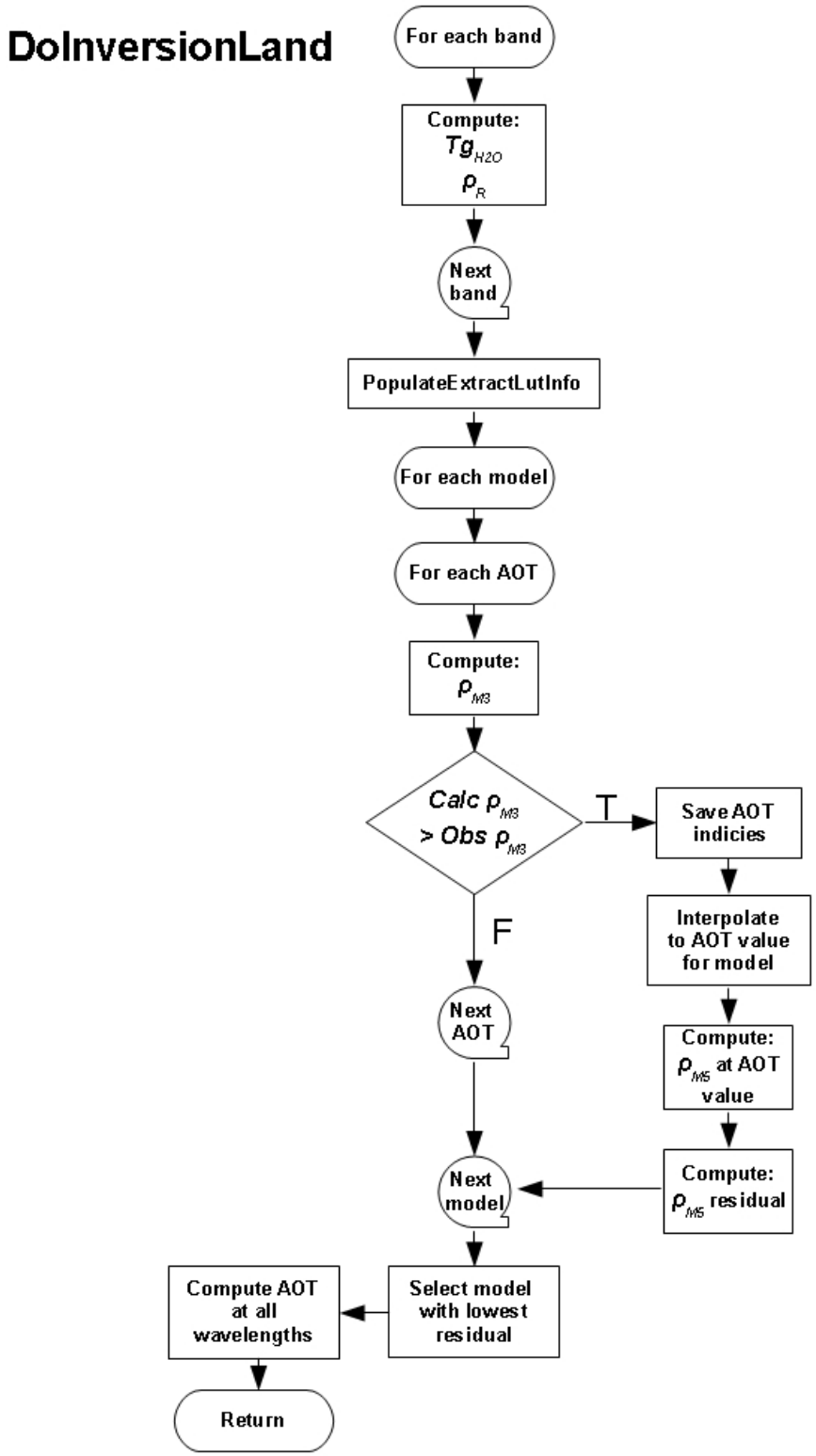

Figure 3.8 Flow chart for core land inversion algorithm.

The spectral signatures are expressed as simple reflectance ratios of M3 to M5 ($\rho_{0.488}/\rho_{0.675}$). Figure 3.8 illustrates the core retrieval over land.

The surface reflectance for the M3 (0.488 μm) and M5 (0.675 μm) bands is calculated for each of the five models and each value of AOT 0.55 μm in the LUT (Section 3.4.2) by solving the Lambertian top-of-atmosphere reflectance equation for ρ_{surf}

$$\rho^{LUT} = T_g^{OG} T_g^{O_3} \left[\begin{array}{l} (\rho_{R+A} - \rho_R(P_0)) T_g^{H_2O}\left(\frac{U_{H_2O}}{2}\right) + \rho_R(P) \\ + T_g^{H_2O}(U_{H_2O}) T_{R+A}(\theta_0) T_{R+A}(\theta_S) \frac{\rho_{surf}}{1 - S_{R+A}\rho_{surf}} \end{array} \right] \quad (3.23)$$

Where,

- P_0 is the standard pressure = 1 atm, a constant.
- θ_0 is the solar zenith angle, θ_s is the view zenith angle, P is the actual pressure [atm].
- Tg^{og} is the gaseous transmission of the gases other than ozone or water vapor (CO_2, O_2, N_20, and CH_4), Tg^{o_3} is the ozone gaseous transmission, $Tg_{H_2O}(U_{H_2O})$ is the water vapor gaseous transmission for the total integrated amount of water vapor (U_{H_2O}).
- $Tg_{H_2O}(U_{H_2O}/2)$ is the water vapor gaseous transmission for half of total integrated amount of water vapor (U_{H_2O}).
- $\rho_R(P)$ is the Rayleigh intrinsic reflectance (molecules only) at pressure P.
- ρ_{R+A} is the atmospheric intrinsic reflectance (molecules and aerosols),
- $T_{R+A}(\theta_0)$ is the total (direct and diffuse) downward atmospheric transmission,
- $T_{R+A}(\theta_s)$ is the total (direct and diffuse) upward atmospheric transmission,
- S_{R+A} is the atmospheric spherical albedo, and
- ρ_{surf} is the surface reflectance.

$\rho_{TOA}(\tau_a)$ is measured by VIIRS in each wavelength. All other quantities besides ρ_{surf} can be calculated using radiative transfer codes given a specific geometry, a surface pressure, an aerosol optical thickness (denoted by τ_a in the above equation), an aerosol model and column measurements of the various gas absorbers. In the VIIRS retrieval the column gas concentrations are either provided by ancillary data or assumed from climatology. See Section 3.1. The surface pressure is derived from a digital elevation map, given the latitude-longitude of the observed pixel. See Section 3.1.

Thus, for each wavelength, AOT and model in the LUT, the above equation can be solved for ρ_{surf}. Because the solution for each wavelength is computed independently, there is a different surface reflectance ratio for each model, for each AOT. The best AOT at 0.55 μm for each model is the

value that satisfies the expected surface reflectance ratio between the 0.488 μm and 0.675 μm bands for vegetated surfaces (0.578 from Section 3.4.3). Thus, there are initially five solutions to the inversion, one for each of the five models. These five solutions are exact solutions with the only residual due to interpolation between AOT nodes in the LUT, a relatively minor value. In order to select the best aerosol model and thereby select a single value for AOT at 0.55 μm, we solve for the surface reflectance at 0.412 μm, 0.445 μm and 2.25 μm using the AOT at 0.55 μm for that model. Now because there are multiple wavelengths and multiple surface reflectance ratios involved, the solution is not exact and has to be fit in a least squares sense. For each model, we compute a residual based on the expected 0.412 μm, 0.445 μm and 2.25 μm to 0.672 μm surface reflectance ratio from Table 3.6.

$$\mathrm{Re}\,sidual = \sum_{\lambda}^{5}\left[\rho_{\lambda\_surf\_Cal} - \rho_{0.672\_surf\_Cal}\left(\frac{\rho_{\lambda\_surf\_\exp}}{\rho_{0.672\_surf\_\exp}}\right)\right]^2 \qquad (3.24)$$

The 5 λs (wavelengths) refer to 0.412 μm, 0.444 μm, 0.488 μm, 0.672 μm and 2.257 μm, although the 0.488 μm and 0.672 μm contribute little to the residual because they are already an exact solution to Eq. (3.23). The model with the lowest residual is selected, determining both the AOT at 0.55 μm value and the aerosol model. The AOT at all other wavelengths is then computed using the spectral dependence defined by the chosen aerosol model, with the selected AOT at 0.55 μm.

The core VIIRS retrieval differs from the MODIS Dark Target algorithm in two fundamental ways. First, the VIIRS algorithm chooses between 5 discrete models, never combining them. In contrast, the MODIS algorithm combines two bimodal models, one dominated by fine mode and one dominated by coarse mode. Second, the VIIRS algorithm solves Eq. (3.23) for ρ_{surf} and then fits the surface reflectance ratios to expected values. The MODIS algorithm uses expected values of surface reflectance ratios to estimate ρ_{surf}. It then solves Eq. (3.23) for τ_a at one wavelength (0.47 μm) and fits the calculated top-of-atmosphere reflectance at another wavelength (0.67 μm) to the directly measured value from MODIS, allowing for different combinations of fine-dominated and coarse-dominated models.

3.5 Retrieval of size parameter

The aerosol size parameter currently produced by the VIIRS aerosol algorithm is the Ångström Exponent (AE) defined in Equation (1.3). This product follows directly from the inversion of spectral AOT over ocean and land. Over ocean, the AE product is calculated from the AOT derived in bands M7 and M9 (0.862 and 1.60 μm, respectively) as,

$$AE\_ocean = -\frac{\ln(\tau_{M7}) - \ln(\tau_{M9})}{\ln(0.865) - \ln(1.61)} \qquad (3.25)$$

Note that the choice of bands used to calculate AE_ocean in VIIRS differs from the choices used in the corresponding MODIS product. MODIS offers two AE_ocean products, one calculated using the wavelength pair, 0.55 μm and 0.86 μm, and the other using 0.86 μm and 2.1 μm.

Over land, the AE product is calculated from the AOT derived in bands M2 and M5 (0.444 and 0.672 μm, respectively) as,

$$AE\_land = -\frac{\ln(\tau_{M2}) - \ln(\tau_{M5})}{\ln(0.445) - \ln(0.672)} \tag{3.26}$$

This wavelength pair is similar to the MODIS Collection 5 AE_land product, which uses 0.466 μm and 0.646 μm. However, MODIS has discontinued its AE_land product for lack of skill in the inversion. Preliminary validation of the VIIRS AE_land also shows little skill in the size parameter retrieval over land.

There is an opportunity in the future for VIIRS to produce a different or additional size parameter such as particle effective radius, but not at this time.

3.6 Suspended Matter

Suspended Matter is the third product of the VIIRS aerosol algorithms. Unlike AOT and size parameter, suspended matter does not follow from the MODIS aerosol algorithm heritage. The Suspended Matter product currently produced by VIIRS is a classification of the type of aerosol encountered in the retrieval. It is applied only when the aerosol loading quantified by the retrieved AOT exceeds a specified threshold, and it is applied over both ocean and land. The classification categories are: volcanic ash, dust, smoke, sea salt, not determined and none. The smoke category includes all aerosol types not identified as volcanic ash, sea salt, dust or undetermined, and it is primarily a fine-mode dominated aerosol type, most likely derived from combustion processes. In this way the suspended matter smoke category includes both traditional smoke from biomass burning sources and non-light absorbing sulfate particles from burning fossil fuels in developed economies.

Volcanic ash is identified in the VIIRS Cloud Mask (VCM) and is passed to the aerosol algorithm via one of the VCM flags that are read as input to the aerosol algorithm. The aerosol algorithm then simply passes that information, unchanged, to the suspended matter output in the aerosol product. The VCM-derived designation of volcanic ash supersedes all internal classifications described below.

Discriminating between dust and smoke classifications proceeds differently over ocean and over land. In both cases, AOT must be greater than 0.15 to proceed. If not, then the Suspended Matter returns the 'None" category.

Over ocean, the classification is based on the η parameter from Equation (3.13) in Section 3.3.4. Dust arises from wind erosion processes producing an aerosol dominated by the coarse mode

with effective radii greater than 1.0 μm (See Table 3.2). Smoke and other combustion-generated aerosols are produced from gas-to-particle conversion processes that result in particle size distributions dominated by the fine mode with effective radii less than 1.0 μm and usually less than 0.4 μm. Note that even though each particle type is dominated by particles in specific size ranges, the tails of the individual mode size distributions extend into a broad range of sizes. Thus, even though dust is a coarse mode aerosol, it contains particles found at sizes below 1 μm. However, in general if η exceeds a certain value it can be considered to be primarily smoke, if it falls below a different threshold it can be designated as dust. Currently the suspended matter over ocean classifies the aerosol as smoke when $\eta > 0$. The algorithm classifies the aerosol as dust when $\eta < 0.2$. When $0.2 < \eta < 0.5$, and AOT < 0.3, then the category sea salt is chosen. When η falls between 0.2 and 0.5, but AOT is greater than 0.3, then the Undetermined category is chosen. These thresholds may unrealistically exclude dust, because η for dust a distance downwind from its source often exceeds 0.2. Less restrictive thresholds may be applied in the future.

Over land, the suspended matter classification is based on the aerosol model chosen during the retrieval. See Section 3.4.2. Of the five possible aerosol models for the land retrieval in Table 3.5, if the 'dust' model is retrieved, meaning that it produces the smallest residual in Equation (3.24), then the suspended matter classification flag over that land pixel will be designated as dust. If any of the other 4 models are retrieved, then the suspended matter flag will be smoke.

The suspended matter product reports the retrieved classification along with important quality flags. These flags are set depending on the quality flag of the associated IP AOT product, whether volcanic ash is indicated from the VIIRS cloud mask, and the aerosol loading. Details of the suspended matter quality flag are given in Appendix C.3.

Suspended matter is produced at the sensor resolution, nominally 0.75 km, similarly to the Intermediate products (Section 3.7), but it is an Environmental Data Record (EDR) that is scheduled to be released to the public. The algorithm also computes smoke concentration using an empirical approach. Details can be found in the Suspended Matter ATBD (SM ATBD, released 2011).

3.7 Definition of IP and EDR products

All of the algorithms described above, and all of the aerosol products, AOT, AE and suspended matter are derived for every VIIRS pixel at the native pixel resolution of the sensor, which is 0.742 x 0.259 km at nadir (Table 2.1; Section 2.2). Nominally this resolution will be referred to as 0.75 km. The VIIRS aerosol products produced at 0.75 km resolution are referred to as Intermediate Products (IP), except suspended matter, which is a final product at this resolution that is scheduled for public release. An IP product is made available within the VIIRS processing environment to other groups requiring quantitative measures of aerosol properties to produce their products. For example, land surface reflectance retrieval requires aerosol information for atmospheric correction of the measured spectral radiance at top of atmosphere.

The aerosol algorithm, itself, makes use of the aerosol IP product to produce the aerosol Environmental Data Record (EDR) products. The aerosol EDR products are aggregated from the 0.75 km aerosol IP product by arranging the IP products in arrays of 8 x 8, resulting in a nominal EDR product of 6 km at nadir based on the 64 IP aerosol retrievals. Note this is a fundamental deviation from the heritage MODIS Dark Target procedure. The VIIRS algorithm *first retrieves aerosol products* at each appropriate pixel at the sensor resolution then aggregates these retrieved aerosol parameters to a larger retrieval box. In contrast, the MODIS algorithm *first groups observed radiance* at the native sensor resolution, averages to obtain a single representative spectral radiance for the box and retrieves one set of aerosol products for that box. The VIIRS method is more computationally intensive but achieves full aerosol retrievals at relatively fine resolution in the IP product.

The VIIRS aerosol EDR products include both AOT and Ångström Exponent (Section 3.5), over both ocean and land. These are currently available to the public. The VIIRS aerosol IP products include AOT and Ångström Exponent (Section 1.2). Suspended Matter is a special case, an EDR that is produced at the nominal 0.75 km resolution. It is scheduled for public release, but is not yet available to the public.

3.7.1 NAAPS fill for IP product

The VIIRS aerosol IP product was originally intended as a service to other algorithms within the VIIRS processing environment. These other algorithms that require aerosol information before processing their products require aerosol information at all pixels. Because the VIIRS aerosol algorithm purposely avoids situations ill-suited for an aerosol retrieval (clouds, bright surfaces, sunglint, turbid water, inland water, etc.) there may be pixels and entire regions without an aerosol retrieval. This leaves the dependent algorithms unable to proceed with their retrieval. In order to provide aerosol information for every pixel, even those determined to be unsuitable for an aerosol retrieval, the VIIRS aerosol IP products fill the retrieval gap with a combination of interpolation from nearby retrievals and model results from an operational aerosol chemical transport model, the Naval Aerosol Analysis and Prediction System (NAAPS) or from climatology.

Using model or climatology data to fill in for missing retrievals is done only at the IP level. There is no model data in the VIIRS aerosol EDR products. Furthermore, there is a flag in the IP product that clearly identifies when the source of a pixel's aerosol information comes from NAAPS or from climatology, making it easy to mask out the ancillary data if it is deemed unsuitable for a specific application of the IP data.

The protocol is to go first to NAAPS to fill in for missing data, and only if NAAPS is also missing, to go to climatology.

3.7.1.1 The interpolation algorithm

The estimate of AOT over pixels not retrieved directly by the aerosol algorithm can be obtained

either by interpolating from surrounding retrievals or by using ancillary data, in this case either NAAPS results or climatology. Whether the gaps are filled by interpolation or by ancillary data, we refer here to the procedure as the "interpolation algorithm".

After the AOT retrieval is done for all retrieved pixels in a whole granule of x**,** y pixels, the algorithm attempts to fill missing pixels by interpolation between the nearest retrieved pixels The NAAPS / climatology is used only if the total weight of retrieved pixels within a certain neighborhood (searching window) of a current missing pixel is insufficient for interpolation. As a result, the algorithm fills small missing areas with interpolated AOTs, before it fills inner parts of extended missing areas (deserts, snow/ice) with NAAPS or monthly mean climatology AOT and provides a smooth transition from interpolation to NAAPS /climatology at the edges of extended missing areas.

In general, AOT for the current missing pixel $\tau_{miss}(i_0,j_0)$ is calculated as a weighted sum of interpolated AOT, $\tau_{int}(i_0,j_0)$, and the NAAPS/climatology AOT, τ_{clim}:

$$\tau_{\text{miss}}(i_0, j_0) = p_{\text{int}}\,\tau_{\text{int}}(i_0, j_0) + p_{\text{clim}}\,\tau_{\text{clim}}(i_0, j_0) \tag{3.27}$$

$$p_{\text{int}} + p_{\text{clim}} = 1 \tag{3.28}$$

$\tau_{int}(i_0,j_0)$ is calculated as a weighted sum of retrieved AOT values $\tau_{ret}(i_0,j_0)$for all pixels (i,j)within a searching window surrounding the current pixel. Accumulation of the weighted sum is performed sequentially over expanding squares, from the center of the searching window to its edges:

$$S_K = \sum_{i=i_0-K}^{i_0+K} \sum_{j=j_0-K}^{j_0+K} w(i-i_0, j-j_0) \tag{3.29}$$

$$\tau_{\text{int},K(i_0,j_0)} = \frac{1}{S_K}\left[\sum_{i=i_0-K}^{i_0+K} \sum_{j=j_0-K}^{j_0+K} w(i-i_0, j-j_0)\,\tau_{ret}(i,j)\right] \tag{3.30}$$

where K=1,2,…,DIST, i,j are coordinates of pixels, neighboring to the current bright one, DIST is a maximum distance (in pixels) from the current pixel within which pixels are participating in the interpolation. In fact, DIST determines the size of the searching window, which is 2*DIST+1. The final AOT interpolated estimate, $\tau_{int}(i_0,j_0)$ is defined as,

$$\tau_{\text{int}}(i_0, j_0) = \tau_{\text{int,K 0.5}}(i_0, j_0) \tag{3.31}$$

where K0.5 is equal to the minimum K value at which,

$$S_{K0.5} \geq 0.5 S_{DIST} \tag{3.32}$$

S_{DIST} is the maximum possible value of the accumulated sum for the entire searching window:

$$S_{DIST} = \sum_{i=i_0-DIST}^{i_0+DIST} \sum_{j=j_0-DIST}^{j_0+DIST} w(i-i_0, j-j_0) \tag{3.33}$$

The weights *w* are determined as follows:

$w(i-i_o,j-j_o) = f(i-i_o,j-j_o)$ if the (i,j) pixel is "retrieved",

$w(i-i_o,j-j_o) = 0$ if the (i,j) pixel is "missing".

The function $f(i-i_o,j-j_o)$ decreases with the distance from the current pixel:

$f(i-i_o,j-j_o) = \exp(-((i-i_o)^2+(j-j_o)^2)/(2\sigma))$, $\sigma=(DIST/3)^2$.

This way of pixel accumulation, from the window center to its edges and stopping when the condition (Eq. (3.32)) is met, allows suppressing the influence of the far outliers within the searching window if there are enough retrieved pixels for interpolation in the close neighborhood of the missing pixel. On the other hand, if the number of retrieved pixels at the window center is insufficient, the interpolation accounts for distant retrievals at the edges of the searching window. Another advantage of this method of interpolation is that it requires the accumulation of fewer pixels than accumulation over the entire searching window. This reduces execution time required for interpolation.

The maximum value of S_{DIST}, S_{max}, takes place if all pixels within the entire searching window are retrieved:

$$S_{\max} = \sum_{i=i_0-DIST}^{i_0+DIST} \sum_{j=j_0-DIST}^{j_0+DIST} f(i-i_0, j-j_0) \tag{3.34}$$

Intuitively, in this case the best interpolation accuracy is achieved. The interpolation accuracy deteriorates when the number of retrieved pixels within the window is getting less or when they move further from the window center. Since this corresponds to decreasing S_{DIST} from S_{max} to lesser values, the ratio S_{DIST}/S_{max} can be used as a measure of interpolation accuracy. When S_{DIST}/S_{max} becomes less than a certain threshold value Δ, the algorithm invokes NAAPS or climatology to construct an estimated AOT as a weighted sum of interpolation and NAAPS/climatology (Eq. (3.27)). Accordingly, relative contributions of interpolation and NAAPS / climatology into the final AOT estimate are:

$p_{int} = 1$, $p_{clim} = 0$, if $S_{DIST}/S_{MAX} \geq \Delta$ or the NAAPS / climatology AOT is unavailable,

$p_{int} = S_{DIST}/S_{max}/\Delta$, $p_{clim}=1 - S_{DIST}/S_{max}/\Delta$ if the NAAPS / climatology AOT is available and $S_{DIST}/S_{MAX}<\Delta$.

As a result, the algorithm involves two user-defined parameters: the half-size of a searching window, DIST, and the interpolation threshold Δ. In our tests, we put DIST=20 and Δ=0.25.

The interpolation algorithm marks pixels, filled with interpolation, NAAPS / climatology and with the mixture of both with a special flag, qf_data.climo (the three bit in the third quality flag for interpolation/NAAPS/Climatology processing). This flag, which is initially set to 0 for all non-retrieved pixels, is reset to the following values after the interpolation:

qf.data.climo = 0 if value is achieved without either interpolation or NAAPS/climatology,
qf_data.climo = 1 if value is achieved through interpolation,
qf_data.climo = 2 if value is achieved through both interpolation + NAAPS / climatology,
qf_data.climo = 3 if value is achieved through only NAAPS / climatology.

Users should be aware that using the IP product with filled or interpolated values introduces sharp gradients into spatial distribution of the product. Figure 3.9 illustrates these sharp gradients and how judicious use of the qf.data.climo flags will identify the affected pixels. No NAAPS/climatology pixels are designated as “high quality”, in the final products, so if users simply restrict their use of VIIRS AOT products to “high quality”, they will avoid encountering any NAAPS/Climatology pixels altogether. This is demonstrated in the bottom panel of Figure 3.9 for the IP product.

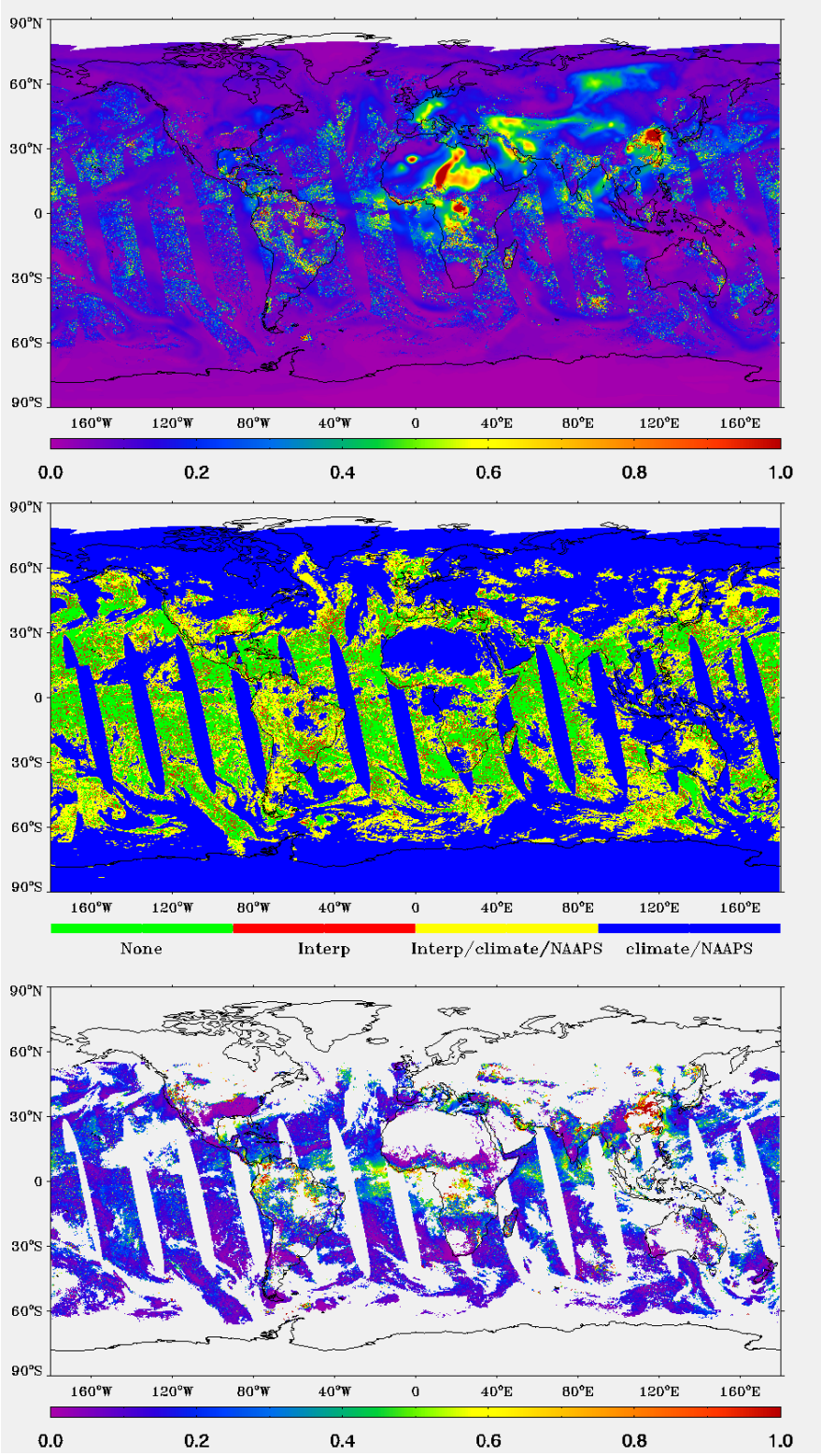

Figure 3.9 VIIRS IP AOT product for Feb. 24, 2013. (Top) AOT field including pixels filled with NAAPS/Climatology and/or interpolated. (Middle) the data.climo quality flag indicating source of

each pixel. The 'None' category in green depicts true retrievals from satellite data. (Bottom) AOT field for 'high quality' IP product that includes only pixels with qf.data.climo = 0.

3.7.2 Aggregation to EDR

The VIIRS aerosol EDR product is the main output of the VIIRS aerosol algorithm. It is constructed by aggregating 8 x 8 arrays of retrieved AOT pixels at the IP resolution. The EDR aggregation algorithm does not use the interpolated/filled IP pixels described in Section 3.7.1.1, and includes only IP pixels of qf_data.aotqf <= 1. The aggregation procedure makes use of a system of quality checks and filtering, resulting in a more robust product than the IP product, though at reduced spatial resolution. Figure 3.10 illustrates the procedure.

Each IP aerosol value is identified with a collection of data quality flags that identify situations that potentially may degrade the product. With some situations, the product is so degraded that no retrievals are made. Such cases include certain missing inputs and situations inappropriate for retrieval as described in Sections 3.3.1 and 3.4.1. These situations are identified as "not produced" by the top level IP quality flag and the AOT, Ångström Exponent and Suspended Matter fields contain fill values. These are the pixels denoted as "missing" in the interpolation procedure of Section 3.7.1.1. The next category of IP quality flags is "excluded". These pixels contain retrieved values for AOT, and may also for Ångström Exponent and Suspended Matter, but the algorithm encountered missing inputs whose absence in the retrieval will severely affect results. Also excluded are retrievals of AOT at 550 nm either negative or greater than 2.0, and retrievals of Ångström Exponent less than -1.0 or greater than 3.0. "Excluded" aerosol IP pixels will not be included in the EDR aggregation. The final two IP quality categories: "degraded" and "high quality" are both included in the aggregation. "Degraded" IP retrievals may be affected by low solar elevation angle, adjacent clouds, cloud shadows, thin cirrus, volcanic ash, soil dominant pixels or inability to reduce the retrieval residual to below an acceptable threshold. Ångström Exponent IP products are also degraded for AOT at 550 nm less than 0.15. Despite the possibility of degradation, these IP pixels are considered for the EDR product, but will be flagged at lower qualities.

The aggregation algorithm is a cascade of logical 'IF" statements that attempts to weed out less robust situations, or at least flag those situations as lower quality at the EDR level. If the 8x8 EDR cell contains at least 17 IP AOT retrievals of "high quality", the EDR AOT will be produced from these high quality pixels only, and the resulting EDR product will be labeled as "high quality". The IP pixels in that EDR cell are sorted according to the AOT at 550 nm. The darkest 20% and brightest 40% are discarded and the EDR AOT is calculated from the average of the remaining high quality IP AOT values.

The Ångström Exponent IP retrievals go through a similar set of thresholds. There must be at least 17 Ångström Exponent IP retrievals labeled as "high quality" for a high quality Ångström Exponent EDR product. The EDR is produced only from high quality IP Ångström exponents that are sorted according to AOT at 550 nm, with the darkest 20% and brightest 40% discarded before the Ångström Exponent values are averaged from the remaining pixels.

If there are insufficient high quality IP pixels to produce a high quality EDR, the thresholds are relaxed and "degraded" pixels are included in the sorting and final averaging. All EDR retrievals that use "degraded" IP pixels are flagged as either "medium" or "low" EDR quality retrievals. The aggregation logic is displayed as a flowchart in Figure 3.10, and the details can be found in the Aerosol_Product_Users Guide_V4.docx.

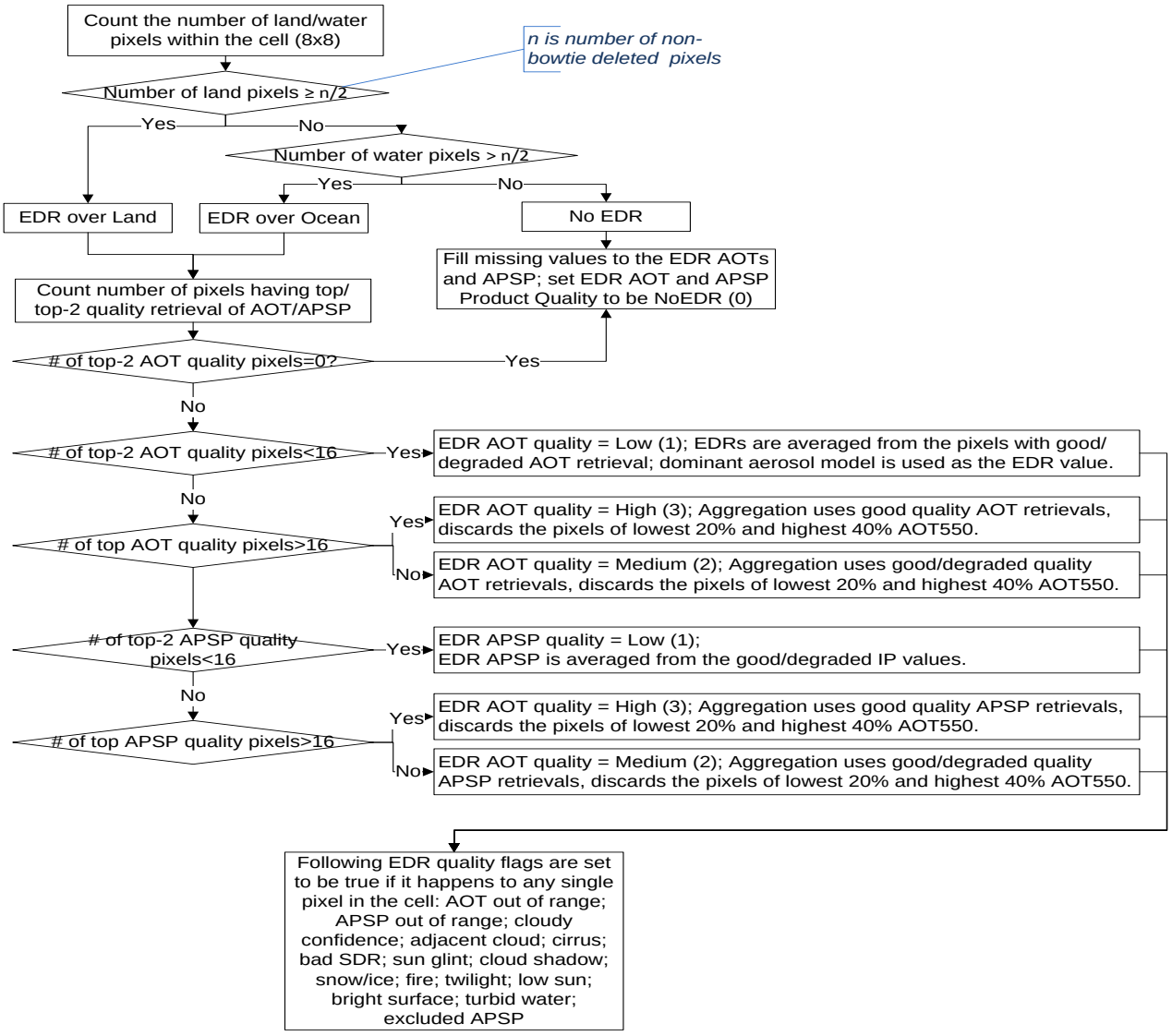

Figure 3.10 IP to EDR aggregation flow chart.

3.8 Quality flag considerations

Quality flags are an essential component of the VIIRS aerosol products. These flags are produced specifically for each product: EDR and IP; AOT, Ångström Exponent and Suspended Matter. They

report an overall quality of the retrieved product, trace the origin of the values in the product array and provide diagnostic information on the algorithm results. The accuracy, precision, uncertainty and general usefulness of each product can be significantly different for products labeled by different quality flags. Thereby, users are strongly cautioned to access and consider quality flag information in conjunction with the retrieved aerosol parameters.

The IP product quality flags provide top level information on the overall quality of each pixel aerosol retrieval for AOT, Ångström Exponent and Suspended Matter separately. This top level quality is unpacked from the top byte and cascades from QF=00 (integer value 0) denoting "high quality" to QF=01 (integer value 1) denoting "degraded" to QF=10 (integer value 2) denoting "excluded" to finally QF=11 (integer value 3) denoting "not produced". Only IP QF =0 or 1 are used in the aggregation to the EDR product. See Section 3.7.2. The IP quality flags also provide information from the cloud mask, land/sea and day/night masks, the history of how the retrieval handled different internal avoidance masks (i.e. glint masks, etc.), and other situations encountered during the retrieval that may affect quality, such as extreme solar zenith angles. The IP quality flags also indicate whether the aerosol value at this pixel is derived 100% from satellite inputs at that pixel, or whether the values have been interpolated from nearby pixels or whether the information has been supplemented with predictions from the NAAPS model. See Section 3.7.1.

For the EDR product there are 5 bytes of quality flags relaying information about the AOT and Ångström Exponent retrievals. The top level bytes provide information on the overall quality of the AOT and Ångström Exponent products in the nominal 6x6 km^2 retrieval cell, based on the aggregation procedure and the quality flags of the IP pixels used within that retrieval cell. Here the cascades runs from QF=00 (integer value 0) denoting "not retrieved" to QF=01 (integer value 1) denoting "low" quality to QF=10 (integer value 2) denoting "medium" quality to QF=11 (integer value 3) denoting "high" quality. *Note that the cascade of integer quality values for the EDR product runs oppositely to that of the IP product.* An EDR QF=3 denotes a *high quality* retrieval, while an IP QF=3 denotes "*not produced*".

The EDR quality flags are set based on how many IP pixels of which IP QF are used in the aggregation. An EDR QF=3 denotes that a minimum of 17 IP pixels of QF=0 (high IP quality) are used in the aggregation and that no IP pixels of QF > 0 (less than high quality) are used to make the EDR product. An EDR QF=2 denotes that at least 16 IP pixels of either QF=0 or 1 are used to make the EDR product. An EDR QF=1 denotes that less than 16 pixels of either QF=0 or 1 are used to make the EDR product, and an EDR QF=0 denotes that no EDR product is produced.

The remaining bytes of the EDR quality flag contain diagnostic information on the pixels aggregated into the EDR product including which aerosol models were used and whether any pixels in the 8x8 array might be affected by cloud contamination, glint, cirrus, snow/ice, shadows, low sun angle, bright surfaces, etc. In the case of the aerosol model indicator, the quality flag denotes the dominant aerosol model of the 8x8 retrievals in the EDR cell. There is also an indicator of low AOT causing exclusion of the Ångström Exponent product.

The Suspended Matter quality flag is only one byte containing quality information on "detection", "type" and "smoke concentration". The reason for separate quality flags for "detection" and "type" is that detecting an aerosol event is easier and can be done with confidence at lower aerosol loading than determining the aerosol type in the event. Thus, the AOT threshold for a high quality suspended matter product to detect an event is AOT > 0.5, while the threshold for a high quality typing is AOT > 1.0. For suspended matter the cascade of quality runs similarly to the EDR cascade, from 00 (integer value 0) being "not produced" to 11 (integer value 3) being "high quality". The quality is taken from the IP retrieval quality flags directly, except IP QF = 'high quality' or 'degraded' are downgraded to Suspended Matter QF =1 (excluded) if AOT at 550 nm < 1.0. The Suspended Matter product is only produced with confidence if there is sufficient aerosol loading. Also, if volcanic ash is identified via the input information from the VIIRS Cloud Mask, the quality is reset to QF=3 no matter the IP QF and no matter the aerosol loading.

Details of the quality flags can be found in this document in Appendix C, and in the JPSS Operational Algorithm Description Document for VIIRS aerosol products (AOT, APSP & SM) Intermediate Product (IP)/Environmental Data Records (EDR) Software, and also in the Aerosol_Product_Users Guide_V4.docx.

4.0 PRELIMINARY VALIDATION

Serious validation of the VIIRS aerosol products began on 2 May 2012, about six months after the launch of Suomi-NPP. The six month delay allowed the primary input parameters used by the aerosol algorithm spectral refectances (SDRs) and cloud mask products (VCM) to have opportunity to characterize and adjust their at-launch algorithms. Product evaluation began with data collected on 2 May 2012 and continues with data collected through March 2013.

Figure 4.1 gives a time line of important VIIRS aerosol validation milestones during this period. Changes in the algorithm dictated 2-3 time intervals in the preliminary validation analysis. These intervals are:

Land (**L1**: May-Sep 2012; **L2**: Dec. 2012-Jan. 2013; and **L3**: Feb.-Mar. 2013)
Ocean (**O1**: May-Sep 2012; **O2**: Dec. 2012.-Mar. 2013)

The interval between **L1** and **L2** or between **O1** and **O2** is not analyzed because of a processing error introduced on Oct. 15, 2012 at 15:19 GMT and corrected on Nov. 27, 2012 at 14:58 GMT. VIIRS aerosol data should not be used from 15 October to 27 November 2012.

The L3 period is fundamentally different from the previous land periods because a Processing Coefficient Table (PCT) change implemented on Jan. 22, 2013 at 17:28 GMT. The PCT change substituted new surface reflectance ratios in the land algorithm, and affected only the land algorithm, not the ocean algorithm. Table 3.6 shows both sets of surface reflectance ratios. The "at launch" ratios were used by the algorithm during periods **L1** and **L2**. The "current" ratios were implemented during the PCT change and are used during **L3,** and beyond.

The preliminary validation described in this section will label plots either by **L1**, **L2**, **L3**, **O1**, **O2** descriptions, or by 'PCT' or 'IDSP' designations. PCT indicates the plot was created using the same algorithm applied operationally during **L3**, but applied off-line to earlier data for testing purposes. IDSP indicates the plot used the results of the operational algorithm in effect at that time. Thus, 'PCT' results use the 'current' surface ratios of Table 3.6, and 'IDSP' results use the 'at launch' surface ratio values. All examples avoid the period, 15 October to 27 November 2012.

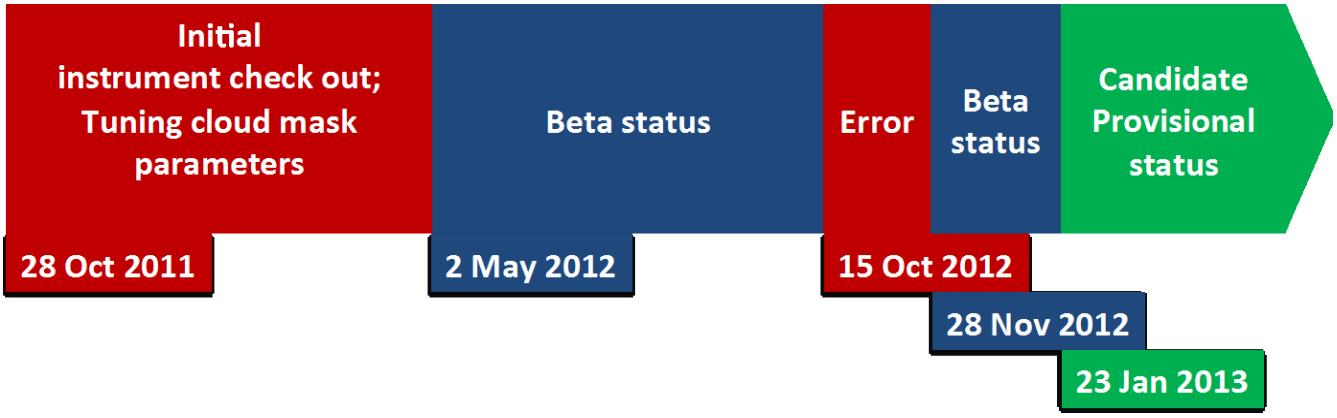

Red periods:	Product is not available to public, or product should not be used.
Blue periods:	Product is available to public, but it should be used with caution, known problems, frequent changes.
Green period:	Product is available to public; users are encouraged to evaluate.

Figure 4.1 Time line of VIIRS aerosol product milestones and product status.

4.1 Validation Data Sets

The VIIRS AOT and Ångström Exponent products have been compared with aerosol products derived from observations of the AErosol RObotic NETwork (AERONET) (Holben et al., 1998) and Maritime Aerosol Network (MAN) (Smirnov et al., 2009), and with the Moderate Resolution Imaging Spectroradiometer (MODIS) onboard the NASA Earth Observing System (EOS) satellites (Terra and Aqua) (Remer et al., 2005; Levy et al., 2007). VIIRS Suspended Matter has been compared with Cloud-Aerosol Lidar and Infrared Pathfinder Satellite Observations (CALIPSO) products. Comparisons include direct collocations of various match-up criteria, and also comparisons of monthly statistics without the benefit of direct collocation.

AERONET Level 2 Quality Assured direct sun observations of AOT are accurate to within 0.01. However, because the VIIRS evaluation is proceeding in near-real time, the match-ups used here in

this evaluation are Level 1.5 and have not been quality assured. This does not mean that the AERONET accuracy is systematically degraded from 0.01, but that there could be localized stations where this accuracy standard is not met. Nonetheless AERONET provides the best means of quantitatively validating satellite-derived AOT parameters. However, validation stations are spatially limited and do not offer a complete global evaluation. Especially lacking in the land-based AERONET data base are opportunities to evaluate aerosol products over oceans.

The MAN observational network, under the AERONET umbrella, is based on the results of handheld sunphotometers deployed on a variety of ships traversing the open oceans, either on research cruises or from merchant marine ships that follow the shipping lanes. The inherent accuracy of the handheld devices coupled with the human component of making the measurements on a rolling ship render the MAN AOT to be less accurate (0.02) than at the land-based robotic AERONET stations (Smirnov et al., 2009). Also, data continues to be scarce in the MAN network.

The MODIS aerosol product used in the comparisons is the Collection 5 Dark Target product over land and ocean. The MODIS product has been in production for a dozen years, has undergone continuous evaluation during this time and is considered to be a characterized product with well-understood error bars, which are stated to be ±0.03±0.05AOT over ocean and ±0.05±0.15AOT over land. The advantage of the MODIS comparisons is the broad regions that can be covered and the vast number of collocations.

Because of CALIOP's depolarization and color ratio capabilities this instrument is able to confidently discriminate between dust and other types of aerosol. CALIOP's maps of dust and non-dust aerosol are the primary reality-check on the VIIRS-retrieved Suspended Matter product.

Both qualitative and quantitative assessments are made. The qualitative assessment compares maps of VIIRS aerosol EDRs to similar products from MODIS and CALIOP to show that the VIIRS products indeed "look like" aerosol products. The quantitative assessment describes the level of agreement in terms of accuracy (bias) and precision (standard deviation of differences between retrievals and reference data).

4.2 VIIRS vs. MODIS

VIIRS EDRs are characterized in their relationship to MODIS aerosol data, which is itself a validated product. The analysis here relies on direct collocation between VIIRS and MODIS, following these criteria:

- MODIS (Level 2) and VIIRS (IP/EDR) AOT are matched in time within 5 minutes
- VIIRS AOT from nearest pixel falling within a MODIS 10 km box.
- Both MODIS over Land and over Ocean AOTs are filtered with MODIS Cloud Fraction = 0 (from aerosol cloud mask)
- MODIS AOT is filtered with the best MODIS Quality Assurance Land and Ocean Flag
- VIIRS AOT is filtered with QF=3 (high quality)

Figure 4.2 shows the VIIRS EDR and MODIS global collocated ocean mean AOT averaged over the 4 month period Dec. 2012 through Mar. 2013 (**O2**). These VIIRS data benefit from MODIS' ability to screen data and select pixels for retrieval. VIIRS EDR reproduces the MODIS Dark Target picture of the global aerosol distribution with somewhat smaller VIIRS AOT at high latitude oceans and somewhat higher AOT at tropical latitudes.

Figure 4.3 shows the VIIRS EDR and MODIS global collocated land and ocean mean AOT averaged over the two month period Feb.-Mar. 2013 (**L3**). This is a shorter period than shown in Figure 4.2. Here, we see that the land AOT is biased high against MODIS in some regions (e.g. the Amazon in South America) and biased low in other regions (e.g. India and China). However, there has been an overall improvement in bringing down the global land high bias seen in VIIRS retrievals over the **L1** and **L2** periods. A demonstration of that improvement is seen in Figure 5.3 and Figure 5.4, where the new ratios (PCT) are implemented for the exact same data as the operational algorithm using the at launch ratios (IDPS). The result is a reduction in overall bias between VIIRS and MODIS from 0.050 to -0.002.

Figure 4.4 shows the scatter plots of VIIRS versus MODIS calculated from the collocated data sets. Both EDR and IP products are shown. The ocean plots are for the **O2** time period, and the land plots are for the **L3** time period. The terms accuracy, precision and uncertainty are used to quantify the evaluation. Accuracy refers to the mean bias between the two data sets. Precision is the standard deviation of the scatter, and uncertainty is the sum of accuracy and precision. As the scattered points gravitated towards the 1:1 line, accuracy (bias) and precision (scatter) should go to zero. Over ocean, VIIRS matches MODIS very well with accuracy less than 0.01, precision less than 0.05 and correlation coefficients ~0.93 for both the EDR and IP product. Over land, the EDR product matches MODIS better than the IP product, with accuracy about the same (~-0.05), but with better precision (0.15 vs. 0.19) and higher correlation coefficient (0.85 vs. 0.78).

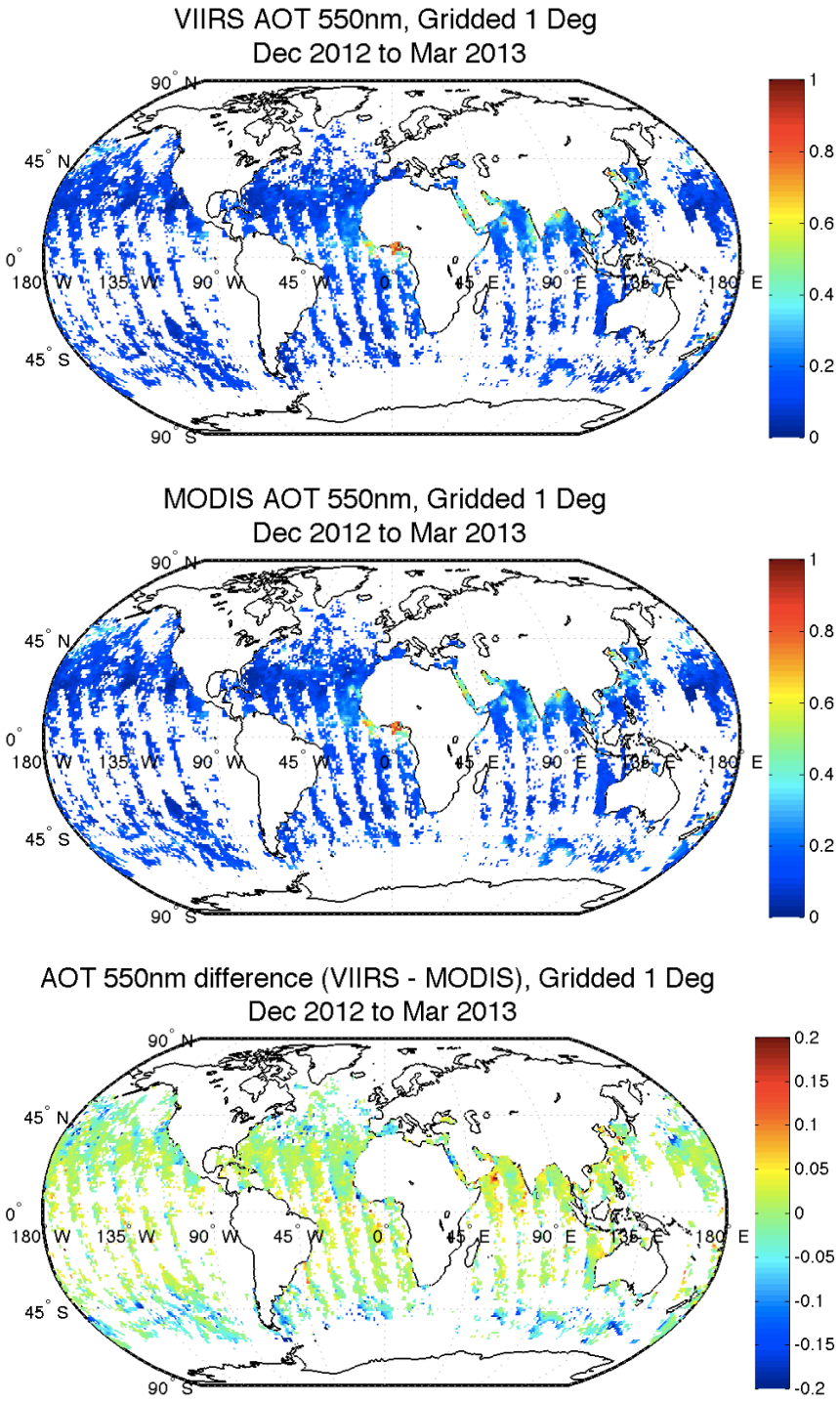

Figure 4.2 Dec. 2012 through Mar. 2013 mean collocated EDR AOT at 550 nm over ocean from VIIRS (top), MODIS (center) and the difference of VIIRS – MODIS (bottom).

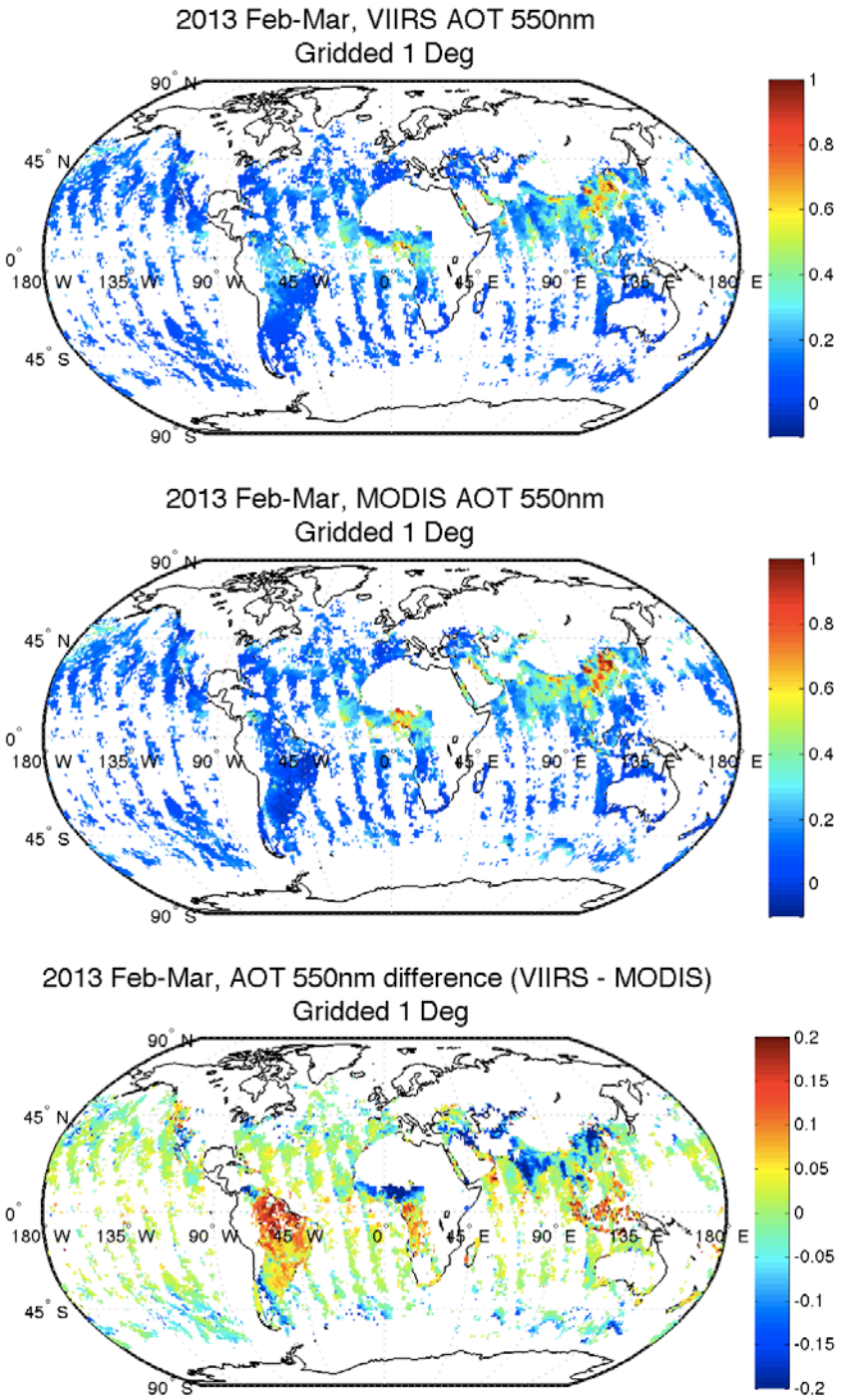

Figure 4.3 Feb.-Mar. 2013 mean collocated EDR AOT at 550 nm over land and ocean from VIIRS (top), MODIS (center) and the difference of VIIRS – MODIS (bottom).

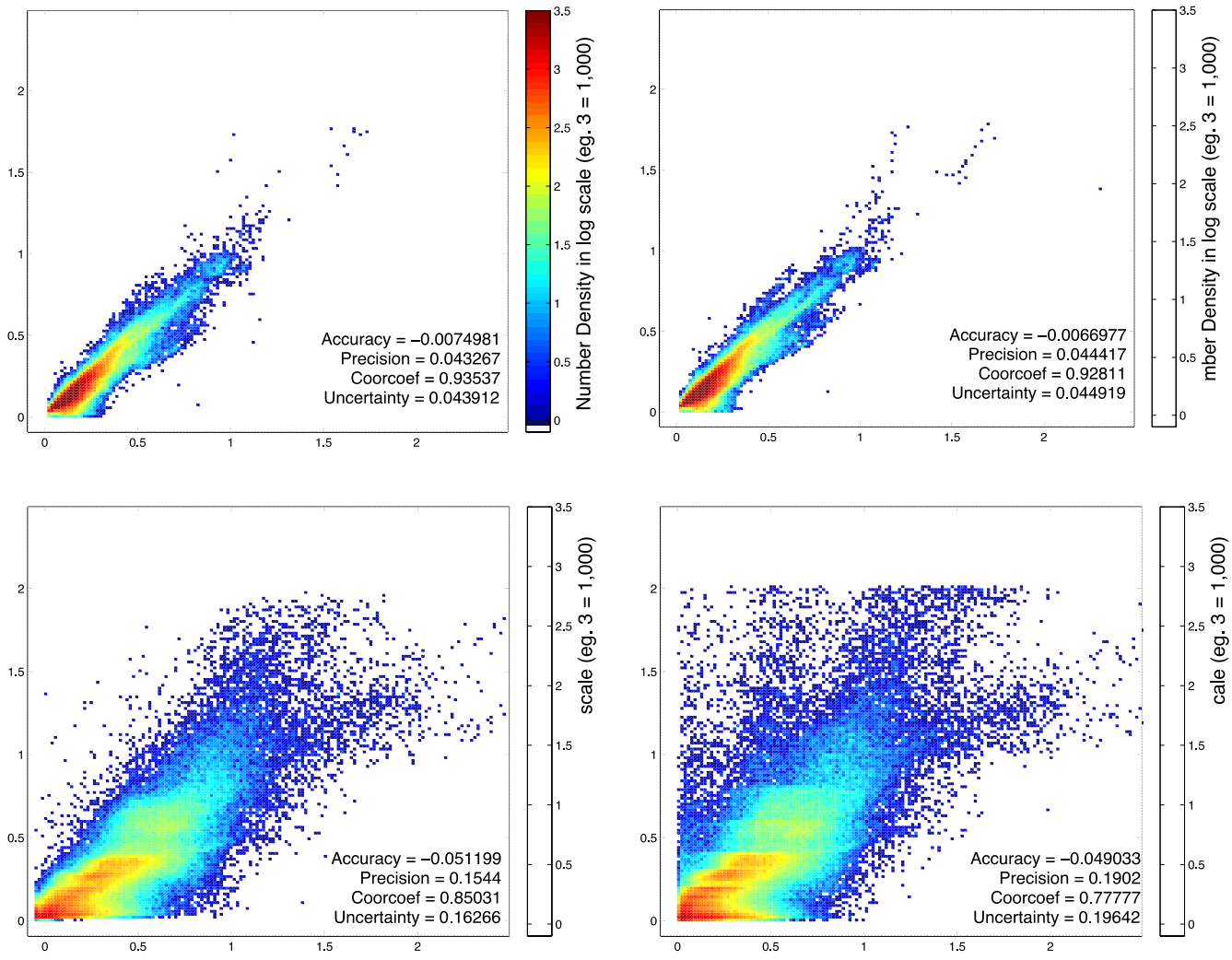

Figure 4.4 Scatterplots of VIIRS AOT plotted against collocated MODIS AOT for over ocean (top) and land (bottom) for the EDR product (left) and the IP product (right). Scatterplots are contoured density plots with each colored contour representing the number of collocations at that point. Ocean plots are for the O2 period, and land plots are for the L3 period.

4.3 VIIRS vs. sunphotometer data (AERONET and MAN)

While comparison with MODIS begins to show how well the VIIRS aerosol products can represent the large scale features of the global aerosol system, and how well VIIRS will be able to continue the heritage data records of its predecessor, the MODIS products themselves contain residual

biases and inaccuracies. Thus, true validation of the VIIRS aerosol product requires quantitative comparison with collocated sunphotometer data, primarily with AERONET, but also with MAN ship-board observations to check retrieval accuracy over ocean away from coastlines.

There is a long history of satellite-sunphotometer collocation protocol that calls on spatio-temporal statistics of the collocation. Here we use the following criteria to determine a collocation:

- AERONET L1.5 Direct Sun retrievals from a maximum of 444 sites (including the high spatial density DISOVER_AQ sites) are averaged within **±30 minutes** of VIIRS overpass time.

- Best quality VIIRS AOTs (QF=0 for IP; QF=3 for EDR) within a radius of **27.5 km** from the AERONET site are averaged.

- A minimum of **five best quality VIIRS AOT** retrievals and **two AERONET observations** must be available within the spatial and temporal constraints.

- AERONET AOT data, if observed at wavelengths other than 550 nm, are interpolated to 550 nm using AOT 440 nm and 670nm.

Figure 4.5 shows the scatter plots between VIIRS-retrieved EDR AOT and AERONET observations, and also the geographical distribution of the AERONET stations providing the collocations in the scatter plots. The color of each dot denotes the mean difference between the VIIRS-retrieved parameter and the AERONET-observed counterpart. Land retrievals are shown on the left and ocean retrievals at coastal AERONET stations are shown on the right. The land period is **L3**, and the ocean period spans both **O1** and **O2**. The VIIRS EDR over ocean retrieval of AOT compares very well with AERONET observations near coasts and islands. Correlation = 0.84, accuracy (bias) is less than 0.015 and precision is about 0.08. Over land, the agreement is also very good with correlation of 0.88, absolute accuracy less than 0.015 and precision of 0.11. The maps show that while the validation set is global, it is heavily weighted to the eastern U.S. and western Europe where the algorithm performs well. Over south Asia it appears to be biased low and in the intermountain west of the U.S., it is biased high. These regional biases against AERONET are not in phase with the biases against MODIS seen in Figure 4.3. MODIS itself experiences biases against AERONET, and also the locations of each AERONET station may not exactly represent the conditions of the larger geographical region. For these reasons, the VIIRS products must be evaluated with both AERONET and with other satellite products.

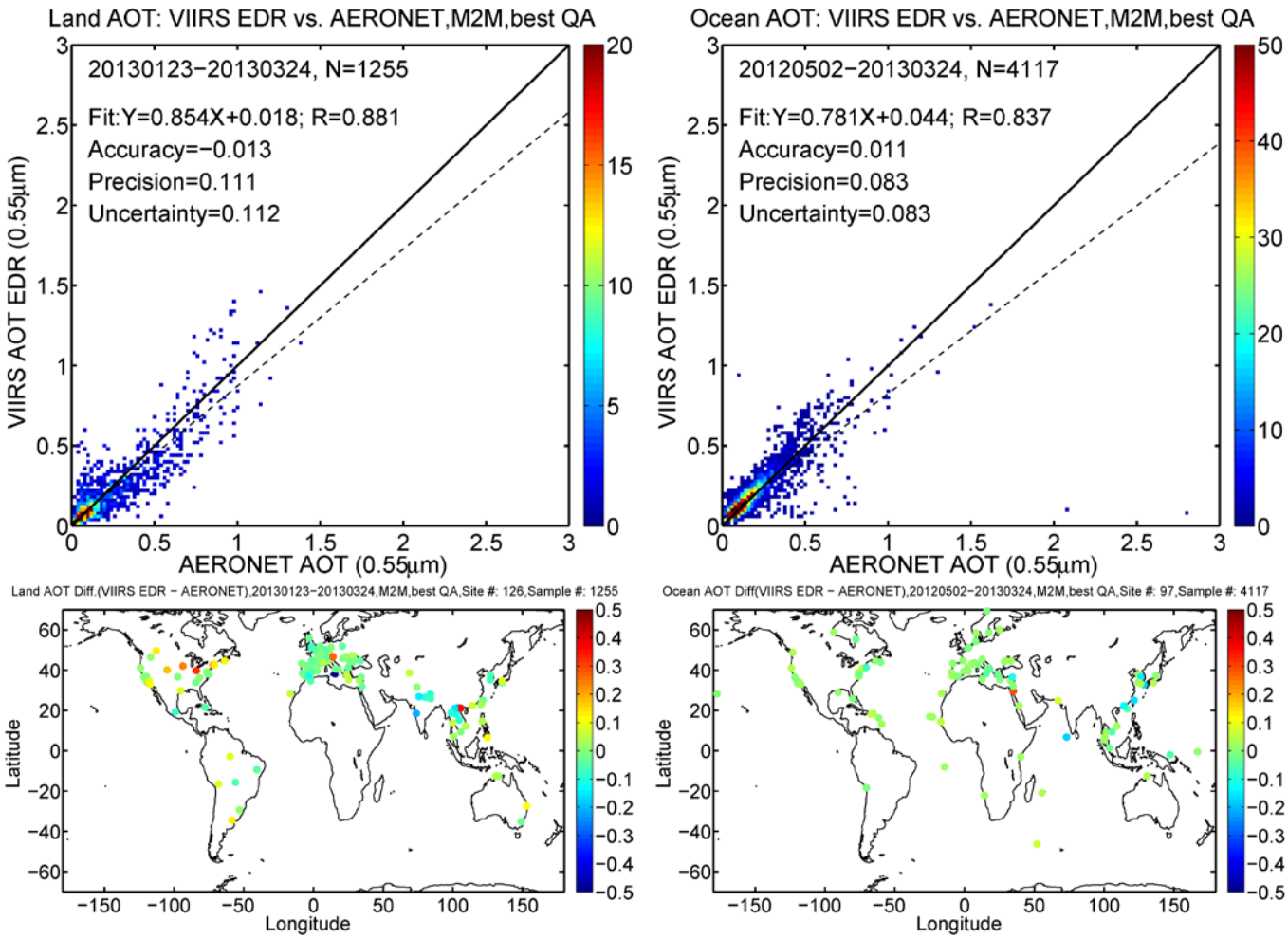

Figure 4.5 (Top) Scatter plot of VIIRS EDR AOT against AERONET observations for the land product (left) and the ocean product at coastal stations (right). The period of evaluation for land is Feb. – Mar. 2013 (L3), and for ocean it is May 2012 – March 2012, excluding Oct. 15 to Nov. 27, 2012 (O1 and O2). (Bottom) Geographical distribution of the AERONET stations providing the collocations in the scatter plots. The color of each dot denotes the mean difference between the VIIRS-retrieved parameter and the AERONET-observed counterpart.

A similar set of plots is shown in Figure 4.6, but for the IP product. Note only high quality IP retrievals are used in this evaluation so that no NAAPS/climatology or interpolated pixels are included. There is a modest degradation of quality in the ocean product in going from EDR to IP. The correlation, accuracy and precision all degrade slightly, but the IP ocean AOT remains valid. There is a more significant degradation in quality over land when moving from the EDR product to the IP product. The degradation can be seen in the scatter plot, in the regional map beneath and in the validation statistics.

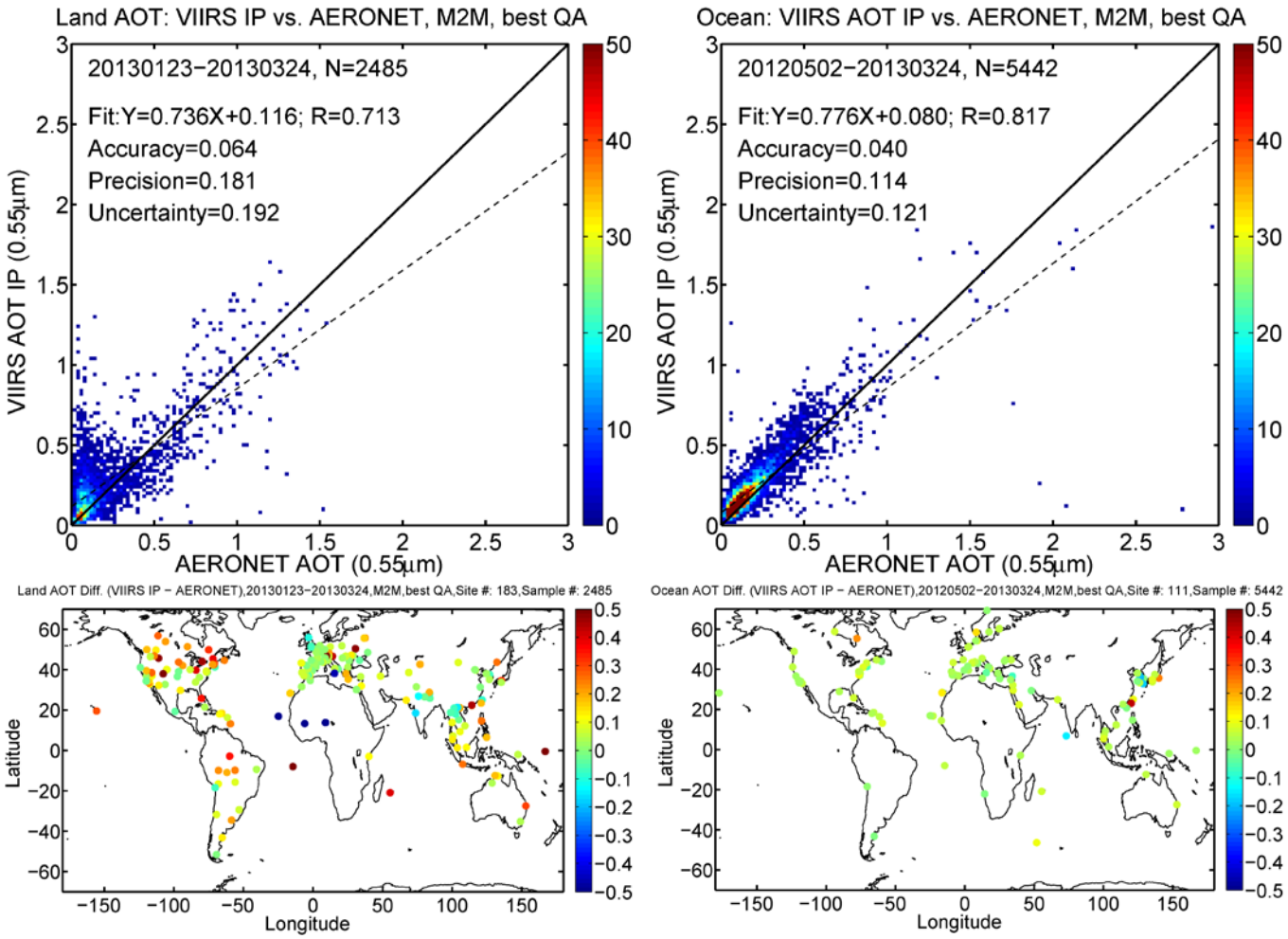

Figure 4.6 Same as Figure 4.5, but for the IP product.

Figure 4.7 shows the comparison between VIIRS AOT retrievals over open ocean and the MAN observations, for both EDR and IP products. MAN data relies on ocean cruises and data is much sparser than from the land-based AERONET network. Thus, the number of collocations are limited. Still, there is a sufficient number of samples to show that the VIIRS over ocean AOT retrieval matches the ship-board measurements extremely well with accuracy less than 0.01, precision ~0.09 and correlation coefficient greater than 0.83.

Figure 4.8 and Figure 4.9 show scatterplots between VIIRS retrieved Ångström exponent(AE) and AERONET observations for land (left) and coastal ocean (right), for the EDR product (Figure 4.8) and the IP product (Figure 4.9). The plots are similar to plots Figure 4.5 and Figure 4.6. The Ångström exponent products do not match their collocated ground truth as well as the AOT products. There appears to be some skill, but with much scatter in the over ocean EDR product, but little to no skill in the IP product or in either of the land products.

The summary of the validation for AOT is given in Table 4.1 and for the Ångström exponent in Table 4.2. These tables also show comparable evaluation of Aqua-MODIS, Terra MODIS and MISR aerosol products for the same time periods for MODIS and for a subset of the time period for MISR, land and ocean separately. We see from these tables that **VIIRS is meeting or exceeding the accuracy, precision and correlation of the well-established MODIS products.**

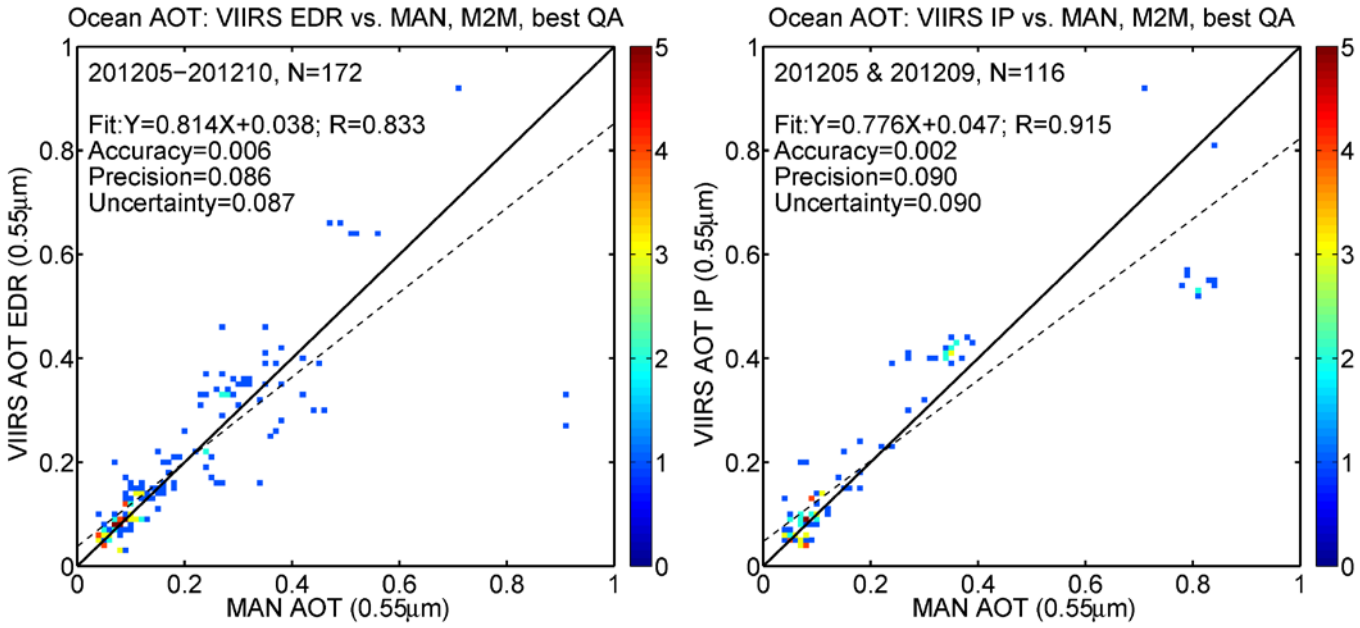

Figure 4.7 Scatterplots of VIIRS AOT retrieval versus MAN AOT observations made from shipboard measurements over open ocean. On the left is the VIIRS EDR retrievals. On the right is the IP retrievals.

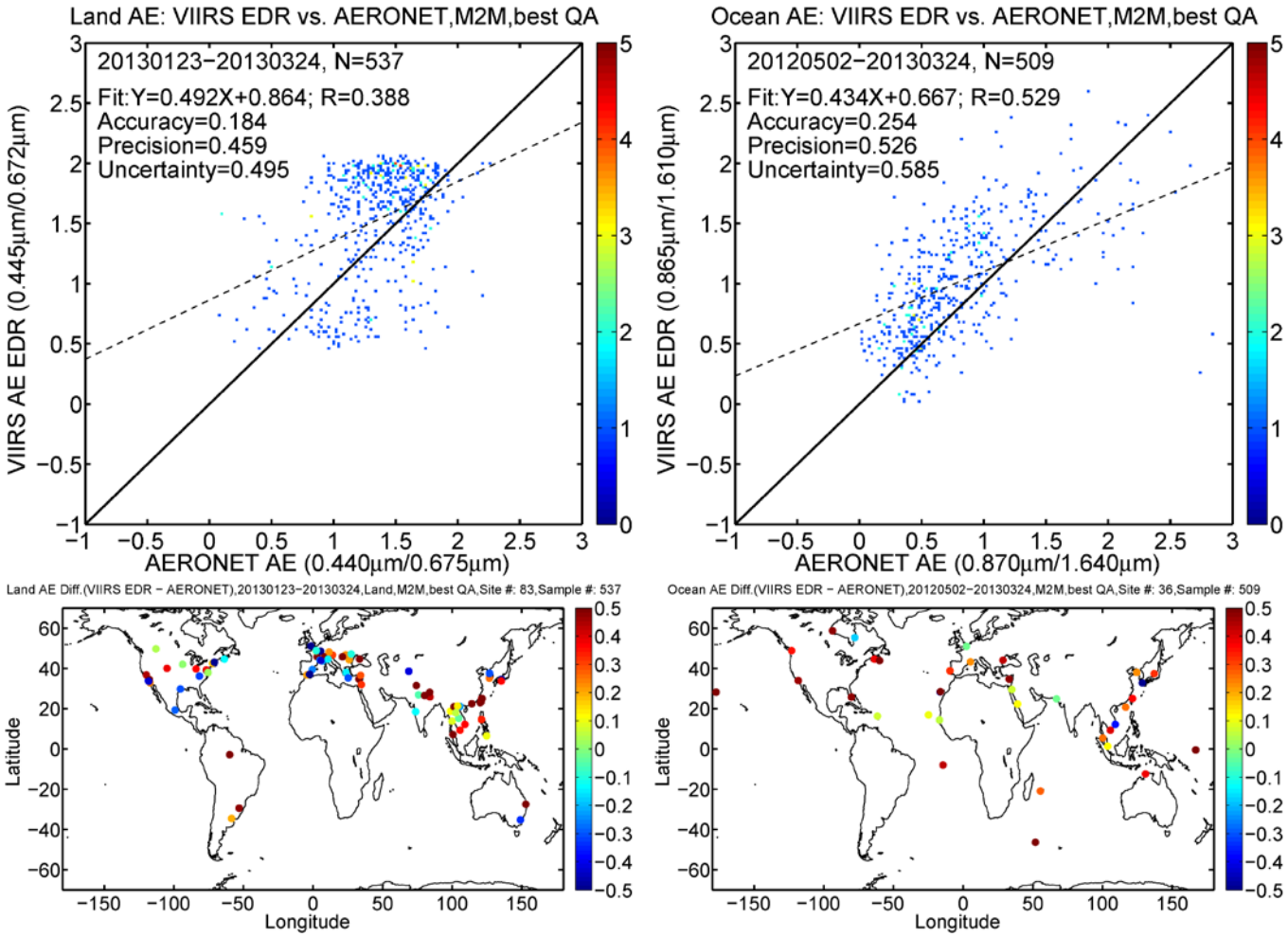

Figure 4.8 Same as Figure 4.5, but for the EDR Ångström exponent product.

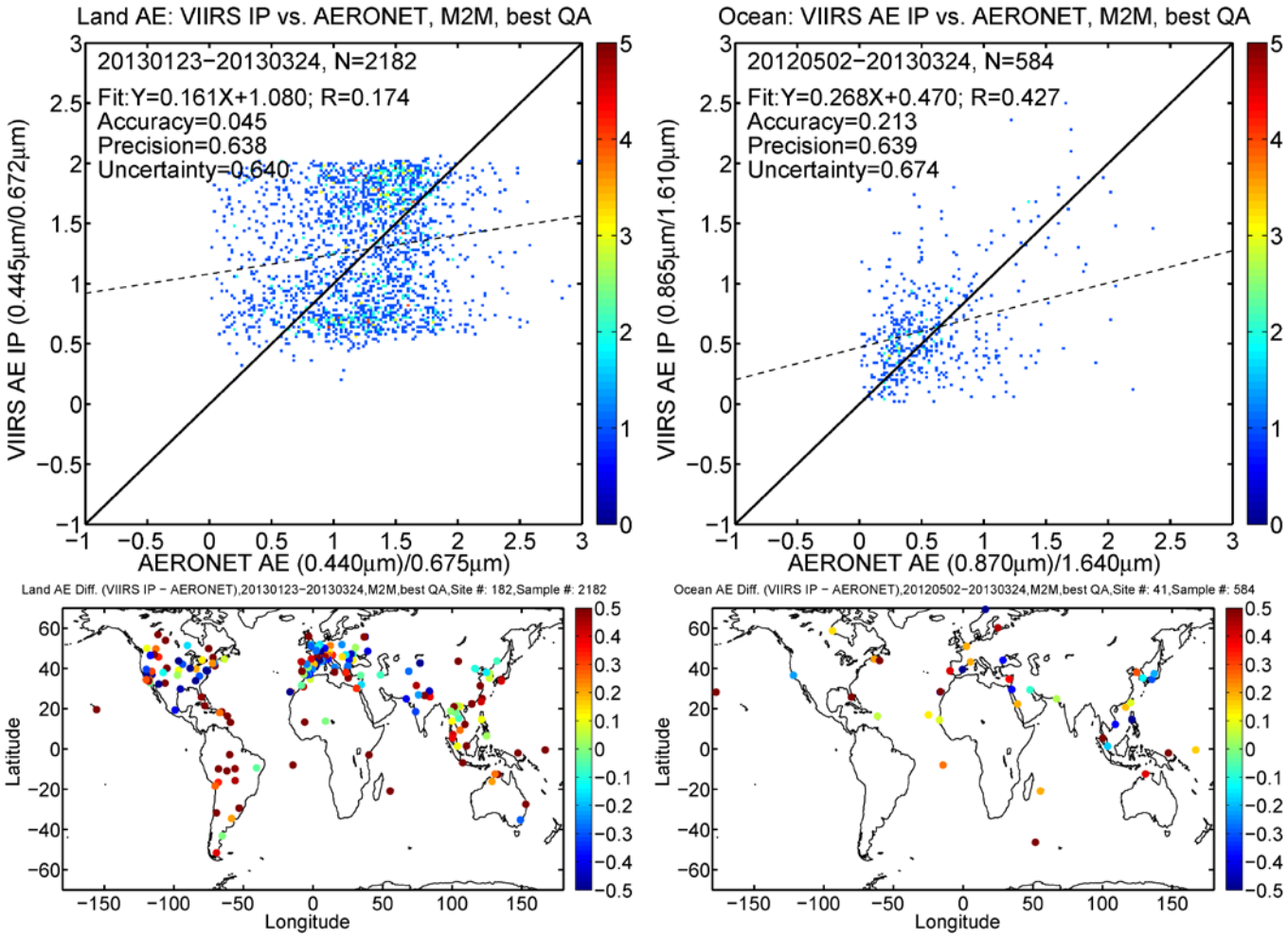

Figure 4.9 Same as Figure 4.8, but for the IP Ångström exponent product.

Table 4.1 Collocation statistics of VIIRS, Aqua-MODIS (MYD04), Terra-MODIS (MOD04) and MISR AOT product against AERONET for the appropriate time periods defined in Figure 4.5 and Figure 4.6.

EDR	**VIIRS**	**AQUA MODIS**	**TERRA MODIS**	**MISR**	**VIIRS**	**AQUA MODIS**	**TERRA MODIS**	**MISR**
AOT	**LAND**				**OCEAN**			
Sample Size	1125	1026	1269	718	4117	4742	4495	911
Accuracy	-0.013	-0.014	-0.043	-0.009	0.011	0.006	0.010	0.038
Precision	0.111	0.143	0.140	0.133	0.083	0.117	0.087	0.059
Uncertainty	0.112	0.144	0.146	0.134	0.083	0.117	0.087	0.071
Cor Coef	0.881	0.858	0.887	0.845	0.837	0.795	0.871	0.957
IP	**VIIRS**	**VIIRS**						

AOT	LAND	OCEAN						
Sample Size	2485	5442						
Accuracy	0.064	0.040						
Precision	0.181	0.114						
Uncertainty	0.192	0.121						
Cor Coef	0.713	0.817						

Table 4.2 Collocation statistics of VIIRS, Aqua-MODIS (MYD04), Terra-MODIS (MOD04) and MISR Ångström Exponent product against AERONET for the appropriate time periods defined in Figure 4.8 and Figure 4.9.

EDR	VIIRS	AQUA MODIS	TERRA MODIS	MISR	VIIRS	AQUA MODIS	TERRA MODIS	MISR
Ångström Exponent	**LAND**				**OCEAN**			
Sample Size	537	601	701	718	509	787	737	91
Accuracy	0.184	-0.272	-0.248	-0.071	0.254	-0.128	-0.230	0.153
Precision	0.459	0.686	0.675	0.404	0.526	0.639	0.726	0.393
Uncertainty	0.495	0.738	0.719	0.411	0.585	0.652	0.761	0.422
Cor Coef	0.388	0.175	0.216	0.611	0.529	0.579	0.563	0.714
IP	**VIIRS**	**VIIRS**						
Ångström Exponent	**LAND**	**OCEAN**						
Sample Size	2182	584						
Accuracy	0.045	0.213						
Precision	0.638	0.639						
Uncertainty	0.640	0.674						
Cor Coef	0.174	0.427						

4.4 Suspended matter evaluation: VIIRS vs. CALIOP

The VIIRS suspended matter product categorizes major aerosol events into volcanic ash, dust, smoke and none. See Section 3.6. An example of the global distribution of the suspended matter product showing the dominant type in each latitude-longitude grid square for the month of March 2013 is given in Figure 4.10. The algorithm requires AOT_550 = 0.50 for suspended matter to be detected and 1.0 for the type to be reported. Thus, only major aerosol events are classified. Volcanic ash is determined from the VIIRS cloud mask, and it supersedes the other categories identified within the aerosol algorithm itself. However, currently the VIIRS cloud mask has turned off the volcanic ash flag, pending improvements to the detection algorithm.

The product, as seen in Figure 4.10, is not performing adequately. There is very little dust aerosol identified. There are regions identified with smoke events that most likely have more to do with snow melt over land than with an actual event.

Dust can be identified from space due to its large particle size and non-spherical shape. Large particles decrease spectral dependence and nonsphericity introduces a different polarization signal from molecules or sphericial particles. CALIOP, with its two channel lidar system and depolarization detection capabilities is able to separate dust from other types of aerosol. Figure 4.11 shows the monthly dust fraction calculated from the VIIRS suspended matter product and from CALIOP measurements. The CALIOP measurements show a band of dust stretching from the Caribbean Sea at 60 W longitude to the east coast of Asia at 120 E longitude, and covering the Sahara, Middle Eastern and Asian deserts, all known dust sources. This global distribution of dust aerosol from CALIOP is as expected from 30 years of observations and modeling of the global aerosol system. In contrast the VIIRS dust fraction barely registers dust anywhere on the planet, just a little bit in west Africa and East Asia.

The Suspended Matter is undergoing an in depth evaluation as to how to best improve its dust-detection capabilities over both land and ocean, and also how to decrease false positives in the smoke detection.

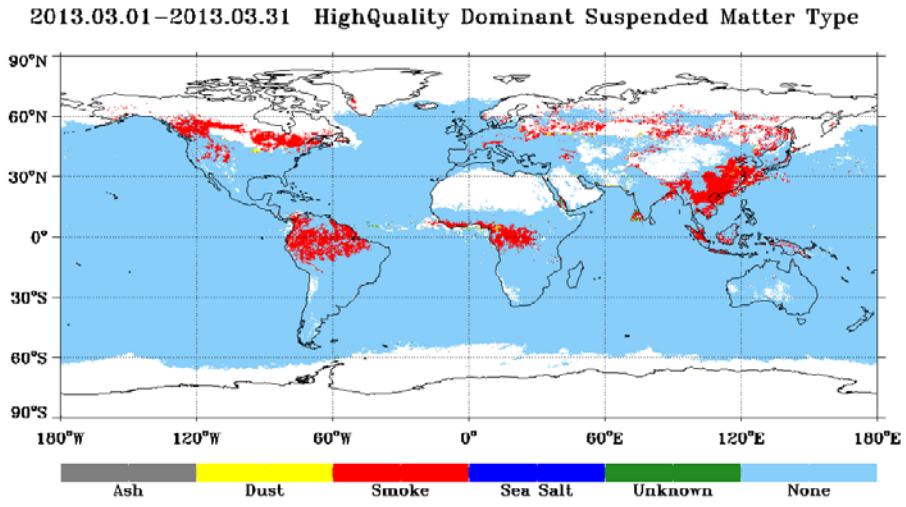

Figure 4.10 Suspended matter product for March 2013.

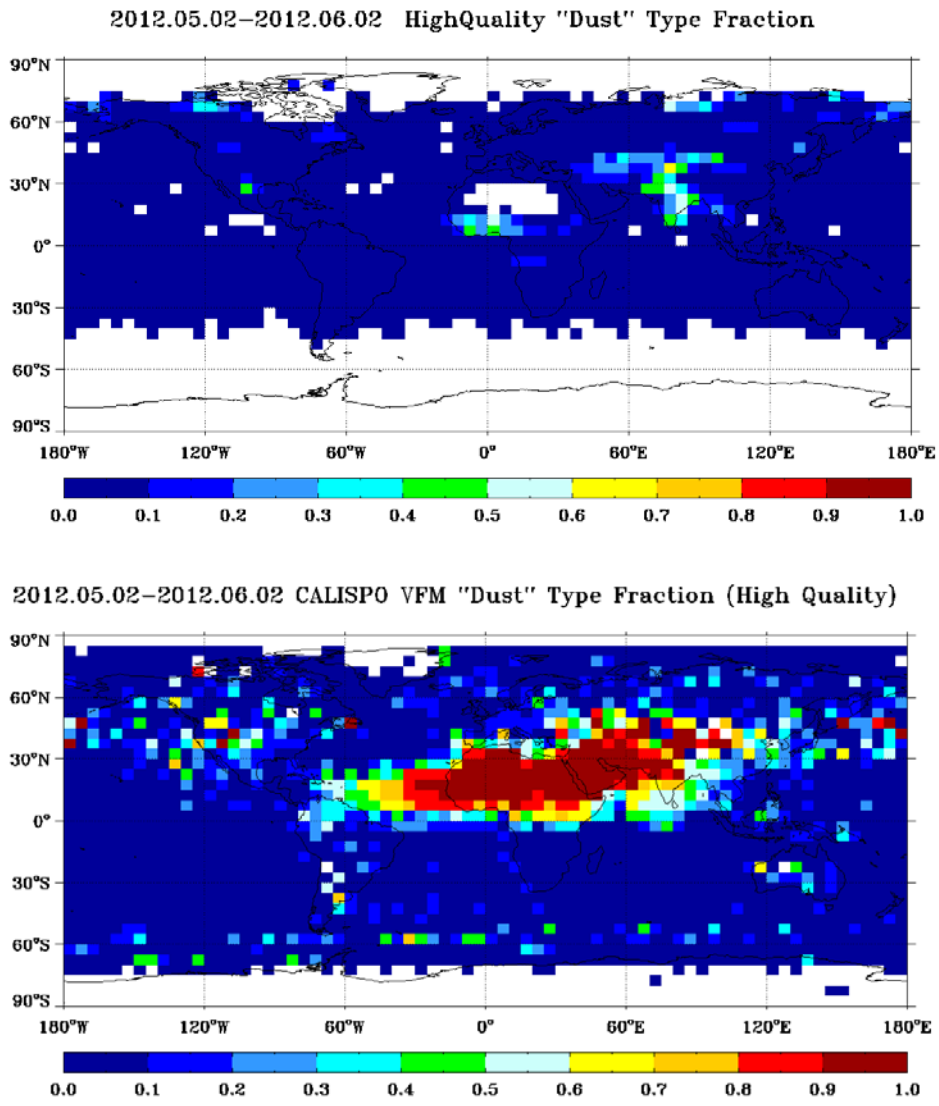

Figure 4.11 Distribution of dust fraction from the Suspended Matter product for the time period 2 May to 2 June 2012 (top). Dust fraction calculated from the CALIOP vertical feature finder product (bottom).

5.0 FUTURE UPDATES

The evaluation exercises in Section 4.0 show that VIIRS aerosol products are providing quantitative aerosol information. The exercises also point to inadequacies in some of the current products and algorithms.

The ocean AOT is matching MODIS, AERONET and MAN very well, and at this time, no further improvement is needed. The ocean Ångström Exponent matches less well, but is still returning a useable product in the EDR. We note that the VIIRS Ångström Exponent matches validation at

least as well and often better than does MODIS. There are no immediate plans to adjust the ocean algorithm, as described in Section 3.3.

The land AOT showed a systematic high bias against AERONET and MODIS before the algorithm change of 22 January 2013. Analysis of the original problem, the modification to the PCT that was implemented in January 2013, the results of that implementation and plans for further modifications to the algorithm code itself are given below (Section 5.1).

The suspended matter product is not useable at this time. A few small changes, as well as the introduction of a dust index are being explored. We note that Suspended Matter is a new product, having no predecessor in the MODIS suite of products, and so is unexplored territory, which will take longer to come to maturity.

The land Ångström Exponent is currently inadequate, although in the EDR, at least apparently better than its MODIS predecessor. The land AOT product must be improved first and the land Ångström Exponent re-evaluated before plans can be made to improve the currently ailing land Ångström exponent. An assessment will be made at that time as to whether there is sufficient information content in the VIIRS observations to compute a useful Ångström exponent. We note here that the Collection 6 MODIS algorithm will not be producing an Ångström exponent or any particle size parameter over land, having concluded after several tries that the information content does not exist in the MODIS spectral range. This conclusion may be true for VIIRS, as well, but further study is needed.

5.1 Plans for land AOT

The high bias originally seen in the over land AOT product (Figure 5.3) could have been due to several possibilities. 1) Cloud contamination introduced by the VIIRS cloud mask. 2) Other contamination introduced by inadequate filtering of the input data (Section 3.4.1). 3) Incorrect aerosol models (Table 3.5). 4) Incorrect surface reflectance ratios. 5) Inadequacy of the core retrieval to find a proper solution (Section 3.4.4). 6) Undetected coding error. While each of these is a possible explanation, the last two are unlikely.

Because the high bias persisted over many geographical and meteorological conditions, and because the high bias existed even in very low aerosol loading situations, the dominant reason for the bias was likely (4) incorrect assumptions for surface ratio. The at-launch ratios shown in Table 3.6 were derived from atmospheric correction of MODIS reflectances using roughly 40 AERONET stations. MODIS bands are similar to, but not exactly the same as the VIIRS bands in terms of central wavelength and band width. There was no reason to expect that these MODIS-derived ratios would work seamlessly in the VIIRS retrieval, and the evidence was that they did not.

VIIRS data and products (SDR, geolocation, VIIRS cloud mask, ancillary data and aerosol IP retrievals) were collected over AERONET stations and matched in time to AERONET AOT

observations. Then an atmospheric correction was performed using Equation (3.23) with AERONET supplying the AOT (τ_A). This resulted in retrieved surface reflectance values in bands M1, M2, M3, M5 and M11. The correction was done five times for each of the five land aerosol models Table 3.5, and the results over the five models were averaged. Five months of data (2 May 2012 to 2 October 2012) were processed. Only situations with low aerosol loading and low variability, as defined by at least 3 AERONET observations within 30 minutes of overpass, AERONET AOT_550 ≤ 0.10, and standard deviation ≤ 0.20. Only high quality VIIRS IP retrievals were used, pixels had to be within 5 km of the AERONET station and any elevation changes within those 5 km needed to be ≤ 100 m. An additional level of filtering was imposed that required the standard deviation of the results of averaging the five models to be ≤ 5%.

Figure 5.1 shows the retrieved surface ratio between bands M3 and M5 as a function of the old VIIRS AOT retrieval error, where the VIIRS retrieval uses the at-launch values for the surface reflectance ratios. When the AOT retrieval error is zero, the retrieved surface ratio is close to the old assumed value in the algorithm (0.578). When the ratio is higher than the old assumed value, which it is through most of the data analyzed, VIIRS develops a high bias against AERONET. This explains the persistent high bias in the land AOT seen during the validation period (May – September 2012 corresponding to **L1** from Section 4.0). Replacing the at-launch surface ratio with a higher value (0.645) will bring down the VIIRS AOT high bias in a global sense. However, individual retrievals will still be subject to errors because of large fluctuations in surface reflectance ratios as a function of vegetation amount and soil type. This is clearly seen in Figure 5.4. The at-launch values of surface reflectance ratios produce a global high bias when compared with MODIS. Changing to the current surface reflectance ratios lowers the global bias, but introduces regional biases that can be either high or low.

The current MODIS aerosol algorithm uses relationships between surface reflectance in different bands that are a function of the "greenness" of the surface. This greenness is quantified by the same *Bright_Index* of Equation (3.20). We note that the VIIRS surface reflectance ratios that are retrieved through the methodology described here are strongly monotonically dependent on the *Bright_Index*. See Figure 5.2. This suggests that if the algorithm uses dynamic surface reflectance ratios, dependent on the *Bright_Index*, not only will the global high bias in land AOT be reduced, but that the precision in retrievals will be improved as well.

Thus, the plan for improving the over land AOT retrieval has been a two-step approach, with the first step implemented already and the second step in preparation. First, modify the global surface reflectance ratios by substituting the values in Table 3.6 for the old at-launch values. This has been done by changing the PCT without modifying internal code, which went into effect on Jan. 22, 2013. The change has reduced the overall high bias in the over land product. Second, modify the algorithmic code to change the global surface ratios to become 2nd order polynomial functions dependent on the *Bright_Index*. The reason for the two-step approach is that PCT changes can be implemented into the processing stream much faster than actual changes to the code itself. Each step will make a major improvement to the product. Figure 5.4 and Figure 5.5 illustrate the improvement to the land AOT with each step. When these changes have been implemented, the land products, both AOT and Ångström Exponent will be re-evaluated. Further steps may be

needed, but until these changes are implemented and evaluated, more subtle issues cannot be addressed.

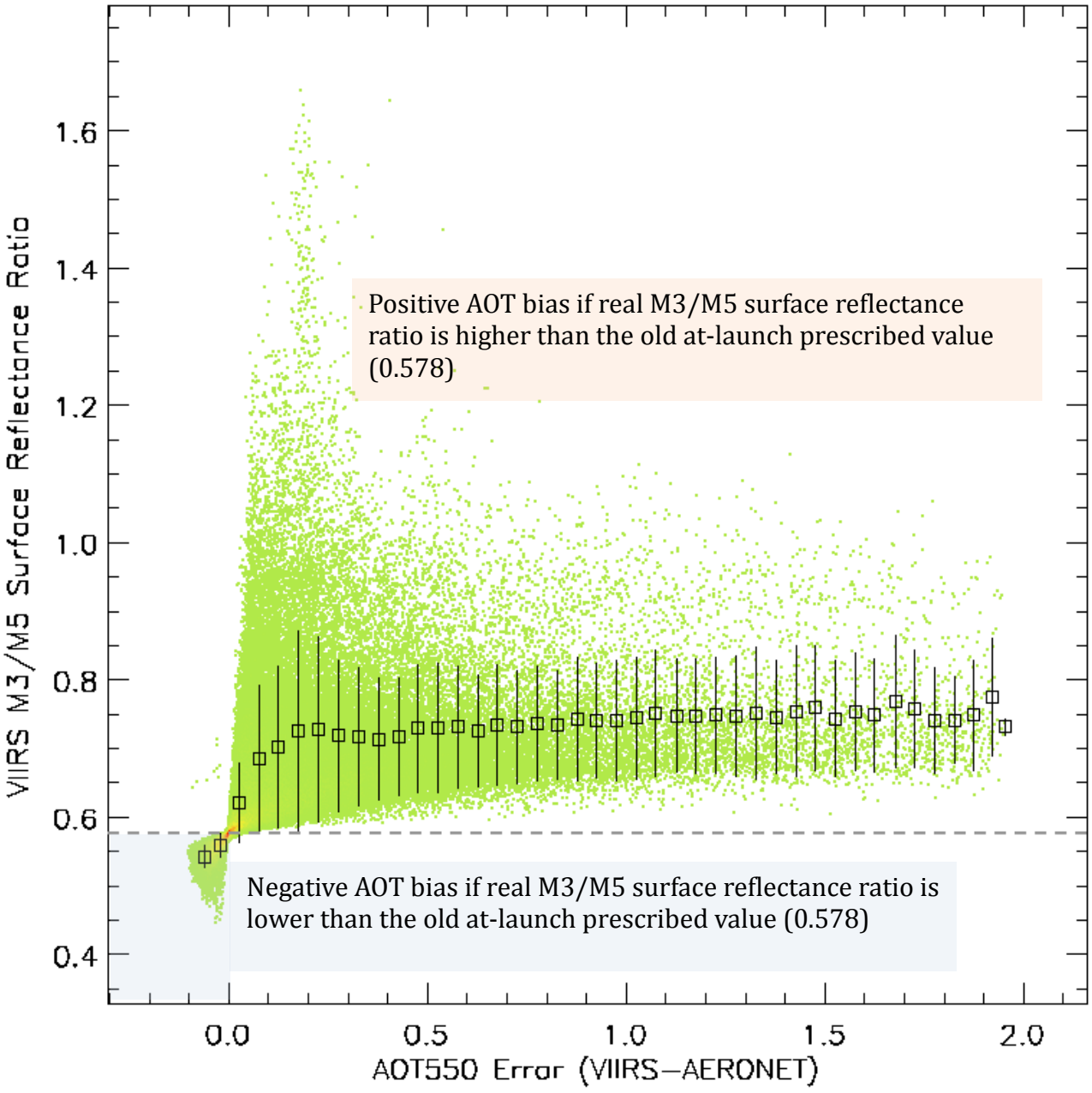

Figure 5.1 Retrieved surface reflectance ratio between bands M3 and M5 at collocated AERONET stations as a function of the VIIRS – AERONET AOT at 0.55 μm.

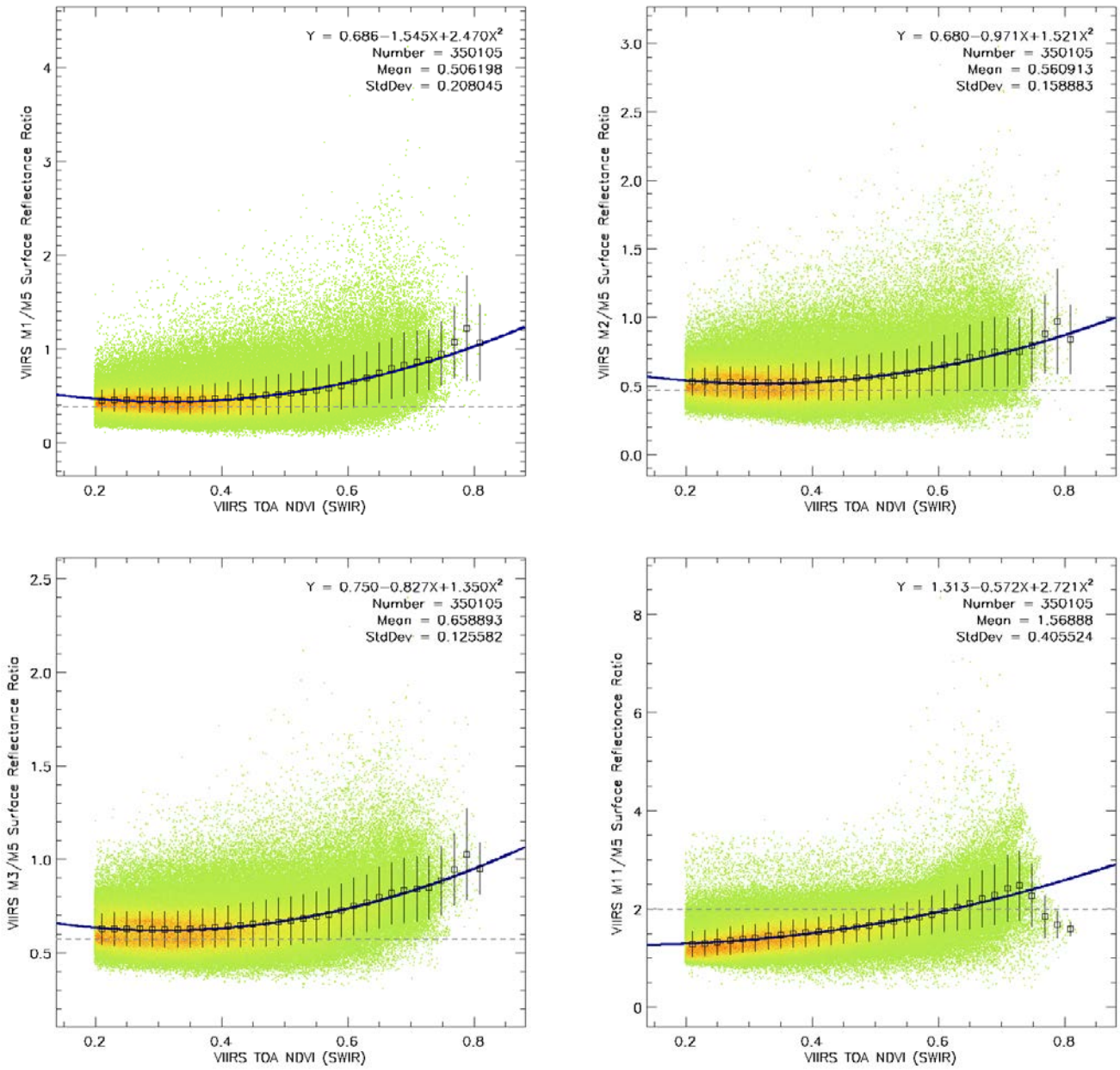

Figure 5.2 Retrieved surface reflectance ratios as a function of VIIRS Bright_index, here called TOA NDVI (SWIR). This terminology follows from the MODIS heritage.

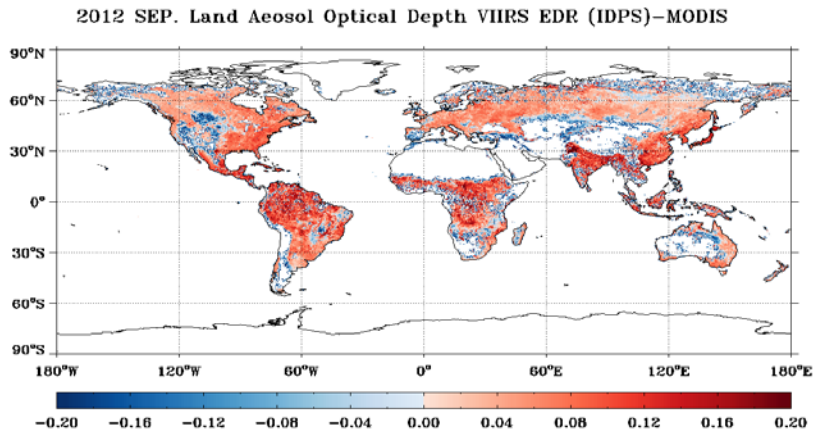

Figure 5.3 September 2012 difference in monthly mean AOT produced from VIIRS aerosol code running at-launch surface reflectance ratios and corresponding MODIS monthly mean values.

Bias	0.050
StdDev	0.084
Global VIIRS AOT	0.204
Global MODIS AOT	0.155

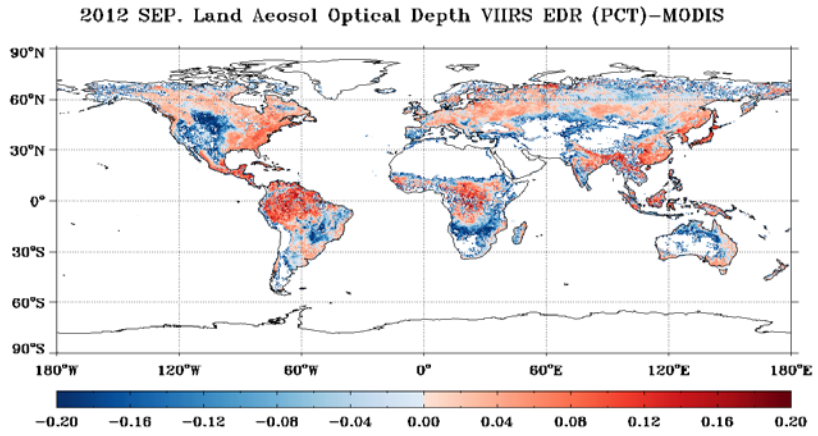

Figure 5.4 September 2012 difference in monthly mean AOT produced from VIIRS aerosol code running current Table 3.6 surface reflectance ratios and corresponding MODIS monthly mean values.

Bias	0.002
StdDev	0.098
Global VIIRS AOT	0.153
Global MODIS AOT	0.155

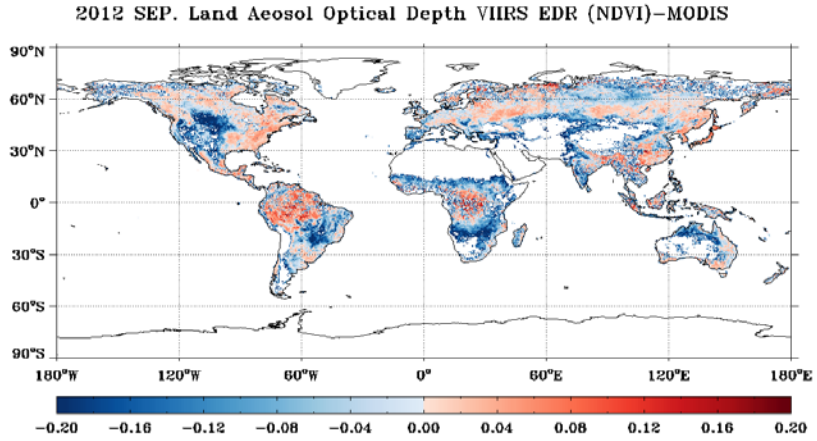

Figure 5.5 September 2012 difference in monthly mean AOT produced from VIIRS aerosol code running proposed $NDVI_{SWIR}$ dependent surface reflectance ratios and corresponding MODIS monthly mean values.

Bias	0.029
StdDev	0.098
Global VIIRS AOT	0.126
Global MODIS AOT	0.155

Concluding Remarks

The VIIRS aerosol algorithm continues to be a work in progress. At this point in time, roughly 18 months post-launch, preliminary validation of the products yields very promising results, especially for the products having MODIS heritage. Analysis and modifications of the algorithm will continue, in order to extract the maximum information from the VIIRS measurements, and to monitor and adjust to possible instrument characterization changes. Likewise this document is a living document that will evolve in concert with the algorithm and products.

6.0 REFERENCES

Baker, N., Joint Polar Satellite System (JPSS) Aerosol Optical Thickness (AOT) and Particle Size Parameter Algorithm Theoretical Basis Document (ATBD), JPSS Ground Project code 474, 474-00049, GSFC JPSS Aug. 6, 2011 released.

Born, M. and E. Wolf (1975). Principles of Optics, Fifth Edition, Pergamon Press.

Charlson, R. J., S. E. Schwartz, J. M. Hales, R. D. Cess, J. A. Coackley Jr., J. E. Hansen, and D. J. Hofman (1992). Climate forcing of anthropogenic aerosols. Science, 255, 423-430.

Cox, C., and W. Munk (1954). Statistics of the sea surface derived from sun glitter. J. Mar. Res., 13, 198-208.

Diner, D.J., J.C. Beckert, T.H. Reilly, C.J. Bruegge, J.E. Conel, R. Kahn, J.V. Martonchik, T.P. Ackerman, R. Davies, S.A.W. Gerstl, H.R. Gordon, J-P. Muller, R. Myneni, R.J. Sellers, B. Pinty, and M.M. Verstraete, "Multiangle Imaging SpectroRadiometer (MISR) description and experiment overview," *IEEE Trans. Geosci. Remt. Sensing,* **36** (1998): 1072-1087.

Dubovik, O., B. N. Holben, T. F. Eck, A. Smirnov, Y. J. Kaufman, M. D. King, D. Tanré, and I. Slutsker, 2001, "Variability of absorption and optical properties of key aerosol types observed in worldwide locations", J. Atmos. Sci., 59,590-608.

Eck, T. F., B. N. Holben, J. S. Reid, O. Dubovik, A. Smirnov, N. T. O'Neill, I. Slutsker, and

Eck, T.F., B. N. Holben, J.S.Reid, O.Dubovik, A.Smirnov, N.T.O'Neill, I.Slutsker, and S.Kinne, "Wavelength dependence of the optical depth of biomass burning, urban and desert dust aerosols, " *J. Geophys. Res.,* **104** (1999) : 31 333-31 350.

Ferrare, R. A., R. S. Fraser, and Y. J. Kaufman (1990). Satellite remote sensing of large-scale air pollution: Measurements of forest fires smoke, J. Geophys. Res., 95, 99119925.

Fraser, R.S., "Satellite measurement of mass of Sahara dust in the atmosphere." *Appl. Opt.,* **15** (1976): 2471–2479.

Geogdzhayev, I. V. and M. I. Mishchenko, 1999. Preliminary Aerosol Climatology for the Period of NOAA-9 Observations (http://gacp.giss.nasa.gov)

Griggs, M. (1975). Measurements of atmospheric aerosol optical thickness using ERTS-1 data, J. Air pollut. Control Assoc., 25, 622-626.

Hansen, J. E., and A. A. Lacis (1990). Sun and dust versus greenhouse gases: An assessment of their relative roles in global climate change. Nature, 346, 713-719.

Higurashi A. and T. Nakajima, "Development of a two channel aerosol retrieval algorithm on global scale using NOAA AVHRR." *J. Atmos. Sci*., **56** (1999): 924–941.

Holben, B.N., T.F. Eck, I. Slutsker, D. Tanré, J.P. Buis, A. Setzer, E.F. Vermote, J.A. Reagan, Y.J. Kaufman, T. Nakajima, F. Lavenue, I. Jankowiak, and A. Smirnov (1998). AeroNet – A federated instrument network and data archive for aerosol characterization, Remote Sensing of the Environment, 66:(1) 1-16.

Intergovernmental Panel on Climate Change (IPCC) (1994). Radiative Forcing of Climate Change. Edited by B. Bolin, J. Houghton, and L. G. M. Filho, UNEP, World Meteorol. Organ., Geneva.

Kahn, R.A., B.J. Gaitley, M.J. Garay, D.J. Diner, T. Eck, A. Smirnov, and B.N. Holben, "Multiangle Imaging SpectroRadiometer global aerosol product assessment by comparison with the Aerosol Robotic Network. " *J. Geophys. Res*. **115,** D23209 (2010), doi: 10.1029/2010JD014601.

Kaufman, Y. J., R. S. Fraser, and R. A. Ferrare (1990). Satellite measurements of large-scale air pollution methods, J. Geophys. Res., 95, 9895-9909.

Kaufman, Y. J., and D. Tanré (1996). Algorithm for Remote Sensing of Tropospheric Aerosol from MODIS, http://eospso.gsfc.nasa.gov/atbd/modistables.html.

Kaufman, Y. J., D. Tanré, L. A. Remer, E. F. Vermote, A. Chu, and B. N. Holben (1997). Operational remote sensing of tropospheric aerosol over land from EOS moderate resolution imaging spectroradiometer. *J. Geophys. Res*., 102, 16971-16988.

Kaufman, Y. J., A. E. Wald, L. A. Remer, B. Gao, R. Li, and L. Flynn (1997). The MODIS 2.1-.m Channel-Correlation With Visible Reflectance for Use in Remote Sensing of Aerosol. *IEEE Trans. on Geoscience and Remote Sensing*, 35, 1286-1298.

King, M. D., D. M. Byrne, B. M. Herman, and J. A. Reagan (1978). Aerosol size distribution obtained by inversion of optical depth measurements. J. Atmos. Sci., 35, 21532167.

Kneizys, F. X., E. P. Shettle, W. O. Gallery, J. H. Chetwynd, Jr., W. L. Abreu, J. E. A. Selby, R. W. Fenn and R. A. Mc- Clatchey, (1980). Atmospheric transmittance radiance: Computer Code LOWTRAN 5. Environ. Res. Pap. No. 697, Air Force Geophysics Laboratory, 233 pp.

Koepke, P. (1984). Effective reflectance of oceanic whitecaps, Appl. Opt., 23, 1816-1823.

Kotchenova,S.Y., Vermote, E.F., Matarrese,R., and Klemm, F.J., 2006: Validation of a vector version of the 6S radiative transfer code for atmospheric correction of satellite data. Part I: path radiance, *Appl. Opt*., 45, 26, 6762-6774.

Levy RC, L.A. Remer, S. Mattoo, E.F. Vermote, and Y.J. Kaufman (2007). A second-generation algorithm for retrieving aerosol properties over land from MODIS spectral reflectance. *J. Geophys. Res*., **112**, D13211,.

Li, R. R., Y. J. Kaufman, B. C. Gao, and C. O. Davis (2003). Remote Sensing of Suspended Sediments and Shallow Coastal Waters, *IEEE Trans. Geosci. Remote Sens*., 41, 559-566.

Mekler Y., H. Quenzel, G.Ohring, and I.Marcus , "Relative atmospheric aerosol content from ERTS observations." *J. Geophys. Res*., **82**(1977):967–972.

Mie, G., Beiträge zur Optik trüber Medien, speziell kolloidaler Metallösungen. *Ann. Physik*, **25** (1908): 377–445.

Mishchenko, M. I., A. A. Lacis, B. E. Carlson, and L. D. Travis (1995). Nonsphericity of dust-like tropospheric aerosols: Implications for aerosol remote sensing and climate modeling, Geophys. Res. Letters, 22, 1077-1080.

O'Neill, N.T., T.F.Eck, B.N.Holben, A.Smirnov, O.Dubovik, and A.Royer, "Bimodal size distribution influences on the variation of Angstrom derivatives in spectral and optical depth space, " *J. Geophys. Res.*, **106 (**2001), 9787-9806.

Petitcollin F. and Vermote E. F. 2001, Land surface reflectance, emissivity and temperature from MODIS middle and thermal infrared data., accepted in R.S.E.

Rao, C.R.N, EP McClain, and LL Stowe, "Remote sensing of aerosols over the oceans using AVHRR data theory, practice, and applications." *Int. J. Remote Sens.* **10**(4–5), (1989): 743–749.

Remer, L.A. and Y.J. Kaufman, 1998, Dynamic aerosol model: Urban/Industrial aerosol, Journal of Geophysical Research, 102, 16849-16859.

Remer L.A., Y.J. Kaufman, D.Tanré, S.Mattoo, D.A. Chu, J.V. Martins, R.R. Li, C. Ichoku, R.C. Levy, R.G. Kleidman, T.F. Eck, E. Vermote, B.N. Holben, "The MODIS aerosol algorithm, products and validation," *J. Atmos. Sci*., **62**(2005): 947–973.

Roger J.C and Vermote E. F., 1998, A method to Retrieve the Reflectivity Signature at 3.75.m from AVHRR data, Remote Sensing of the Environment, 64:103-114.

SM ATBD: Suspended Matter Algorithm Theoretical Basis Document: 474-00046 http://npp.gsfc.nasa.gov/science/sciencedocuments/474-00046__VIIRS_Suspended_Matter_ATBD_Rev-_20110422.pdf

Smirnov, A., B. N. Holben, I. Slutsker, D. M. Giles, C. R. McClain, T. F. Eck, S. M. Sakerin, A. Macke, P. Croot, G. Zibordi, P. K. Quinn, J. Sciare, S. Kinne, M. Harvey, T. J. Smyth, S. Piketh, T. Zielinski, A. Proshutinsky, J. I. Goes, N. B. Nelson, P. Larouche, V. F. Radionov, P. Goloub, K. Krishna Moorthy, R. Matarrese, E. J. Robertson, and F. Jourdin, "Maritime Aerosol Network as a component of Aerosol Robotic Network," *J. Geophys. Res.*, **114,** D06204, (2009), doi:10.1029/2008JD011257.

Stowe L. L., R. Hitzenberger, and A. Deepak, Report on *Experts Meeting on Space Observations of Tropospheric Aerosols and Complementary Measurements*, WCRP-48, WMO/TD-No. 389, World Meteorological Organization, (1990).

Stowe, L. L., A. M. Ignatov, and R. R. Singh (1997). Development, validation, and potential enhancements to the second-generation operational aerosol product at the National Environmental Satellite, Data, and Information Service of the National Oceanic and Atmospheric Administration, *J. Geophys. Res*., 102, 16,923-16,934.

Tanré, D., M. Herman, and Y. J. Kaufman (1996). Information on aerosol size distribution contained in solar reflected spectral radiances. *J. Geophys. Res*., 101, 19,04319,060.

Tanré D., L.A. Remer, Y.J. Kaufman, S. Mattoo, P.V. Hobbs, J.M.Livingston, P.B. Russell, and A. Smirnov , "Retrieval of aerosol optical thickness and size distribution over ocean from the MODIS airborne simulator during TARFOX." *J. Geophys. Res.,* **104**, D2 (1999): 2261–2278.

Tanré D., F.M. Bréon, J.L. Deuzé, O. Dubovik, F. Ducos, P. François, P. Goloub, M. Herman, A. Lifermann, F. Waquet, "Remote sensing of aerosols by using polarized, directional and

spectral measurements within the A-Train: the PARASOL mission," *Atmos. Meas. Tech.*, **4 (**2011):1383-1395, doi:10.5194/amt-4-1383-1395-2011.

VCM ATBD: VIIRS Cloud Mask Algorithm Theoretical Basis Document: 474-00033. Prepared by N. Baker. Released February 2013. http://npp.gsfc.nasa.gov/science/sciencedocuments/474-00033_ATBD-VIIRS-Cloud-Mask_B.pdf

Vermote, E., D. Tanré, 1992, Analytical expressions for radiative properties of planar Rayleigh scattering media, including polarization contributions, J.Quant. Spectrosc. Radiat. Transfer, 47,4, 305-314.

Vermote, E., D. Tanré, J.L. Deuzé, M. Herman, and J.J. Morcette, 1997a. 6S User Guide Version 2.

Vermote, E., D. Tanré, J.L. Deuzé, M. Herman, and J.J. Morcette, 1997b. Second Simulation of the Satellite Signal in the Solar Spectrum, 6S: An Overview, IEEE, Trans. On Geo. Remote Sensing, VOL 35, 1997.

Vermote, E. F., Saleous, El, N. Z. and Justice, C. O.: Atmospheric correction of MODIS data in the visible to middle infrared: first results, Remote Sens Environ, 83(1-2), 97–111, doi:10.1016/S0034-4257(02)00089-5, 2002.

Wen, G., S. Tsay, R. F. Cahalan, and L. Oreopoulos, 1999. Path radiance technique for retrieving aerosol optical thickness over land. J. Geophys. Res., 104D, 3132131332.

APPENDIX A Coefficients for gaseous transmission and molecular scattering calculations

WAVELENGTHS in μm (λ)
lambda: 0.412000, 0.445000, 0.488000, 0.555000, 0.672000, 0.746000, 0.865000, 1.24000, 1.38000, 1.64000, 2.25000

MOLECULAR OPTICAL THICKNESS at 11 wavelengths (τ_R^{λ})
moltau: 0.318910, 0.233620, 0.160500, 0.0977900, 0.0441580, 0.0288570, 0.0160540, 0.00367060, 0.000000, 0.00131190, 0.000331280

OZONE COEFFICIENTS (a_{O3}) in Eq. (3.1):
o3cof: 0.000285210, 0.00287980, 0.0180350, 0.0838500, 0.0433130, 0.0106730, 7.67350e-005, 1.52580e-008, 0.000000, 0.000000, 0.000000

CONSTANT SPECIES COEFFICIENTS (a_0, a_1, b_0, b_1, c_0 *and* c_1) in Eq. (3.4):
tgoga0: -0.000280560, -2.83280e-005, -0.000117540-9.96060e-005, -0.00198180, -0.00183480, -2.75520e-005, -0.000904070, 0.000000, -0.0209480, -0.0470690

tgoga1: 0.00116490, 0.000103750, 0.000366230, 0.000311280, 0.00846380, 0.00397870, 0.00112460, 0.00737160, 0.000000, 0.00393730, 0.0398200

tgogb0: 0.000281710, 2.90410e-005, 0.000120750, 0.000102420, 0.00177870, 0.00209930, 8.43890e-006, 1.24250e-005, 0.000000, 0.00301690, -0.0126610

tgogb1: -0.00111620, -0.000102150, -0.000375200, -0.000322650, -0.00954910, -0.00513400, 0.000202290, -0.000592510, 0.000000, 0.0403560, -0.0422850

tgogc0: 7.43100e-005, 7.52440e-006, 3.12710e-005, 2.64560e-005, 0.000519320, 0.000496360, 2.69090e-006, 0.000146410, 0.000000, 0.00425260, 0.00771930

tgogc1: -0.000304890, -2.70540e-005, -9.67470e-005, -8.17780e-005, -0.00231570, -0.00107000, -9.68680e-006, -0.00118650, 0.000000, 0.00454670, -0.0136530

WATER, COEFFICIENTS:

pwcof1: 4.04370e-005, -7.23950e-007, 6.77590e-006, -0.000122860, -0.000517040, -0.00533640, -0.00251020, -0.00377030, 0.000000, -0.00115360, -0.00162120

pwcof2: -0.000986480, -0.000124690, -0.000372640, -0.000247090, -3.06490e-005, 0.00186690, 0.000712850, 0.00238370, 0.000000, 0.000863490, 0.00101020

pwcof3: -7.37470e-006, 7.14210e-008, -1.22700e-006, 2.07450e-005, 7.73180e-005, 0.000872150, 0.000381480, 0.000591240, 0.000000, 0.000137830, 0.000265270

APPENDIX B Parameters needed in ocean core inversion

B.1 Atmospheric spherical albedo at actual surface pressure

$S_{R+A}(P,Aer)$ is the atmospheric (Rayleigh and aerosol) spherical albedo, which is a function of the surface pressure (P) and aerosol model (Aer). Since $S_{R+A}(P,Aer)=1-\int_0^1 \mu T(\mu)\,d\mu$, where $T(\mu)$ is the transmission for $\mu=\cos\theta$, if we ignore the water vapor dependence, which is a second order effect, we can write $S_{R+A}(P,Aer)$ in terms of a reference pressure as,

$$S_{R+A}(P,Aer)=(S_{R+A}(P_o,Aer)-S_R(P_o))+S_R(P).$$

$S_{R+A}(P_o,Aer)$ is stored in the pre-calculated LUT for each aerosol model (Aer) and optical thickness. The $S_R(P)$ term is calculated from an analytical expression,

$$S_R(P)=\frac{1}{4+3\tau_R}\left[3\tau_R-4E_3(\tau_R)+6E_4(\tau_R)\right],$$

where E3 and E4 are exponential integral functions defined as,

$$E_n(x)=\int_1^\infty \frac{e^{-xt}}{t^n}dt.$$

The integrals satisfy the recurrence relationship:

$$n\,E_{n+1}(x)=e^{-x}-x\,E_n(x)$$

that is used to compute $E_4(x)$ and $E_3(x)$ from $E_1(x)$ approximated by

$$E_1(x)=\sum_{i=0}^{5} a_i x^i-\log(x).$$

The coefficients are:

a_0= -0.57721566,
a_1= 0.99999193,
a_2= -0.24991055,
a_3= 0.05519968,
a_4= -0.00976004,
a_5= 0.00107857.

The approximation for $E_1(x)$ is accurate to within 2e-07 for $0<x<1$.

B.2 Normalized integrated downward irradiance by sunglint directional reflectance

$\overline{\rho_G}$ is pre-computed in a LUT depending on the geometry and AOT for a particular aerosol model. Unlike the main retrieval LUT that is indexed by solar and sensor view angles, AOT and aerosol model, the sunglint LUT is indexed by three angular variables: solar zenith, sensor zenith and relative azimuth. Table B.1 provides the bins of the sunglint LUT. Intermediate values are found with linear interpolation.

Table B.1 Nodes of the sunglint Look-Up Table

Argument	Dimension	Bins
550 nm AOT	15	0.01, 0.05, 0.10, 0.15, 0.20, 0.30, 0.40, 0.60, 0.80, 1.00, 1.20, 1.40,1.60, 1.80, 2.00
Solar Zenith Angle	21	0°, 4°, 8°, 12°, 16°, 20°, 24°, 28°, 32°, 36°, 40°, 44°, 48°, 52°, 56°, 60°, 64°, 68°, 72°, 76°, 80°
Satellite Zenith Angle	21	0°, 4°, 8°, 12°, 16°, 20°, 24°, 28°, 32°, 36°, 40°, 44°, 48°, 52°, 56°, 60°, 64°, 68°, 72°, 76°, 80°
Relative Azimuth	21	0°, 9°, 18°, 27°, 36°, 45°, 54°, 63°, 72°, 81°, 90°, 99°, 108°, 117°, 126°, 135°, 144°, 153°, 162°, 171°, 180°

$\overline{\rho_G^*}$ is the reciprocal of $\overline{\rho_G}$, which is extracted from the same LUT, but with view and sensor zenith angles swapped.

B.3 Sunglint spherical albedo

The sunglint spherical albedo $\overline{\overline{\rho_G}}$ is a band dependent constant set according to Table B.2.

Table B.2 Sunglint spherical albedos.

VIIRS Band	Sunglint Spherical Albedo
M5	0.0661
M6	0.0651
M7	0.0648

M8	0.0640
M10	0.0629
M11	0.0590

APPENDIX C IP, EDR and Suspended Matter Table of Quality Flags

C.1 IP Quality Flags

Table C.1 IP Quality Flags QF1-5

QF1			
Flag	**Values**	**Bits**	**Conditions**

AOT Quality (QF1.1)	00 = 0 =High
	01 = 1 = Degraded
	10 = 2 = Excluded
	11 = 3 = Not Produced
		2	AOTNOTPRODUCED(3):
			• Solar zenith angle > 80°
			• Missing channel reflectance
			  • Over land: M1, M2, M3, M5, M8, M11
			  • Over water: M5, M6, M7, M8, M10, M11
			• Missing ancillary model data
			  • Wind speed, wind direction, precipitable water, surface air temperature, column ozone, surface pressure, surface height
			• Probably or confident cloudy (from QF4.4)
			• Snow/ice present (from QF4.1)
			• Fire present (from QF4.4)
			• Unfavorable surface: inland water or coastal (from QF2.3)
			• Internal test
			  • Over land: sun glint; fire; snow/ice
			  • Over water: sun glint; turbid water; snow/ice
			• Bright surface over land
			  • Bright pixel index ($\frac{M8-M11}{M8+M11}$)<0.05 and Reflectance at M11 > 0.3
			
			AOTEXCLUDED(2):
			• Use tertiary ancillary model data (obsolete)

QF1			
Flag	**Values**	**Bits**	**Conditions**

			• Retrieved AOT550 out of spec range [0,2]
			• Internal test
			  • Missing channel reflectance or brightness temperature (M3,M5,M7,M8,M9,M10,M11,M12, M15, M16 over land; M3,M4,M15,M16 over water)
			AOTDEGRADED(1):
			• 65° ≤ Solar zenith angle < 80°
			• Use secondary ancillary model data (obsolete)
			• Presence of cloud shadow (from QF4.3); cirrus (from QF4.2); adjacent pixel cloud confidence level being probably or confidently cloudy (from QF2.2); volcanic ash (QF4.7)
			• Soil dominant over land (bright pixel index ≤ 0.2)
			• Retrieval residual beyond the threshold
			  • Minimum residual > 0.05 when AOT550 > 0.5 over land
			  • Minimum residual > 0.5 when AOT550 > 0.5 over water
			
			AOTHIGH(0): otherwise

Ångström Exponent Quality (QF1.2)	00 = 0 = High 01 = 1 = Degraded 10 = 2 = Excluded 11 = 3 = Not Produced	2	Set to be same as the Aerosol optical thickness quality (QF1.1) AOTNOTPRODUCED(3): • Nonpositive AOT at channels used for AE calculation (M2 / M5 over land; M7 / M10 over water) AOTEXCLUDED(2): • Out of spec range [-1.0, 3.0] • Low AOT 550(<0.15) AOTDEGRADED(1): AOTHIGH(0): otherwise

QF1			
Flag	**Values**	**Bits**	**Conditions**
Suspended Matter Type Quality (QF1.3)	00 = 0 = High 01 = 1 = Degraded 10 = 2 = Excluded 11 = 3 = Not Produced	2	Set to be same as AOT quality flag (QF1.1) AOTNOTPRODUCED(3); AOTEXCLUDED(2); • 0.15 < AOT550 < 0.5 AOTDEGRADED(1); AOTHIGH(0): if volcanic ash is detected (QF4.7), the SM type quality is set to be AOTHIGH (0) no matter what value QF1.1 is
Cloud Mask Quality (QF1.4)	00 = 0 = Poor 01 = 1 = Low 10 = 2 = Medium 11 = 3 = High	2	Direct copy from VIIRS cloud mask (VCM) without modification

QF2			
Flag	**Values**	**Bits**	**Conditions**
Cloud Detection Result & Confidence Indicator (QF2.1)	00 = 0 = Confident Clear 01 = 1 = Probably Clear 10 = 2 = Probably Cloudy 11 = 3 = Confident Cloudy	2	Direct copy from VCM, with one modification on confident clear case CM_CONF_CLOUDY (3) CM_PROB_CLOUDY(2) CM_PROB_CLEAR(1) CM_CONF_CLEAR(0): if the heavy aerosol flag is turned on in VCM
Adjacent Pixel Cloud Confidence Value (QF2.2)	00 = 0 = Confident Clear 01 = 1 = Probably Clear 10 = 2 = Probably Cloudy 11 = 3 = Confident Cloudy	2	Initially copied from VCM, but subsequently modified to be the most cloudy category available from the adjacent 3x3 pixel cloud confidence flags (QF2.1) CM_CONF_CLOUDY (3) CM_PROB_CLOUDY(2) CM_PROB_CLEAR(1) CM_CONF_CLEAR(0)

QF2			
Flag	**Values**	**Bits**	**Conditions**
Land/Water Background (QF2.3)	000 = 0 = Land & Desert 001 = 1 = Land, No Desert 010 = 2 = Inland Water 011 = 3 = Sea Water 101 = 5 = Coastal 110 = 6 = Ephemeral Water	3	Direct copy from VCM, add a new surface type if ephemeral water is detected in the internal test over land. CM_DESERT (0) CM_LAND (1) CM_IN_WATER(2) CM_SEA_WATER (3) CM_COASTAL (5) AOT_EPHWAT (6): • New type added through internal test over land
Bad SDR (QF2.4)	1 = Yes 0 = No	1	AOTQFYES(1): • If channel reflectance or brightness temperature are missing (<-999.0) Over land: M1-M12,M15,M16 Over water: M3-11, M15,M16 AOTQFNO(0): otherwise

QF3			
Flag	**Values**	**Bits**	**Conditions**
Day/Night Flag (QF3.1)	00 = 0 =Day 01 = 1 =Low Sun, Degraded 10 = 2 = Twilight, Excluded 11= 3 = Night	2	AOTNIGHT (3): Solar zenith angle > 85° AOTSOLZAEX (2): 80° < Solar zenith angle ≤ 85° AOTSOLZADEG (1): 65° < Solar zenith angle ≤ 80° AOTDAY (0): Solar zenith angle ≤ 65°
Interpolation / NAAPS / Climatology Processing Used (QF3.2)	000 = 0 = None 001 = 1 = Interpolation only 010 = 2 = Interpolation & Climatology/NAAPS 011 = 3 = Climatology/NAAPS	3	AOTCLIMO (3): • If there is no good or degraded quality retrieval available within the searching window (41x41 pixels) • Use NAAPS (if available) or climatology AOT550 only; aerosol model information is from climatology AOTINTCLIMO (2): • Ratio of the total weight of pixels with available retrievals to the total weight of all pixels within the searching window < 0.25 • Combine interpolated (weighted average of good/degraded retrievals) and

QF3			
Flag	**Values**	**Bits**	**Conditions**
			NAAPS/climatology AOT550; aerosol model information is from the retrieval with highest weight (if available) or climatology. AOTINT (1): • Above weight ratio ≥ 0.25 • Use interpolated (weighted average of good/degraded retrievals) AOT550 only; aerosol model information is from the retrieval with highest weight (if available) or climatology. AOTNOINTCLIMO (0): • Good/degraded aerosol retrieval is available
Sun Glint (QF3.3)	000 = 0 = None 001 = 1 = Geometry Based 010 = 2 = Wind Speed Based 011 = 3 = Geometry & Wind 100 = 4 = Internal 101 = 5 = Internal & Geometry 110 = 6 = Internal & Wind 111 = 7 = All	3	Over land: determined by internal test Over water: initially copied from VCM and internal test also checks

QF4			
Flag	**Values**	**Bits**	**Conditions**
Snow/Ice (QF4.1)	1 = Yes 0 = No	1	Initially copied from VCM, internal tests also check for snow/ice AOTQFYES (1): • VCM identified or internal tests detected AOTQFNO(0):
Cirrus (QF4.2)	1 = Yes 0 = No	1	Initially copied from VCM, internal tests also check for cirrus over land CM_CLOUD (1): • VCM identified or internal test (over land) detected CM_NO_CLOUD (0)
Cloud	1 = Yes	1	Copied from VCM

QF4			
Flag	**Values**	**Bits**	**Conditions**
Shadow (QF4.3)	0 = No		
Fire (QF4.4)	1 = Yes 0 = No	1	Initially copied from VCM, internal tests also check fire over land CM_FIRE (1) • VCM identified or internal test (over land) detected CM_NO_FIRE (0)
Bright Pixel (QF4.5)	00 = 0 = Dark 01 = 1 = Soil Dominated 10 = 2 = Bright	2	Land only AOTBRIGHT (2): • Bright pixel index $(\frac{M8-M11}{M8+M11})$<0.05 and Reflectance at M11 > 0.3 AOTSOIL (1): • Bright pixel index ≤ 0.2, soil dominated. AOTVEG (0): • Initial value.
Turbid/ Shallow Water (QF4.6)	1 = Yes 0 = No	1	AOTQFYES (1): • Detected by internal test over water AOTQFNO (0)
Ash (QF4.7)	1 = Yes 0 = No	1	Copied from VCM AOTQFYES (1) AOTQFNO (0)

QF5			
Flag	**Values**	**Bits**	**Conditions**
Low AOT – SM Typing Excluded (QF5.1)	1 = Yes 0 = No	1	AOTQFYES (1): • If 0.15 < AOT550 < 1.0 AOTQFNO (0): • AOT550 ≤ 0.15 – no suspended matter • AOT550 ≥ 1.0
Low AOT – SM Detection Excluded (QF5.2)	1 = Yes 0 = No	1	AOTQFYES (1): • If 0.15 < AOT550 < 0.5 AOTQFNO (0): • AOT550 ≤ 0.15 – no suspended matter • AOT550 ≥ 0.5
AOT Out of Spec Range (QF5.3)	1 = Yes 0 = No	1	AOTQFYES (1): • If AOT550 < 0.0 or AOT550 > 2.0 AOTQFNO (0)
APSP Out of Spec Range	1 = Yes 0 = No	1	AOTQFYES (1): • If AE < -1.0 or AE > 3.0

QF5			
Flag	**Values**	**Bits**	**Conditions**
(QF5.4)			AOTQFNO (0)
Low AOT, APSP Excluded (QF5.5)	1 = Yes 0 = No	1	AOTQFYES (1): • If AOT550 < 0.15 AOTQFNO (0)
Residual Threshold Exceeded (QF5.6)	1 = Yes 0 = No	1	AOTQFYES (1): • Minimum residual > 0.05 when AOT550 > 0.5 over land • Minimum residual > 0.5 when AOT550 > 0.5 over water AOTQFNO (0)
		2	Note: Spare bits

C.2 EDR Quality Flags

Table C.2 EDR Quality Flags QF1-5

QF1				
Flag	**Values**	**Bits**	**Conditions**	**Notes**

QF1				
Flag	**Values**	**Bits**	**Conditions**	**Notes**
AOT Quality (QF1.1)	11 = 3 = High 10 = 2 = Medium 01 = 1 =Low 00 = 0 = Not Produced	2	**High:** Number of good quality pixel AOT retrievals > 16 (1/4 the total number of pixels in aggregated horizontal cell) **Medium:** Number of good quality retrievals ≤ 16 and the number of good/degraded quality retrievals ≥ 16 **Low:** Number of good/degraded quality retrievals < 16 **Not Produced:** No good/degraded quality retrievals, neither land or sea water dominant (number of land or ocean pixels < half the number of good/degraded pixels in the horizontal cell), ellipsoid fill in the geolocation, night scan, has a pixel with a solar zenith angle between 80º and 85º but no pixel with a solar zenith angle between 65º and 80º	

QF1				
Flag	**Values**	**Bits**	**Conditions**	**Notes**
APSP Quality (QF1.2)	11 = 3 = High 10 = 2 = Medium 01 = 1 =Low 00 = 0 = Not Produced	2	**High:** Number of good quality pixel APSP retrievals > 16 (1/4 the total number of pixels in aggregated horizontal cell) **Medium:** Number of good quality retrievals ≤ 16 and the number of good/degraded quality retrievals ≥ 16 **Low:** Number of good/degraded quality retrievals < 16 **Not Produced:** No good/degraded quality retrievals, neither land or sea water dominant (number of land or ocean pixels < half the number of good/degraded pixels in the horizontal cell), ellipsoid fill in the geolocation, night scan	
Land, Ocean, or Not Produced (QF1.3)	00 = 0 = Land 01 = 1 = Ocean 10 = 2 = Not Produced	2	**Land:** Number of land/desert pixels ≥ half the total good/degraded pixels within the horizontal cell **Ocean:** Number of sea water pixels > half the total good/degraded pixels within the horizontal cell	
AOT out of Spec Range (QF1.4)	1 = Yes 0 = No	1	**Yes:** AOT at 550 nm of any pixel in the 8x8 horizontal cell is out of spec range (0.0-2.0)	
APSP out of Spec Range (QF1.5)	1 = Yes 0 = No	1	**Yes:** APSP of any pixel in the 8x8 horizontal cell is out of spec range (-1.0-3.0)	

QF2				
Flag	**Values**	**Bits**	**Conditions**	**Notes**
Cloud Contamination (QF2.1)	1 = Yes 0 = No	1	**Yes:** Any pixel in the 8x8 horizontal cell is not confidently clear	
Cloud adjacent to cell (QF2.2)	1 = Yes 0 = No	1	**Yes:** Any pixel in the 8x8 horizontal cell has their cloud adjacency flagged as probably or confidently cloudy	

QF2				
Flag	**Values**	**Bits**	**Conditions**	**Notes**
Cirrus Contamination (QF2.3)	1 = Yes 0 = No	1	**Yes:** Any pixel in the 8x8 horizontal cell has cirrus	
Bad SDR (QF2.4)	1 = Yes 0 = No	1	**Yes:** Any pixel in the 8x8 horizontal cell has bad SDR	
Sunglint (QF2.5)	1 = Yes 0 = No	1	**Yes:** Any pixel in the 8x8 horizontal cell has sunglint	
Cloud Shadow (QF2.6)	1 = Yes 0 = No	1	**Yes:** Any pixel in the 8x8 horizontal cell has cloud shadow	
Snow/Ice (QF2.7)	1 = Yes 0 = No	1	**Yes:** Any pixel in the 8x8 horizontal cell has snow/ice	
Fire (QF2.8)	1 = Yes 0 = No	1	**Yes:** Any pixel in the 8x8 horizontal cell has fire	

QF3				
Flag	**Values**	**Bits**	**Conditions**	**Notes**
Low sun, degraded (QF3.1)	1 = Yes 0 = No	1	**Yes:** Any pixel in the 8x8 horizontal cell has the day/night flag set to 'Low sun, degraded' (65º < Solar zenith angle ≤ 80º)	
Low sun, excluded (QF3.2)	1 = Yes 0 = No	1	**Yes:** Any pixel in the 8x8 horizontal cell has the day/night flag set to 'Low sun, excluded' (80º < Solar zenith angle ≤ 85º)	
Bright surface (land)/Shallow or Turbid Water (ocean) (QF3.3)	1 = Yes 0 = No	1	**Yes:** Any pixel in the 8x8 horizontal cell has a bright pixel (land) or turbid/shallow water (ocean)	
Low AOT, APSP Excluded (QF3.4)	1 = Yes 0 = No	1 4	**Yes:** Any pixel in the 8x8 horizontal cell has excluded APSP	 Spare bits

QF4				
Flag	**Values**	**Bits**	**Conditions**	**Notes**

QF4				
Flag	**Values**	**Bits**	**Conditions**	**Notes**
Land Aerosol Model Index (land) (QF4.1)	100 = 4 = Urban, Polluted 011 = 3 = Urban, Clean 010 = 2 = Smoke, Low Absorption 001 = 1 = Smoke, High Absorption 000 = 0 = Dust	3		Selects the dominant aerosol model (largest number of pixels involved in the EDR aggregation) over land; See AOT ATBD for all model details
		5		Spare bits

QF5				
Flag	**Values**	**Bits**	**Conditions**	**Notes**
Small Mode Aerosol Model (ocean) (QF5.1)	011 = 3 = Fine mode 4 010 = 2 = Fine mode 3 001 = 1 = Fine mode 2 000 = 0 = Fine mode 1 111 = 7 = NA (no ocean)	3		Selects the dominant small mode aerosol model (largest number of pixels involved in the EDR aggregation) over ocean; See AOT ATBD for all model details
Large Mode Aerosol Model (ocean) (QF5.2)	100 = 4 = Coarse mode 5 011 = 3 = Coarse mode 4 010 = 2 = Coarse mode 3 001 = 1 = Coarse mode 2 000 = 0 = Coarse mode 1 111 = 7 = NA (no ocean)	3		Selects the dominant large mode aerosol model (largest number of pixels involved in the EDR aggregation) over ocean; See AOT ATBD for all model details
		2		Spare bits

C.3 Suspended Matter Quality Flags

Table C.3 Suspended Matter Quality Flags QF1-3

QF1				
Flag	**Values**	**Bits**	**Conditions**	**Notes**
Suspended Matter Detection Product Quality (QF1.1)	11 = 3 = High 10 = 2 = Medium 01 = 1 = Low 00 = 0 = Not Produced	2	**High:** Pixel SM type quality is good **Medium:** Pixel SM type quality is degraded **Low:** Pixel SM type quality is excluded **Not Produced:** Pixel SM type quality is not produced	Pixel SM type quality is from Aerosol IP product, it is set by default to the Pixel-level AOT quality (see Table C.1 for conditions) and then changed under the following conditions: **Excluded:** AOT at 550 nm < 0.5 **Good:** If volcanic ash is detected, SM type quality is reset to good no matter what the AOT quality is
Suspended Matter Type Product Quality (QF1.2)	11 = 3 = High 10 = 2 = Medium 01 = 1 = Low 00 = 0 = Not Produced	2	**High:** Pixel SM type quality is good and "Low AOT, SM Typing Excluded" flag is not set (AOT at 550 nm ≤ 0.15 (no SM) or AOT at 550 nm ≥ 1.0) **Medium:** Pixel SM type quality is degraded and "Low AOT, SM Typing Excluded" is not set (AOT at 550 nm ≤ 0.15 (no SM) or AOT at 550 nm ≥ 1.0) **Low:** Pixel SM type quality is excluded or good/degraded plus or along with "Low AOT, SM Typing Excluded" is set (0.15 < AOT at 550 nm < 1.0) **Not Produced:** Pixel SM type quality is not produced	Pixel SM type quality is from Aerosol IP product, it is set by default to the Pixel-level AOT quality and then changed under the following conditions: **Excluded:** AOT at 550 nm < 0.5 **Good:** If volcanic ash is detected, SM type quality is reset to good no matter what the AOT quality is. Low AOT flag is from Aerosol IP product, it is set under the following conditions: **Yes:** 0.15 < AOT at 550 nm < 1.0 **No:** AOT at 550 nm ≤ 0.15 (no SM), AOT at 550 nm ≥ 1.0

QF1				
Flag	**Values**	**Bits**	**Conditions**	**Notes**
Smoke Concentration Product Quality (QF1.3)	11 = 3 = High 10 = 2 = Medium 01 = 1 = Low 00 = 0 = Not Produced	2	**High:** Pixel SM type quality is good and smoke concentration is not larger than the maximum threshold (1000 μg/m^3) **Medium:** Pixel SM type quality is degraded and smoke concentration is not larger than the maximum threshold (1000 μg/m^3 **Low:** Pixel SM type quality is good/degraded and smoke concentration is larger than the maximum threshold (1000 μg/m^3) **Not Produced:** Pixel SM type quality is not produced	Pixel SM type quality is from Aerosol IP product
Land, Ocean, or Not Produced (QF1.4)	00 = 0 = Land 01 = 1 = Ocean 11 = 3 = Not Produced	2	**Land:** Pixel surface type is land or desert **Ocean:** Pixel surface type is sea water	Pixel surface type is from Aerosol IP product

QF2				
Flag	**Values**	**Bits**	**Conditions**	**Notes**
Cloud Contamination (QF2.1)	1 = Yes 0 = No	1	**Yes:** Pixel is neither confidently clear nor probably clear	
Cloud adjacent to cell (QF2.2)	1 = Yes 0 = No	1	**Yes:** Pixel adjacent cloud flag is confident or probably cloudy	
Cirrus Contamination (QF2.3)	1 = Yes 0 = No	1		Copied from Aerosol IP Cirrus Quality Flag
Bad SDR (QF2.4)	1 = Yes 0 = No	1		Copied from Aerosol IP Bad SDR Quality Flag
Sunglint (QF2.5)	1 = Yes 0 = No	1	**Yes:** Pixel has sunglint flag set	

Cloud Shadow (QF2.6)	1 = Yes 0 = No	1		Copied from Aerosol IP Cloud Shadow Quality Flag
Snow/Ice (Q2.7)	1 = Yes 0 = No	1		Copied from Aerosol IP Snow/Ice Quality Flag
Fire (QF2.8)	1 = Yes 0 = No	1		Copied from Aerosol IP Fire Quality Flag

QF3				
Flag	**Values**	**Bits**	**Conditions**	**Notes**
Smoke Concentration out of Expected Range (QF3.1)	1 = Yes 0 = No	1	**Yes:** Pixel smoke concentration is beyond the expected range (0-1000 $\mu g/m^3$)	
Excluded SM typing (QF3.2)	1 = Yes 0 = No	1		Copied from the Aerosol IP SM Typing Excluded Quality Flag
Excluded SM Detection (Q3.3)	1 = Yes 0 = No	1		Copied from the Aerosol IP SM Detection Excluded Quality Flag
Low Sun (QF3.4)	1 = Yes 0 = No	1	**Yes:** IP day/night flag is set to 'Low sun, degraded' ($65º < \text{Solar zenith angle} \leq 80º$)	Day/Night flag is from Aerosol IP Product
Bright Surface/ Shallow or Turbid Water (QF3.5)	1 = Yes 0 = No	1	**Yes:** IP bright pixel or turbid/shallow water flag is set	Bright Surface and Turbid/Shallow Water flag is from Aerosol IP Product
		3		Spare bits